The effect of isolated and nanoencapsulated flavonoids from *Eriocephalus africanus* on apoptotic factors and microRNA expression in cancer

by

Judie Magura

Submitted in fulfilment of the academic requirements for the degree of

Doctor of Philosophy

in

Medical Sciences (Human Physiology)

School of Laboratory Medicine and Medical Sciences,

College of Health Sciences, University of KwaZulu-Natal, Westville, South Africa.
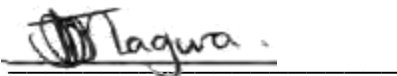
Supervisor: Professor Irene Mackraj

Co-supervisor: Dr Roshila Moodley

June 2020

PREFACE

The research work described in this thesis was conducted by the candidate at the University of KwaZulu-Natal, Westville, South Africa under the supervision of Professor Irene Mackraj and co-supervision of Dr Roshila Moodley.

The contents of this work have not been submitted in any form for any degree to another University, and where use has been made of the work of others, it is duly acknowledged in the text, the results reported are from investigations by the candidate.

_____

Signed: Judie Magura

Date: 30 June 2020

_____

Signed: Prof Irene Mackraj (Supervisor)

Date: 30 June 2020

_____

Signed: Dr Roshila Moodley (Co-supervisor)

Date: 30 June 2020

DECLARATION 1: PLAGIARISM

I, Judie Magura, declare that:

1.   The research reported in this dissertation, except where otherwise indicated or acknowledged, is my original work.

2.   This dissertation has not been submitted in part or in full for any degree or examination at any other university.

3.   This dissertation does not contain other persons' data, pictures, graphs or other information, unless specifically acknowledged as being sourced from other persons.

4.   This dissertation does not contain other persons' writing, unless specifically acknowledged as being sourced from other researchers. Where other written sources have been quoted, then:

a.   Their words have been re-written but the general information attributed to them has been referenced.

b.   Where their exact words have been used, then their writing has been placed in italics and inside quotation marks and referenced.

5. This dissertation does not contain text, graphics or tables copied and pasted from the Internet, unless specifically acknowledged, and the source being detailed in the thesis and in the References sections.

Signed_____

DECLARATION 2: PUBLICATIONS

Publication 1

Judie Magura, Roshila Moodley, Kaminee Maduray & Irene Mackraj (2020): Phytochemical constituents and *in vitro* anticancer screening of isolated compounds from *Eriocephalus africanus*, Natural Product Research, DOI: 10.1080/14786419.2020.1744138

To link to this article: https://doi.org/10.1080/14786419.2020.1744138

1.Presented at the College of Health Science Symposium October 2018 (Oral presentation).

2. Presented at the Gordon Research Conferences, Natural Products and Bioactive Compounds. July 28 - 2 August 2019, Proctor Academy in Andover NH, USA.

Publication 2

Judie Magura, Roshila Moodley & Irene Mackraj: The effect of hesperidin and luteolin isolated from *Eriocephalus africanus* on apoptosis, cell cycle and miRNA expression in MCF-7. Submitted to Journal of Biomolecular Structure and Dynamics. Currently under consideration for publication (corrections submitted).

Abstract submitted for presentation at the European Association for Cancer Research, 26th Congress in Torino Italy, 09-12 June 2021.

Publication 3

Judie Magura, Daniel Hassan, Roshila Moodley & Irene Mackraj: Hesperidin-loaded nanoemulsions improve cytotoxicity, induces apoptosis and downregulates miR-21 and miR155 expression in MCF-7. Submitted to Journal of Drug Targeting.

In preparation of the above manuscripts, I performed all the experiments and interpreted the data. The co-authors contributed in editing and verifying the scientific content as well as editing the manuscript.

Signed _____

ACKNOWLEDGMENTS

Firstly, I would like to acknowledge the exceedingly great power that works inside me through the knowledge of Christ Jesus in whom I live and have my being.

I would also like to express my extreme gratitude to my supervisor Prof. Irene Mackraj for believing in me and giving me an opportunity to study under her. My co-supervisor Dr R. Moodley for her support and commitment to this research.

I would also like to acknowledge the following people for the success of my research:

- My family, my husband Joe, and my kids Israel and Sophia for loving me and supporting me through this work.

- My colleagues, Daniel, Isaiah, Bongisiwe and Nomfundo who supported me through their friendship and lab expertise.

- Prof. B Nkambule, for mentoring me through flow cytometry.

- My friend for life "Sponge", for her unending love and support.

TABLE OF CONTENTS

LIST OF FIGURES

LIST OF TABLES

LIST OF ABBREVIATIONS

AJCC	American Joint Committee on Cancer
ANOVA	Analysis of variance
APAF1	Apoptotic-protease-activating-factor 1
ATR	Attenuated total reflectance
Bad	Bcl-xL/Bcl-2 associated death protein
Bax	Bcl-2-associated x protein
Bcl-2	B-cell Lymphoma 2
Bcl-XL	B-cell Lymphoma-Extra Large
Bid	BH3-interacting domain death agonist
BrdU	Bromodeoxyuridine
Caspase	Cysteine aspartic-specific proteases
cDNA	Complementary DNA
cdk	Cyclin-D dependent kinase
cFLIP	FLICE-like inhibitory protein
^{13}C-NMR	C-13 nuclear magnetic resonance spectroscopy
dATP	Deoxyadenosine triphosphate
DEPT	Distortionless enhancement by polarization transfer
DGCR8	DiGeorge syndrome critical region gene 8-encoded RNA binding protein
DISC	Death-inducing signaling complex
DMEM	Dulbecco's modified eagle medium
DMSO	Dimethylsulfoxide
DNA	Deoxyribonucleic acid

DPBS	Dulbecco's phosphate-buffered saline
DR5	Death receptor 5
DROSHA	A type III ribonuclease
EE	Encapsulation efficiency
EGFR	Epidermal growth factor receptor
ER	Estrogen receptor
ERF	Permeability and retention effect
FADD	Fas-associated death domain
Fas	TNF Receptor superfamily, member 6
FasL	Fas Ligand
FBS	Foetal bovine serum
FDA	Food and Drug Administration
FITC	Fluorescein isothiocyanate
HEK 293	Human embryonic kidney cells
HepG2	Liver hepatocellular carcinoma cells
HER2	Human epidermal growth factor receptor 2
HMBC	Heteronuclear multiple bond coherence
HR-TEM	High resolution-transmission electron microscopy

HR-ESI-MS High resolution-electrospray ionisation-mass spectrometry

HSQC   Heteronuclear single quantum coherence

IR   Infrared

MOMP   Mitochondrial outer membrane permeabilisation

mRNA   Messenger RNA

miRNA   micro RNA

miRISC   miRNA-induced silencing complex

MTT   3-(4,5-dimethylthiazol-2-yl)-2,5-diphenyltetrazolium bromide

MW   Molecular weight

NF-κB   Nuclear factor Kappa Light Chain Enhancer of Activated B

NMR   Nuclear magnetic resonance

PBS   Phosphate buffered saline

PCR   Polymerase chain reaction

PDI   Polydispersity index

PEG   Polyethylene glycol

PLGA   Poly (lactic-co-glycolic acid)

PI   Propidium iodide

PR   Progesterone receptor

RISC   RNA-induced silencing complex

SD   Standard deviation

SLN   Solid lipid nanoparticles

tBID   truncated BID

TLC	Thin layer chromatography
TNF	Tumour necrosis factor
TNM	Tumour node metastasis
TRADD	TNFR-associated death domain
TRAIL	TNF-related apoptosis inducing ligand
UTR	Untranslated region
UV-vis	Ultraviolet- visible
WHO	World Health Organisation
ΔΨm	Mitochondrial electrochemical proton gradient
5-FU	5-Fluorouracil
7-AAD	7-Amino-actinomycin D
ζ	Zeta potential

ABSTRACT

Cancer continues to be a major health burden worldwide, with millions of new cases being diagnosed each year. Among women breast cancer remains a leading cause of cancer-related morbidity and mortality globally, despite the significant advances in detection and individualised treatments. The ideal non-surgical approach for the treatment of breast cancer would be anticancer therapeutics that are delivered directly to the tumour site for complete elimination of cancerous cells without being toxic to surrounding healthy cells. However, current chemotherapeutics encounter numerous challenges due to adverse side effects and progressive drug resistance albeit effective. In light of this, identifying new effective therapies with minimal toxic and chemosensitizing effects as well as target specificity is crucial in combating cancer. Emerging evidence has supported the use of plant-derived chemicals as novel alternative treatment options, owing to their minimal side effects and toxicity.

Plant-derived polyphenols have gained considerable research interest due to their ability to inhibit proliferation, initiate apoptosis and arrest the cell cycle of cancerous cells by modulating related pathways. Furthermore, incorporation of active plant-derived polyphenols into novel technologies such as nanosystems, offers more optimal therapies through improved bioavailability and target specificity. In this regard, this study demonstrates, for the first time, the potential of phytochemicals isolated from the methanolic extract of the medicinal plant, *Eriocephalus africanus*, as an alternative therapeutic strategy in breast cancer treatment using ER-positive human adenocarcinoma (MCF-7) cell lines. Spectroscopic techniques including nuclear magnetic resonance spectroscopy (NMR), infrared spectroscopy (IR) and mass spectrometry (MS) were used to identify the isolated compounds as hesperidin (flavanone), luteolin (flavone) and apigenin (flavone). Preliminary anticancer screening using the 3-(4,5dimethylthiazolyl)-2,5-diphenyl-tetrazolium bromide (MTT) assay revealed hesperidin and luteolin to be potent against MCF-7.

Dysregulated cellular apoptotic death is a hallmark of cancer and chemotherapy resistance; thus, the development of anticancer drugs targeting apoptosis is a widely used, effective anticancer treatment strategy. In this study, the efficacy of hesperidin and luteolin in targeting the apoptotic pathway was evaluated. Treatment of breast cancer cells with hesperidin and luteolin resulted in the downregulated expression of key anti-apoptotic *Bcl-2*; upregulated

expression of pro-apoptotic *Bax* and caspases -8, -9 and -3. In addition, hesperidin and luteolin demonstrated the ability to effect epigenetic control through altering the expression of apoptotic microRNAs (-16, -21 and -34a). Moreover, treatment with hesperidin and luteolin resulted in significant accumulation of MCF-7 apoptotic cells into the G0/G1 and sub-G1 cell cycle phases, respectively. Encapsulation of hesperidin into nanoemulsions improved the cytotoxic and apoptotic effects in MCF-7 without being cytotoxic to non-cancerous human cell lines (HEK 293), halted the progression of the MCF-7 cells in the G2/M phase, and exhibited potential therapeutic activity through inhibiting the expression of oncomirs miR-21 and -155 overexpressed in breast cancer. Encapsulation of luteolin into solid nanoparticles generated from cleaved stearylamine exhibited non-selective cytotoxicity and decreased cell viability ($<$ 10%) in both MCF-7 and HEK 293 cells, thus no further investigations were conducted using luteolin-loaded solid nanoparticles. Collectively, findings from this study provide new evidence on the effects of flavonoids isolated from *E. africanus* on apoptotic and epigenetic control in breast cancer, increasing our knowledge of the molecular basis of their anticancer activity.

1.   CHAPTER ONE: INTRODUCTION AND LITERATURE REVIEW

1.1 Background

Cancer is a rapidly growing disease with the number of deaths increasing considerably worldwide, as it is estimated that by 2025, 20 million new cases would emerge in low- and middle-income countries [1]. Currently, approximately 70% of cancer deaths occur in low- and middle-income countries, with prostate, breast, colorectal and lung being the most common cancers. In men, the most prevalent cancer types occur in the prostate, lung, colon, and rectum, while in women, breast, lung, uterine, and thyroid cancers are more prevalent [2, 3]. According to GLOBOCAN, in 2018, approximately 2 093 876 (lung), 2 088 849 (breast), 1 849 518 (colorectum) and 1 276 106 (prostate) new cases were recorded worldwide [4]. Overall, the data suggests that breast and prostate cancer present with the highest occurrences, globally.

Despite the major advances made in medicine towards cancer treatment, cancer remains a public health concern. Current effective treatments, including chemotherapy and radiotherapy, are often hampered by adverse side effects coupled with progressive chemoresistance [5]. Plant-derived compounds have gained importance as potential alternative treatments for cancer with minimal side effects and anti-proliferative and pro-apoptotic properties [6]. Another drawback in current cancer treatment approaches, is the lack of specificity in drug targeting. Therefore, the application of nanotechnology to drug modification and drug delivery systems have emerged as a promising new therapeutic approach offering improved bioavailability, increased accumulation of drugs at specific disease sites, and overall enhanced efficacy in cancer treatment [3].

1.2 Definition and classification of cancer

Cancer can be described as a group of diseases in which cells abnormally hyper-proliferate, invade normal tissue and eventually spread to the rest of body through blood and the lymphatic system [7]. Cancer is a result of progressive genetic and epigenetic alterations within the cell that leads to uncontrolled cell proliferation associated with evasion of apoptosis, lack of cell cycle arrest, tumour progression and metastasis [1, 8]. Cancer is classified based on the tissue

type or location of origin, for example, cancers originating in the breast, lung and liver are called breast, lung and liver cancer, respectively [9]. Histological classification broadly categorise cancer into; (1) carcinomas, which are cancers that develop from the epithelial tissue lining organs or of the skin (2) sarcomas, malignant tumours in connective tissue such as bone and cartilage, muscle and fat cells; (3) leukaemia referred to as blood or liquid cancers, originating from blood-forming tissue such as bone marrow; (4) lymphomas, malignancies arising from the nodes or glands of the lymphatic system; and (5) myeloma originating from the plasma cells of bone marrow [10, 11]. Tumours can be malignant or benign. Benign tumours are slow-growing, non-cancerous and non-invasive. In contrast, malignant tumours are cancerous, invasive and metastatic [11].

1.2.1 Aetiology and pathogenesis of cancer

The pathogenesis of cancer is multifactorial involving a network of complex mechanisms that are not yet fully understood with each systemic representation shedding more light to the understanding of the disease [12]. Presently, irrespective of the cancer type, the basis of cancer pathogenesis is commonly accepted to arise from genetic damage or alterations in gene expression (mediated by epigenetic mechanisms), within a normal single cell that gives rise to its transformation into a malignant or tumour cell [12, 13]. Several studies have shown that the genomic abnormalities may be induced or initiated by various risk factors including inherited genetic predispositions, random spontaneous DNA replication errors, external factors collectively known as carcinogens (e.g. chemicals, radiation and viruses), or other factors such as tobacco smoke, physical inactivity and an unhealthy diet [13,14]. Consequently, the genetic/epigenetic damage may lead to mutations in key genes such as tumour suppressors, oncogenes, or genes controlling the cell cycle, resulting in inactivation of normal cell growth control and promotion of abnormal cell proliferation, eventually giving rise to cancer [15].

Experimental evidence has demonstrated that the progression of a genetically altered cell to a malignant tumour, though characterised by various pathways and distinct histological features for each cancer type, is a multi-step process consisting of initiation, promotion and progression [15]. As shown in Figure 1, a single cell initially acquires genetic mutations triggered by various stimuli (initiators) and becomes predisposed for neoplastic transformation. The mutated cell proceeds to the lengthy promotion stage where it abnormally proliferates and

reproduces many of its kind (clonal expansion); histologically this condition is called hyperplasia (increase in cell number). Through the progression stage the mutated cells, acquire new mutations, continue to proliferate, change form and grow in tumour size (*in situ* cancer) [13,16,17]. The *in-situ* tumours may remain dormant or acquire other mutations, progress to invade surrounding tissue and become invasive (malignant tumours) [16].
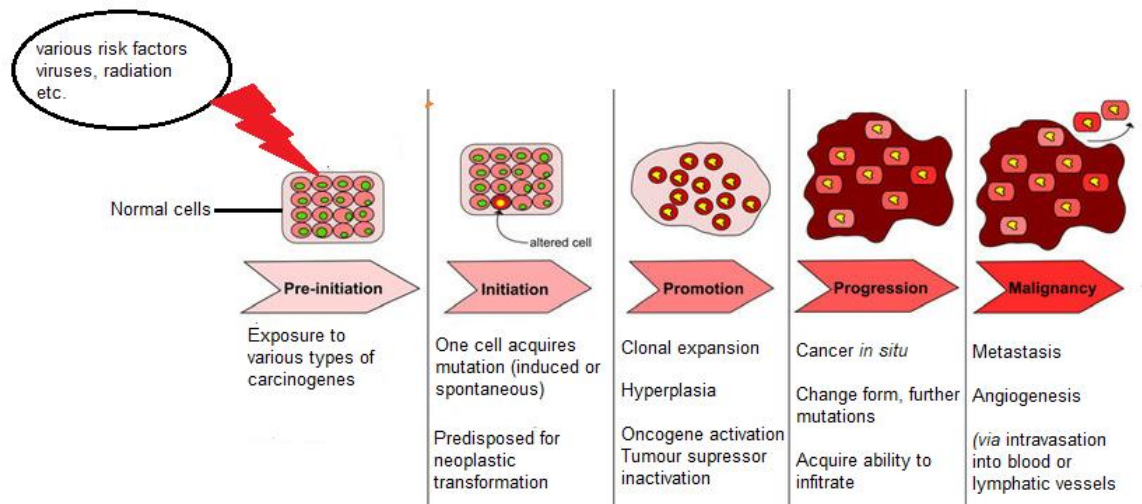
Figure 1. The stages of cancer development: initiation, promotion and progression. The initiation may be triggered by different factors or stimuli including spontaneous errors in DNA replication and various carcinogens. Once initiated the alerted cell acquires the potential to transform from normal to a malignant tumour (Adapted from Kolat et al. 2019 [17]).

Consequently, as the malignant tumours continue to rapidly proliferate, they outgrow the oxygen and nutrient supply of their host tissue vasculature and become oxygen-deprived (hypoxia). Therefore, to sustain this abnormal growth, tumours stimulate the growth of new blood vessels for their own supply through a process called angiogenesis [18]. In addition to maintaining the tumour oxygen and nutrient supply, and waste disposal, angiogenesis enables the tumour cells to invade surrounding tissue and metastasise to distant sites by providing an escape route into the circulation *via* the newly formed blood and lymph systems [19, 20].

1.3 Role of apoptosis in cancer

Apoptosis is a highly organised cell death mechanism essential for healthy tissue development and homeostasis [21]. It serves to remove abnormally proliferating, and/or irreparable DNA

damaged cells, thus protecting genomic integrity and preventing carcinogenesis [22]. Morphological characteristics of apoptosis include nuclear changes such as chromatin condensation, nuclear fragmentation and breakdown, and overall changes such as cellular rounding and shrinkage, volume reduction and blebbing [23]. Apoptosis can be induced by different stimuli, through both intracellular and extracellular signals [24]. This process is initiated and activated by a family of intracellular proteins known as cysteine aspartate-specific proteases (caspases) and regulated by the Bcl-2 family of proteins.

1.3.1 The Bcl-2 family proteins and caspases

The Bcl-2 protein cluster controls cell death mainly through release of cytoplasmic cytochrome *c* and subsequent activation of caspases resulting in mitochondrial apoptosis [25]. The Bcl-2 family is divided into pro-apoptotic effectors (*Bax, Bak*); pro-apoptotic BH3-only proteins (*Bad, Bid, Bik, Bim, Noxa, Puma*) and anti-apoptotic proteins (*Bcl-2, Bcl-xL, Bcl-W, Mcl-1, Bfl-1/A1*) [26, 27]. Anti-apoptotic proteins inhibit apoptosis by preventing the release of mitochondrial cytochrome *c* mediated *via Bax* and *Bad*, while pro-apoptotic proteins promote apoptosis by triggering the release of cytochrome *c* into the cytoplasm [25, 28]. Overall, the balance between pro- and anti-apoptotic proteins determine the fate of the cell; when proapoptotic proteins dominate, apoptosis is induced, while the opposite response causes inhibition [29].

Caspases are a family of cysteine proteases, whose subclassification is based on their distinct function within apoptosis, *viz*. either as initiator caspases (caspase -2, -8, -9, and -10) or effector caspases (-3, -7, and -6) [30, 31]. Caspases usually exist inside the cell, in their inactive form, as procaspases. Upon sensing death signals, initiator caspases initiate apoptosis through cleavage of procaspases into active effector caspases, which mediate cellular degradation through proteolysis, leading to cell death [31]. Activation of initiator caspase-8 normally leads to death receptor-mediated apoptosis, while activation of caspase-9 leads to mitochondria-mediated cell death [32].

1.3.2 Molecular mechanisms of the apoptotic pathway

The apoptotic pathway is initiated by two distinct pathways known as the intrinsic

(mitochondrial) and extrinsic (death receptor). The intrinsic pathway is regulated by the Bcl-2 gene family and involves mitochondrial degradation. It is initiated by various external and internal stimuli, including chemotherapy, DNA damage, oxidative and oncogenic stress, an excess of calcium cations, hypoxia, and growth factor withdrawal (Figure 2) [24]. The stimuli produce intracellular signals, leading to the activation of *Bax* and *Bad*, which accumulate at the mitochondrial outer membrane, oligomerise and mediate mitochondrial outer membrane permeabilization (MOMP), through pore formation and membrane potential changes ($\Delta\Psi$m). The permeabilization results in the release of cytochrome *c*, which then forms an apoptosome with apoptotic protease-activating factor-1 (APAF-1), dATP, and procaspase-9. Subsequently, procaspase-9 is converted to caspase-9, which activates the executioner caspases, which in turn coordinate cell death (apoptosis) [5, 24, 33].

In contrast, the extrinsic (death receptor) pathway is initiated by extracellular death receptors, such as tumour necrosis factor (TNF), death receptor 5 (DR5) and Fas, which bind to their respective ligands, *viz.* TNF, TNF related apoptosis-inducing ligand (TRAIL), and Fas ligand (FasL) [34]. Upon binding to these ligands, death receptors trimerize and promote the binding of adaptor proteins, such as Fas-associated DD protein (FADD) and TNF receptor-associated death domain (TRADD), to initiator procaspases -8 and -10, leading to the formation of the death-inducing signalling complex (DISC). DISC consists of FADD as an adaptor molecule, the cellular FLICE inhibitory proteins (c-FLIPs), procaspase-8 and -10; and its formation leads to the activation of caspase-8 and -10, which promotes apoptosis through direct cleavage of downstream effector caspases such as caspase-3 [35, 36]. The extrinsic and intrinsic pathways may crosstalk through the caspase-8 activated cleavage of BH3 interacting-domain death agonist (Bid) to *tBid*, which targets the mitochondria and activates the pro-apoptotic proteins *Bax* and *Bak*, facilitating the continuation of the intrinsic pathway [24].
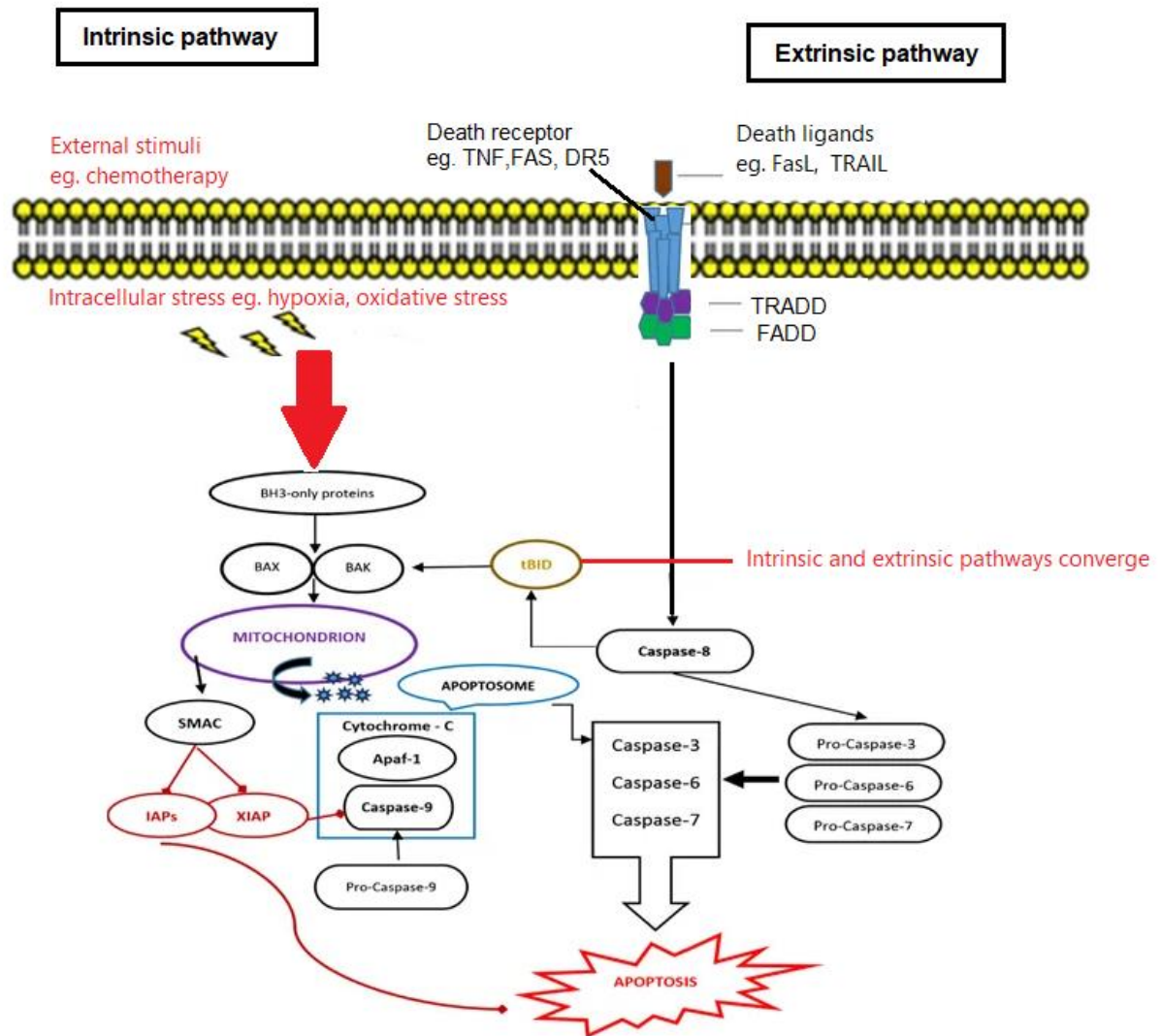
Figure 2. The intrinsic (mitochondrial) and extrinsic (death receptor) apoptotic pathways.

The intrinsic pathway is triggered by intracellular and extracellular stimuli that activates *Bax* and *Bak*. Activation of *Bax* and *Bak* causes MOMP and subsequent release of cytochrome *c* and formation of an apoptosome followed by activation of caspase 9. Caspase 9 activates the executioner caspases 3/6/7, that in turn coordinate cell death (apoptosis). The extrinsic pathway is initiated through the binding of specific death receptors to their ligands followed by activation of caspase 8, which propagates apoptotic cell death through direct cleavage of downstream effector caspases 3/6/7 (Adapted from Baig et al. 2016 [37]).

1.3.3 Apoptosis and cancer progression

Dysregulation of apoptosis has been implicated in the pathophysiology of various diseases, including cancer, AIDS and degenerative diseases [5]. It is clear that progression of cancer is influenced by lack of apoptotic function or evasion of apoptosis resulting in malignant cells not dying [22, 28]. The ability of cancer cells to evade apoptosis is a hallmark of the disease, which promotes uncontrolled propagation of cells resulting in tumour survival, treatment resistance and cancer recurrence [38]. Cancer cells may evade apoptosis through several mechanisms, including overexpression of anti-apoptotic Bcl-2 genes and oncogenes, downregulation of pro-apoptotic Bcl-2 genes and loss of caspase activity [5].

Overexpression of prominent anti-apoptotic genes, *Bcl-2, Bcl-xL,* and *Mcl-1,* have been implicated in apoptosis evasion and treatment resistance in various cancers, including breast, lung and colorectal [39]. Repression of *Bcl-2* in breast cancer has been reported to sensitise cells for treatment and promotes apoptosis [40–42]. Additionally, *Bcl-xL/Mcl-1* inhibitors have been successful in inducing cell death even in most aggressive forms of breast cancer such as triple-negative breast cancer [43]. Notably, inactivation of BH3-only members (*Bad, Puma, Noxa*), and caspases have been shown to promote resistance to pro-apoptotic stimuli and tumour proliferation *in vivo* [44]. Furthermore, since miRNA regulates gene expression in cellular processes, their dysregulation could promote overexpression of anti-apoptotic genes and promote evasion [45, 46]. Hence, inducing or restoring apoptotic function has emerged as an effective approach in preventing cancer progression.

1.4 Cell cycle regulation and cancer

Regulated cellular progression through the cell cycle is essential for maintaining ordered DNA replication, cell division and tissue integrity. The cycle is regulated by specific classes of proteins (cyclins and cyclin-dependent kinases Cdks) and consists of four phases (Figure 3) denoted as 1) G1, where the cells grow and reorganise organelles in preparation for DNA replication, 2) S phase, synthesis phase, cell replicates or copies its DNA 3) G2, second growth phase, cells grow and accumulates proteins for mitosis 4) Mitotic phase, the cell division occurs [47]. Progression of the cell from one phase to another is regulated by a series of checkpoints that ensure all conditions and requirements are met before the cell commits to the next phase.

For example, the G2 checkpoint prevents transition to mitosis if DNA replication is incomplete, by holding the cell in-phase (cell cycle arrest) until all DNA replication is complete. Another vital checkpoint occurs in the M phase, which prevents cell division (mitosis arrest) in response to improper alignment of the daughter chromosomes on the mitotic spindle. The G1 checkpoint also inhibits transition into the S phase in the presence of prior DNA damage and leads to G1 cell cycle arrest until the DNA is repaired [48]. In cases of severe unrepairable DNA or prolonged mitotic arrest, cells commit to apoptotic, autophagic, or necrotic cell death [49, 50].
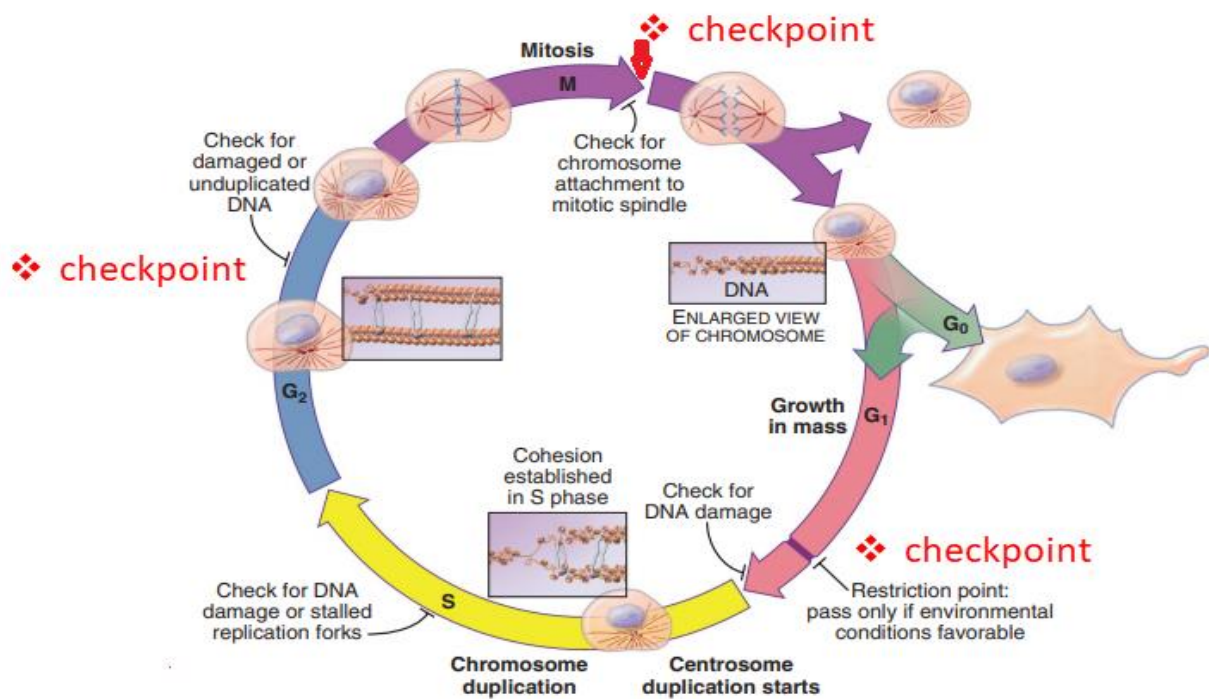
Figure 3. The progression of the cell through the cell cycle. G0 denotes the phase where nondividing cells enter, this is not necessarily permanent as in some cases cells re-enter the cycle. G1 the first growth phase, S synthesis phase, G2 second growth phase, M denotes mitosis where the cell divides and cytokinesis the separation of the cytoplasm (Adapted from Introduction to the Cell Cycle 2017 p. 648 [48]).

However, in cancer pathogenesis, cancer cells often acquire genetic and epigenetic mutations that disable checkpoints, impair the ability to induce cell cycle arrest, and allow progression of cancer cells through the cycle despite their multiple genome impairments. This sustained progression promotes uncontrolled proliferation of cancer cells with defective genomes and

often results in tumour metastasis and treatment resistance. Thus, anticancer approaches that promote cell cycle arrest and subsequent cell death, show promising potential in cancer treatment [51]. Different cytotoxic stimuli have been successful in halting breast cancer cell progression at different cycle phases, leading to apoptosis, such as G2/M phase [52], S and G2/M phase [53], G1/M [54], and S phase [55].

1.5 Role of microRNA in cancer

MicroRNAs (miRNA) have recently gained recognition as key post-transcriptional regulators of several cellular signalling processes, including apoptosis, cell cycle and proliferation [56]. MiRNA are small non-coding RNA, approximately 18-24 nucleotides in length, that regulate gene expression through binding to the 3′ untranslated region (3′ UTR) of the target mRNA, resulting in either mRNA degradation or inhibition of translation [57]. The inhibition of mRNA translation or its degradation depends on the extent of mRNA-miRNA nucleotide sequence complementarity; perfect matching leads to mRNA degradation, whereas partial matching or mismatch results in inhibition of translation [58]. The biosynthesis and mechanisms of miRNA regulation of their target mRNA are shown in Figure 4. Briefly, the miRNA gene is first transcribed by RNA polymerase II into a long primary miRNA, then processed by Drosha/DGCR8 microprocessor complex into 70 -120 nucleotide long precursor miRNA (pre-miRNA) possessing a stem-loop structure and a 2-nucleotide overhang at the 3′- cleavage end [45, 59]. The precursor miRNA is then transferred into the cytoplasm by binding to a Ran-dependent nuclear transport receptor protein, exportin 5 [59]. Following transfer into the cytoplasm, the pre-miRNA is processed into mature RNA duplexes (20-22 nucleotides) by the Dicer/TRBP/PACT complex [56]. By helicase action, the duplex RNA is separated into single miRNA strands. The thermodynamic stability of the duplex 5′- end influences the separation of the strands. Normally the miRNA strand that is unstable at 5′-end is incorporated into the RNA-induced silencing complex (RISC) and guides the miRNA-induced silencing complex (miRISC) to mismatch pairing with the target mRNA, resulting in translation inhibition. The strand that is at the stable 5′- end is usually degraded. Therefore, miRNA negatively regulates the expression of their target mRNA [56, 59].
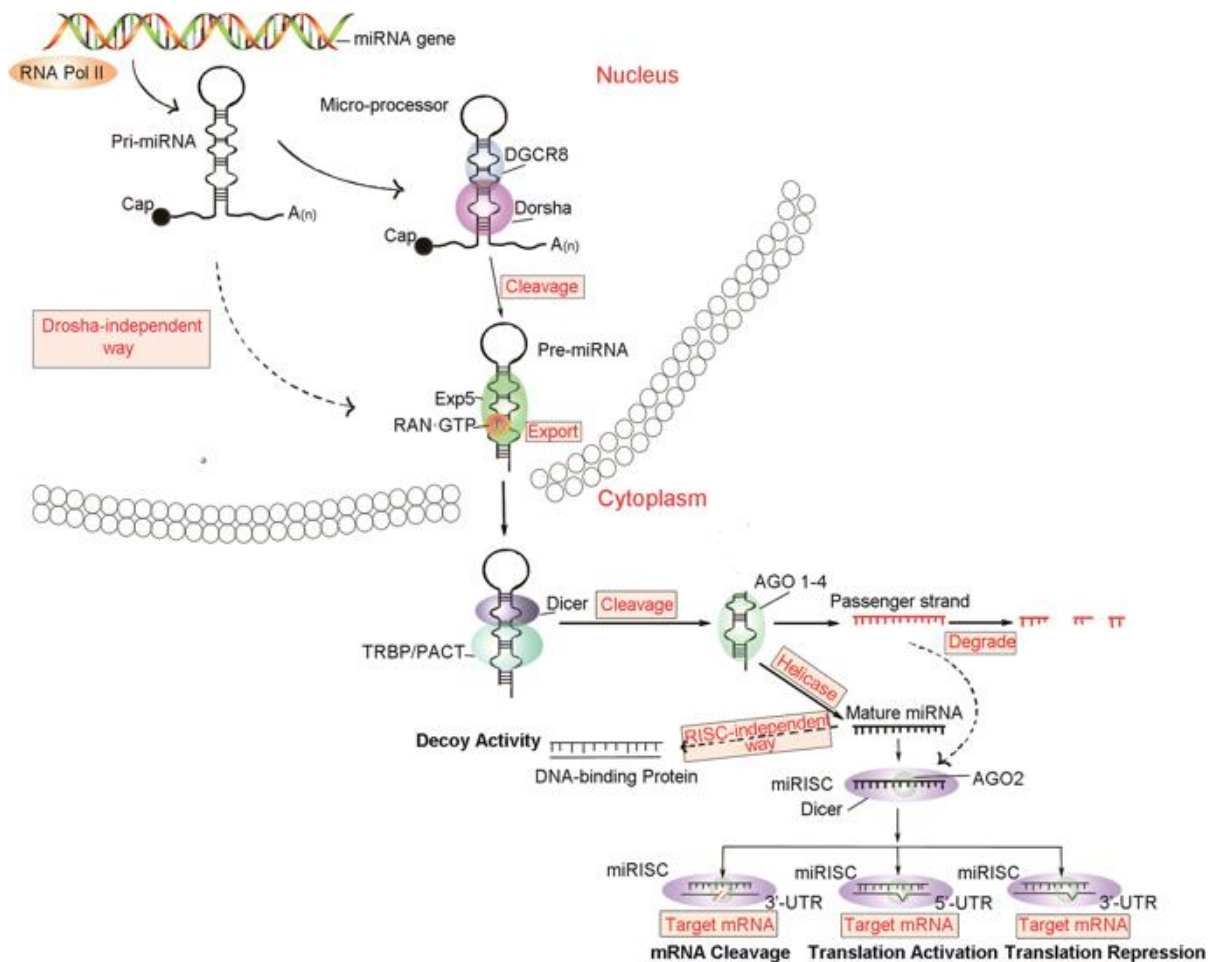
Figure 4. The biosynthesis of miRNA and the mechanisms of their regulation of target mRNA. The solid arrows indicate the classical pathway which includes Drosha, whereas the dotted lines indicate the non-classical Drosha-independent way (Adapted from Si et al. 2019 [56]).

Recent evidence has indicated that the expression of miRNAs is dysregulated in various human cancers. MiRNAs function as either oncogenes or tumour suppressors by regulating the expression of fundamental target genes [60]. MicroRNAs from the miR-15a/16 cluster have been shown to act as tumour suppressors, inhibiting cell proliferation, promoting cell cycle arrest and apoptosis [61]. MiR-15a/16 is often silenced or deleted in various cancer types. Previous studies have demonstrated that miR15a/16 function by targeting oncogenes such as Bcl-2, Mcl-1 and cell cycle regulatory genes such as Cyclin D1 [62]. Downregulation of miR15a/16-1 have been indicated to contribute to the pathogenesis of many cancers including

breast cancer, prostate cancer and chronic lymphocytic leukaemia [62–64]. Activation of miR15a and -16 in breast cancer have been shown to downregulate Bcl-2 expression and trigger apoptosis [65]. In MDA-MB-231 breast cancer cells, miR-15a expression was found to be significantly low and upregulation inhibited cell growth and induced G1 cell cycle arrest [63].

MiR-34a is also regarded as a tumour suppressor in human cancer and is often lowly expressed as well. Low miR-34a expression has been correlated with poor overall survival in triple negative breast and lung cancer patients, and with metastasis in breast cancer cells [66, 67]. Notably, the upregulation of miR-34a expression is associated with disease-free survival in cancer [60], promotion of apoptosis and cell cycle arrest in osteosarcoma [68], and sensitisation of MC7/ADR cells to doxorubicin treatment [69].
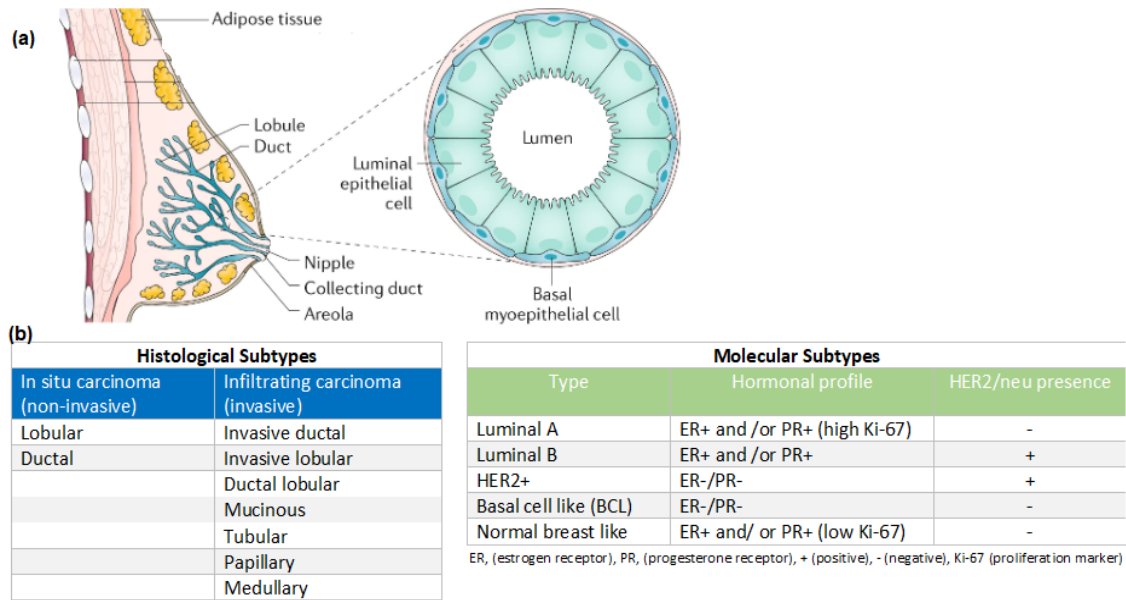
MiRNA such as miR-21 and miR-155 promote cancer progression by inhibiting expression of tumour suppressor genes and are classified as miRNA oncogenes (oncomiRs) [59]. OncomiRs are often overexpressed and exhibit oncogenic activity in human cancer [70]. In addition, downregulation of miR-21 and miR-155 has been shown to correlate with upregulation of proapoptotic *Bid* of Bcl-2 family, caspase-9, increased apoptosis and reduced cell proliferation in cancer cells [71].

1.6 Breast Cancer

1.6.1 Definition and classification

Breast cancer is a complex heterogeneous disease resulting from uncontrolled division and proliferation of the cells lining the mammary glands and ducts [58]. Histologically, breast cancer is broadly classified as either non-invasive (carcinoma *in situ*, which is further subdivided as ductal or lobular), or invasive (infiltrating carcinoma, subtypes include; invasive ductal, invasive lobular, ductal lobular, mucinous, tubular, papillary and medullary) [72]. In keeping with this, over the past 10 years, breast cancer treatment strategies have evolved into more biologically specific therapies, and hence increasingly, the molecular heterogeneity of the disease is now incorporated into a classification scheme [73]. Recent molecular classifications divide breast carcinomas into five groups; luminal A, luminal B, HER-2, basal cell-like and normal breast-like, based on the expression of oestrogen receptor (ER), progesterone receptor

(PR), and the amplification of human epidermal growth factor receptor 2 (HER2/neu) (Figure 2) [74].

(b)

Histological Subtypes	
In situ carcinoma (non-invasive)	Infiltrating carcinoma (invasive)
Lobular	Invasive ductal
Ductal	Invasive lobular
	Ductal lobular
	Mucinous
	Tubular
	Papillary
	Medullary

Molecular Subtypes		
Type	Hormonal profile	HER2/neu presence
Luminal A	ER+ and /or PR+ (high Ki-67)	-
Luminal B	ER+ and /or PR+	+
HER2+	ER-/PR-	+
Basal cell like (BCL)	ER-/PR-	-
Normal breast like	ER+ and/ or PR+ (low Ki-67)	-

ER, (estrogen receptor), PR, (progesterone receptor), + (positive), - (negative), Ki-67 (proliferation marker)

Figure 5. Histological and molecular subtypes of breast cancer. The anatomy of the breast (a) highlights the features implicated in the classification (lobule, duct, luminal epithelial cell, and basal myoepithelial cell). The tables (b) show different subtypes of breast carcinoma (Adapted from (Harbeck et al. 2019 [75]).

1.6.2 Classification of breast cancer according to stage and tumour grade

Identifying the stage of breast cancer and tumour grade is vital for prognosis and establishing effective treatment plans. Breast cancer is classified into five anatomic stages ranging from stage 0 to stage IV, according to the TNM staging system (Table 1), as reported by the American Joint Committee on Cancer (AJCC) [76]. The TNM system can be applied for most types of cancer and describes tumour size (T), lymph node involvement (N) and distant metastasis (M) [72]. Tumour grading classifies the tumours according to the degree of cell abnormality and differentiation as they appear under the microscope. In breast carcinoma the grades are as following; G1-low grade with relatively normal-appearing, well-differentiated cells, G2-moderate differentiation and G3-high grade, poorly differentiated with more abnormally appearing cells [77]. This grading serves as a prognostic tool in predicting how aggressively the tumour will grow and spread.

Table 1. Breast cancer staging according to the American Joint Committee on Cancer (AJCC)

TNM staging system			
Stage 0	Tis	N0	M0
Stage I A	T1	N0	M0
Stage I B	T0	N1mi	M0
	T1	N1mi	M0
Stage II A	T0	N1	M0
	T1	N1	M0
	T2	N0	M0
Stage II B	T2	N1	M0
	T3	N0	M0
Stage III A	T0	N2	M0
	T1	N2	M0
	T2	N2	M0
	T3	N1	M0
	T3	N2	M0
Stage III B	T4	N0	M0
	T4	N1	M0
	T4	N2	M0
Stage III C	Any T	N3	M0
Stage IV	Any T	Any N	M1

T0 = no primary tumour, Tis = carcinoma in situ, T1 = Tumour ≤ 2cm, T2 = Tumour >2cm but ≤5cm, T3 = Tumour >5cm, N0 = No regional lymph node metastases, N1mi = Micro-metastases, N1 = Metastases to movable ipsilateral level I and/or level II axillary lymph nodes, N2 = Metastases to fixed or matted ipsilateral level I and/or level II axillary lymph nodes, N3 = Metastases to ipsilateral level III axillary lymph nodes with/out level I, II axillary lymph nodes involvement, M0 = absence of distant metastasis, M1 = Distant metastasis [76].

1.6.3 Types of breast cancer cell lines for in vitro studies

Mechanistic studies on the efficacy of a new therapeutic intervention using molecules, pharmaceutical drugs, or plant-derived compounds in breast cancer and other diseases, routinely employ *in vitro* testing using specific cell lines as part of the evaluation strategy [78]. Breast cancer cell lines, such as the MCF- 7, have proven to be useful tools for these studies and can be classified according to their molecular subtype, as illustrated in Table 2.

Table 2. Molecular classification of breast cancer cell lines [79]

Cell line	Classification	Hormonal profile
MCF-7	Luminal A	ER^+, $PR^{+/-}$, $HER2^-$
BT474	Luminal B	ER^+, $PR^{+/-}$, $HER2^-$
MDA-MB-453	Luminal	ER^-, PR^-, $HER2^+$
SUM 190	Basal	ER^-, PR^-, $HER2^-$
MDA-MB-231	Basal B	ER^-, PR^-, $HER2^-$
HCC1569	Basal A	ER^-, $PR^{+/-}$, $HER2^+$

ER, (oestrogen receptor), PR, (progesterone receptor), HER2, (Human epidermal growth factor 2) + (positive), - (negative)

1.6.4 Breast cancer epidemiology

According to WHO, breast cancer is the most common cancer in women, with 2.1 million new cases recorded in 2018 globally (approximately one new case per second) and an estimated 627 000 deaths [80]. The incidence of breast cancer is estimated at about 1-in-8 women over a lifetime and is expected to increase steadily with human development [73]. Breast cancer incidence varies regionally across the world, with higher-income areas presenting higher rates *viz*. 92 per 100 000 in North America, and 27 per 100 000 in lower-income regions (Eastern Asia and Middle Africa). However, mortality is higher in low- and middle-income regions [81]. The difference in prevalence between population groups has been attributed to diet, age, genes, ethnicity, lifestyle, among other breast cancer risk factors, as well as the availability and access to resources for early detection [81].

1.7 Therapeutic approaches in cancer

Generally, treatment approaches depend on the type and stage of cancer at the time of first discovery. Currently utilised methods of treatments comprise of surgery, radiotherapy, chemotherapy, hormone therapy, immunotherapy, gene therapy, targeted therapy among many others, used in combination or alone. However, the most commonly used treatments for cancer includes surgery, radiotherapy and chemotherapy [82]. Surgery involves the surgical removal of part or entire tumour mass from a body part and is mostly effective in localised primary tumours, either alone or in combination with radiotherapy or chemotherapy [83]. In breast cancer, breast-conserving surgery has become an established approach in early-stage breast cancer, which involves excision of the tumour (lumpectomy), as opposed to complete removal of the breast (mastectomy) [84]. Breast-conserving surgery is usually preceded or followed by some combination of chemotherapy, radiation or endocrine-therapy to reduce the tumour size as well as ensure minimal risk of metastases and full recovery [85, 86]. The disadvantages of surgery include inability to completely eradicate the peripheral parts of tumours and increased risk of induced acceleration of tumour and metastatic growth as a result of the inflammatory response to surgical trauma [87, 88].

Radiotherapy is based on the use of high energy radiation to kill cancer cells by preventing cell division and proliferation through DNA damage [89]. Radiotherapy is commonly used in combination with surgery, administered after surgical tumour excision to reduce the risk of relapse [90]. Radiation sensitivity is inherently different for each tumour type, with lymphomas being the most sensitive, followed by breast and lung cancer as moderately sensitive, then osteosarcoma and melanoma with poor sensitivity [89]. The disadvantages of radiotherapy include non-selective killing of healthy cells in the peripheries of the tumour masses, limited therapeutic efficacy for distant metastases and progressive tumour radio-resistance [91].

Chemotherapy is regarded as the most effective and widely used systemic treatment for most types of cancers [92]. Chemotherapy employs the use of cytostatic and cytotoxic chemotherapeutic drugs to kill cancer cells by inhibiting growth or halting cell progression and inducing apoptosis [92]. Numerous chemotherapeutic drugs have been explored in cancer treatment including platinum-based (cisplatin), anthracyline-based (doxorubicin, epirubicin and daunorubicin) and paclitaxel-based (Taxol® and Abraxane®) chemotherapies, and combination chemotherapies such as doxorubicin and cyclophosphamide followed by

paclitaxel used in breast cancer therapy [88, 93, 94]. However, due to non-specificity, chemotherapeutic drugs target both cancer cells and healthy cells resulting in numerous adverse side effects such as anaemia, nausea, vomiting and hair loss [95]. Therefore, there remains a need to identify new therapeutic approaches with minimal side effects and enhanced target specificity. Plant-derived drugs have recently gained recognition as alternative cancer treatment options with minimal side effects [24]. An important strategy is the use of nanotechnology in drug development, which offers delivery systems with improved bioavailability and target specificity. Hence, the evaluation of plant-derived compounds using nanotechnology could offer promising alternative treatment options for cancer.

1.7.1 The therapeutic use of medicinal plants and plant-derived compounds in cancer

The increasing development of resistance to treatment, coupled with nonspecific toxicity of traditional chemotherapies poses significant drawbacks in cancer treatment [96]. In light of this, plant-derived compounds have attracted considerable interest as chemotherapeutic and chemopreventive agents in cancer treatment [78]. Plant-derived compounds are typically perceived as non-toxic to healthy cells and are a source of novel molecules for drug discovery [24]. For centuries, plants have been utilized by humanity as medicines and therapies for numerous diseases including cancer, with approximately 60% of current cancer treatments being derived from natural sources [3]. In China, traditional herbal medicine is widely accepted as a form of alternative treatment for cancer and over 400 herbal variants have been registered in the Chinese Herbal registry for cancer therapeutic use [82, 97]. In Africa, where the affordability of modern cancer medicine is a key factor, many cancer patients still rely on readily available plant-derived drugs for their healthcare [98]. Notably, a significant number of new anticancer agents originating from African plants have been tested in clinical trials, for example; curcumin isolated from *Curcuma longa* L (turmeric commonly found in Asia and Africa) and perillyl alcohol isolated from *Lavandula X intermedia* essential oils, which is widely distributed in South and North Africa [99].

Plant-derived compounds have been shown to exhibit potent anti-proliferative and proapoptotic properties against various types of cancers and modulate multiple signalling pathways [100]. Examples include curcumin, a polyphenolic compound, shown to inhibit tumour progression and metastasis in various cancers through suppressing the expression of transcription factor

NF-$_K$B [101]. Moreover, phase II clinical trials of curcumin in pancreatic cancer patients demonstrated significant tumour regression with no toxic effects [99].

Quercetin, a flavonoid, was shown to inhibit proliferation of lung, colon, prostate and breast cancer cells, and induce apoptosis and cell cycle arrest through modulating various pathways [8]. Berberine, an alkaloid, was shown to effect cell cycle arrest at different phases in tumour cells through upregulation of miR-23a, which induces overexpression of cell cycle regulating proteins such as CIP1/p21 and Kip1/p27 and downregulates expression of cyclin-dependent kinases [102]. Epigallocatechin-3-gallate (EGCG), a green tea polyphenol, was shown to promote apoptosis through increasing the *Bax/Bcl-2* ratio, inhibiting the activation of NF-$_K$B and activating caspases [103]. Among cancer therapeutics, two classes of plant-derived compounds, alkaloids and polyphenols are predominant [6]. In this study, we focus on one class of polyphenols identified as flavonoids.

1.7.2 Flavonoids: Classification, structure and therapeutic use in cancer

1.7. 2.1 Classification

Flavonoids constitute the largest group of polyphenolics and are characterised by a C_6-C_3-C_6 basic carbon skeleton [104]. They naturally occur in a variety of plants and are correlated with a plethora of health benefits and low systemic toxicity. Structurally, flavonoids are divided into various classes including flavones, flavanones, flavanols, flavonols, anthocyanidins and isoflavonoids (Figure 6) [5].
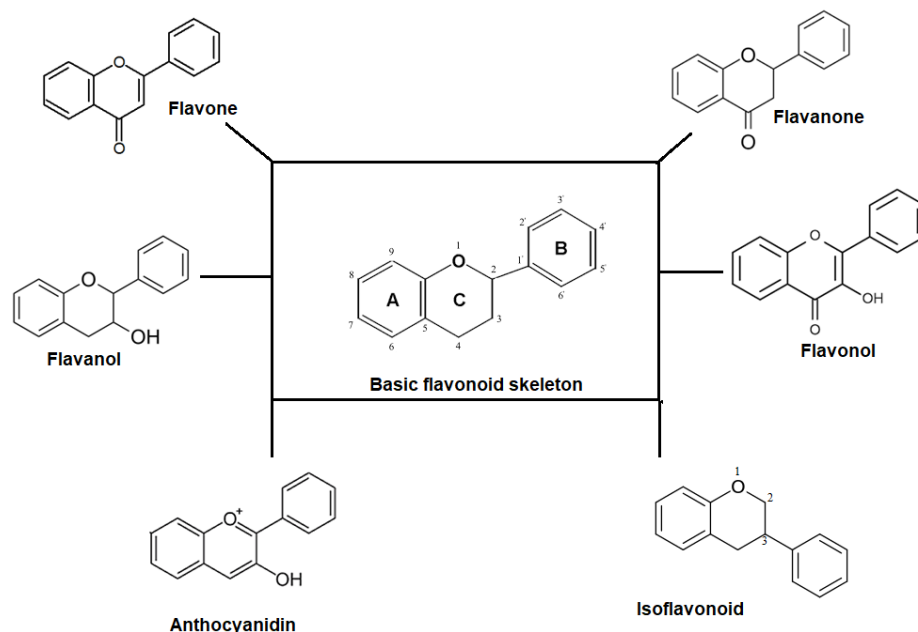
Figure 6. Classification of flavonoids. Classification of flavonoids into six groups; flavone, flavonol, flavanone, flavonol, anthocyanidin and isoflavonoid, based on differences in the molecular structure from the basic flavonoid skeleton, see review by Abotaleb et al. 2019 [5].

1.7.2.2 Structure

The structural variations of flavonoids have been reported to influence their biological activities. These distinctive variations are usually observed in the C-ring, with the presence or absence of a double bond at position 2, OH substitution at position 3 and/or carbonyl at position 4. In the A and B rings, differences occur in the number and position of -OH or -OCH$_3$ substitutions; and the presence of glycol moiety usually in the A ring [104]. Previous studies comparing the cytotoxic effects of 23 structurally different flavonoids in MCF-7, MDA-MB231, and prostate cancer cell lines, demonstrated that the presence of 2,3 double bond enhanced cytotoxicity [105]. Flavones, with B-ring hydroxyl group substitution and a double bond in the C-ring, proved to be potent proteasome inhibitors and inducers of apoptosis in tumour cells [106]. Furthermore, methoxylation in the A-ring showed strong antiproliferative activity in cancer cells treated with the flavonoids, nobiletin and sinensetin [107].

1.7.2.3 Therapeutic use in cancer

A growing number of epidemiological studies indicate that a high intake of dietary flavonoids is correlated with lower incidence of various cancers, including breast cancer [108]. Several *in vitro* and *in vivo* studies have demonstrated the ability of flavonoids to inhibit cell proliferation, invasion and metastasis, and promote cell cycle arrest and apoptosis, and modulate molecular events in carcinogenesis [109]. As discussed before, cancer cells may become resistant to chemotherapeutic treatment, resulting in tumour propagation and metastasis. Flavonoids have been shown to halt the propagation of resistant cells by promoting cell death or re-sensitising the cancer cells to chemotherapeutic treatments [110].

Flavones possessing a 2,3 double bond and hydroxyl groups, such as apigenin and luteolin, found in spinach and aromatic flowering plants, respectively, have shown anticancer activity in human breast, prostate and colorectal cancer [5, 110]. With luteolin and apigenin, inhibition of PI3K/Akt and activation of the fork-head box protein, resulted in the induction of apoptosis and cell cycle arrest in MCF-7 and TNBC cells [108]. Luteolin was shown to exhibit apoptotic efficacy in MCF-7 through activation of the caspase cascade, PARP inactivation, cytochrome *c* release, and inhibition of *Bcl-2* expression [111]. Combination treatment of apigenin and cisplatin enhanced cytotoxic and apoptotic effects in MCF-7 through modulation of tumour suppressor p53 [112], and in prostate cancer stem cells through downregulating anti-apoptotic *Bcl-2*, *survivin* and *sharpin* expression, and upregulating pro-apoptotic caspase-8 and p53 expression [113]. Through blockage of the signal transducer and activator of transcription 3, apigenin reversed drug resistance in adriamycin-resistant breast cancer cells (MCF-7/ADR) [114].

Flavanones, characterised by the absence of a double bond at position 2 in the C-ring, include hesperidin, aglycone hesperetin and naringenin, which are abundantly distributed in citrus fruits [115]. Hesperetin and naringenin are the most studied citrus flavonoids while studies on hesperidin are minimal. Hesperetin exerted pro-apoptotic effects in MDA-MB-231 and MCF7 cells through the intrinsic mitochondrial pathway [5]. Hesperidin was shown to induce phosphatidyl-serine externalisation, activation of caspases, the release of cytochrome *c,* collapse of mitochondrial membrane potential, and increases *Bax*: *Bcl-2* ratio to promote proapoptotic effects in breast cancer cells [116]. Hesperidin was also found to reduce cell proliferation and promote G2/M phase cell cycle arrest in gallbladder cancer cells [117].

Naringenin exhibited antiproliferative effects through modulation of Bcl-2 family genes, activation of caspases, cell cycle arrest in G0/G1 phase, activation of extrinsic and intrinsic apoptotic pathways, impairment of glucose uptake and induction of mitochondrial dysfunction in a wide range of human cancer cells including breast cancer [115].

Naturally occurring flavonoids have proven to be potent agents in cancer treatment and prevention, however, owing to their varying bioavailability and poor systemic delivery, their success in clinical use is affected and limited [108]. Therefore, there is an urgent need to explore different options to improve their bioavailability and develop effective drug delivery systems.
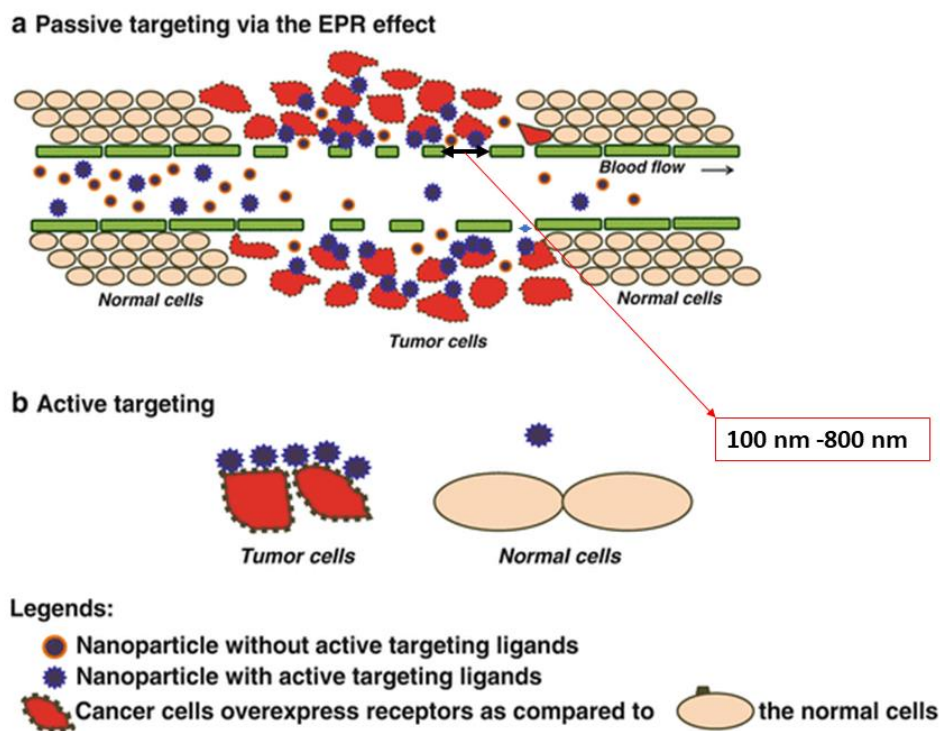
1.7.3 Nanoencapsulated plant-derived compounds in cancer therapeutic strategies

Nanoencapsulation can offer an attractive alternative approach for improving putative therapeutic properties of plant-derived compounds such as bioavailability, stability, and site-specific targeted and controlled delivery in cancer. Nanoencapsulation is a technique that encompasses encapsulating or entrapping bioactive compounds into a nanoscale carrier or system of a size range of 1-1000 nm [118]. The nanocarrier preserves the bioactive compound from premature gastrointestinal degradation, improves therapeutic efficacy, solubility, and bioavailability of the bioactive compound due to the increased surface area per unit volume, and increases compound accumulation into the target cancer cell [119]. Furthermore, nanocarriers can be fine-tuned for optimised therapeutic effect through adjusting their size and shape, alternating their chemical composition and modifying their surface properties such as surface charge, surface coating or PEGylation, and attaching functional groups or targeting moieties [120].

Various nanocarriers such as nanoemulsions, solid lipid nanocarriers, liposomes, polymeric micelles dendrimers, and many others have been developed and are currently being optimised for improved drug delivery systems. Lack of site-specific delivery is among the major drawbacks of current chemotherapies and clinically used anti-cancer compounds [3]. Nanoencapsulation enables preferential accumulation of the active drug at the diseased site through passive or active targeting. *In vitro* drug delivery into the intracellular target site can be achieved through endocytosis (internalisation through engulfment). Endocytosis can be activated through selective binding of ligands, attached on the nanosystems, onto the cell surface receptors or through non-selective binding based on electrostatic interactions [121]. *In*

vivo, the tumour vasculature is characterised by an irregular structural network with immature, tortuous, leaky and hyperpermeable vessels [122]. In addition to the aberrant vessels, tumours also have acidic microenvironments (low pH in comparison to healthy cells) and lack lymphatic drainage [123]. This unique morphology of solid tumours allows for passive drug delivery (Figure 7). Depending on the tumour type, the tumour endothelial cell lining gaps can be enlarged up to 70 times more than normal endothelium (700 nm tumour endothelium *vs.* 10 nm normal endothelium) [120]. Hence, drugs delivered in nano-systems due to their size and the leaky vasculature, and lack of lymphatic drainage can selectively accumulate and be retained in the tumour site through the enhanced permeability and retention effect (EPR) [124].

The acidic pH (range 6.5 - 6.8) of the solid tumours is also exploited for passive delivery of drugs by the use of nano-systems with acidic pH-responsive transition as part of their physicochemical properties [123]. Likewise, surface coating of nanocarriers with poly (ethylene glycol) PEG enhances stealth properties, prolongs systemic circulation time, and enhances the accumulation of encapsulated drugs to the tumour site through passive targeting [125]. Active targeting involves affinity-based recognition of receptors on the target cell surface by biological ligands conjugated to the drug-loaded nanosystems, resulting in selective drug accumulation at the tumour site [126]. Receptors overexpressed on cancer cell surfaces include HER2, epidermal growth factor receptor (EGFR), folate, integrins, and transferrin. Moieties used as target ligands include proteins, carbohydrates, monoclonal antibodies, vitamins and peptides [127].

a Passive targeting via the EPR effect

Blood flow →

Normal cells

Tumor cells

Normal cells

100 nm -800 nm

b Active targeting

Tumor cells

Normal cells

Legends:
- Nanoparticle without active targeting ligands
- Nanoparticle with active targeting ligands
- Cancer cells overexpress receptors as compared to the normal cells

Figure 7. Schematic representation of (a) passive and (b) active targeting for drug delivery in solid tumours. In passive targeting nanoparticles selectively accumulate at the tumour site through the enhanced permeability and retention effect (EPR). However, in active targeting, nanoparticles exploit both the EPR effect and selective binding of the active ligands conjugated to their surface to overexpressed receptors on the tumour cell surface (Upponi & Torchilin 2014 [128]).

Incorporation of plant-derived compounds into nanocarriers have shown great potential in improving their efficacy in cancer treatment. For example, the encapsulation of epigallocatechin-3-gallate (EGCG), a green tea derived polyphenol, into polymeric nanosystems resulted in ten-fold drug-dose advantage in exerting pro-apoptotic and antiangiogenic effects against prostate cancer in contrast to free EGCG [129]. Quercetin-loaded solid lipid nanoparticles demonstrated an increased apoptotic index in comparison to free quercetin in MCF-7 breast cancer cells [130]. Similarly, kaempferol-loaded mucoadhesive nanoemulsions exhibited decreased cell viability in contrast to free kaempferol, and induced apoptosis in glioma cells [131]. Together, this evidence shows the potential of nanosystems to circumvent the drawbacks of using unmodified bioactive compounds and existing chemotherapeutics in cancer treatment.

1.8 *Eriocephalus africanus*

Eriocephalus africanus is an evergreen, aromatic, indigenous plant widely distributed in the south-western Cape region of South Africa. *E. africanus* is commonly known as '*wild rosemary,*' owing to its leaf morphology (Figure 8) being similar to that of culinary rosemary (*Rosmarinus officinalis* L); however, it is a member of the Asteraceae family and genus *Eriocephalus* [132].

Taxonomy
Family: Asteraceae
Genus: *Eriocephalus*
Species: *Eriocephalus africanus*
Common name: *Wild rosemary*

Figure 8. *Eriocephalus africanus*, of the family Asteraceae, commonly known as 'wild rosemary,' (a) shows the aerial view of *wild rosemary* and (b) close-up morphology of the plant [132].

1.8.1 Traditional use, biological activity and phytochemical constituents

Traditionally, *E. africanus* is used to treat dermal diseases, heart conditions and inflammation. Infusions of this plant are used in herbal remedies such as diuretics and the treatment of gastrointestinal disorders, as well as coughs and fever [133]. However, despite its acclaimed ethnomedicinal uses, only a few scientific studies report on its antioxidant [134] and antibacterial properties [135]. Currently, there are no reports on the anticancer properties of *E. africanus*, although several plants from its family (Asteraceae) have been reported to possess anti-carcinogenic abilities [136]. The phytochemical constituents of the Asteraceae family

include polyphenols, alkaloids and terpenes including sesquiterpene, possessing numerous disease curative and preventive properties [137].

1.9 Problem statement

Cancer, including breast cancer, continues to be one of the leading causes of death worldwide. Despite the considerable advances made in the treatment of cancer over the past two decades, existing therapies have demonstrated several drawbacks, including low bioavailability, adverse side effects, non-selective toxicity to healthy cells, development of chemoresistance and lack of target specificity, in some cases. In light of these drawbacks, the development of alternative efficient therapeutics with minimal toxicity is needed in the treatment of cancer. Plant-derived molecules are emerging as potential alternative treatment options with typically low toxicity. Moreover, the incorporation of phytochemicals into novel nano-drug systems is showing significant enhancement in their efficacy, bioavailability and target specificity. It is within this context that this study was conducted, to investigate the potential of *Eriocephalus africanus*, a medicinal plant, with little scientific validation despite belonging to a family (Asteraceae) with well recognised anticarcinogenic abilities.

1.10 Aim

The aim of this study was to isolate and characterise phytocompounds from *Eriocephalus africanus* L., investigate their effects on cytotoxicity, cell cycle progression, apoptotic and epigenetic control in breast cancer using human breast adenocarcinoma cell lines (MCF-7) and develop nanosystems for their encapsulation, which were evaluated for safety and efficacy as anticancer agents against MCF-7.

Objectives

- To isolate, characterise and identify the secondary metabolites from the methanolic extract of *E. africanus* using column chromatography and spectroscopic techniques (IR, MS and NMR)
- To screen for potential anticancer activity of the isolated compounds *via* the MTT assay

- To determine the cytotoxicity of the selected compounds against MCF-7 at varying concentrations and duration *via* the MTT assay
- To evaluate the apoptotic activity and effect on cell cycle progression of the selected compounds using flow cytometric techniques
- To determine the effect of the phytocompounds on expression of key apoptotic mRNA and miRNA using quantitative Real-Time PCR
- To synthesise lipid-based nanosystems for the selected phytocompounds
- To evaluate the physicochemical properties of the synthesised nanosystems in terms of surface morphology, polydispersity index (PDI), zeta potential (ZP), encapsulation efficiency and *in vitro* drug release
- To determine the safety of the synthesised nanosystems through *in vitro* cytotoxicity against non-cancerous human embryonic kidney cells (HEK 293) and haemolytic studies
- To evaluate their efficacy and anticancer therapeutic potential in breast cancer using MCF-7 cell lines

1.11 Novelty of the study

This study is among the first in providing a scientific basis for the medicinal properties of *E. africanus*. It demonstrates the potential of the plant as a source of flavonoids as well as the potential of plant-derived flavonoids and flavonoid-loaded nanosystems for the development of alternative treatments targeting the apoptotic pathway in breast cancer.

1.12 Thesis overview

The research findings of this study are presented in this thesis in the form of research manuscripts:

Chapter one: Provides the introduction with a brief background to the study and a literature review focusing on topics relevant to the study. The problem statement, aim and objectives are also outlined in this chapter.

Chapter two: **Manuscript one -** Highlights the isolation of phytochemicals from the methanolic extract of *E. africanus*, the spectroscopic characterisation of the isolated compounds and the preliminary screening for their anticancer activity. This chapter is a first-authored experimental article published in the ISI accredited journal, Natural Product Research.

Chapter three: **Manuscript two -** Reports the effects of isolated flavonoids on the apoptotic and cell cycle machinery in MCF-7, and their effect on expression of key apoptotic miRNA. This study is a first-authored experimental article currently under revision by the ISI accredited Journal of Biomolecular Structure and Dynamics (corrections submitted).

Chapter four: **Manuscript three -** Details the synthesis of novel hesperidin-loaded nanoemulsions (HP-NEM), presents the physicochemical properties of HP-NEM, safety evaluations and highlights the potential of HP-NEM as cytotoxic agents and inhibitors of oncomirs miR-21 and miR-155 expression in breast cancer cell lines. This study is a first-authored experimental article under review in the ISI accredited Journal of Drug Targeting.

Chapter five: Provides the synthesis and overall conclusions of the research findings from this study. Recommendations for further research are also summarised.

REFERENCES

[1]   Lewandowska AM, Rudzki M, Rudzki S, et al. Environmental risk factors for cancer –
        review paper. Annals Agric Environ Med Institute of Rural Health 2019; 26(1):1–7.

[2]   Hassanpour SH, Dehghani M. Review of cancer from perspective of molecular. J
        Cancer Res Pract Medknow 2017; 4(4):127–29.

[3]   Khan T, Gurav P. PhytoNanotechnology: Enhancing delivery of plant based anti-cancer
        drugs. Front Pharmacol 2018; 8:1002.

[4]   All cancers excl. non-melanoma skin cancer. WHO factsheet http://gco.iarc.fr/today

[5]   Abotaleb M, Samuel SM, Varghese E, et al. Flavonoids in cancer and apoptosis.
        Cancers (Basel) 2019; 11(1).

[6]   Sun LR, Zhou W, Zhang HM, et al. Modulation of multiple signaling pathways of the
        plant-derived natural products in cancer. Front Oncol 2019; 9: 1153.

[7]   Ahmad R, Ahmad N, Naqvi AA, et al. Role of traditional Islamic and Arabic plants in
        cancer therapy. J Trad Complementary Medicine 2017; 7 (7):195-204.

[8]   Tang SM, Deng XT, Zhou J, et al. Pharmacological basis and new insights of quercetin
        action in respect to its anti-cancer effects. Biomed Pharmacother 2020; 121:109604.

[9]   Glodkowska-Mrowka E, Stoklosa T. Next generation sequencing in oncology. In:
        Clinical applications for Next-Generation Sequencing. Elsevier Inc 2016; pp. 63–74.

[10]   Mitra S, Ganguli S, Chakrabarti J. Introduction. In: Cancer and noncoding RNAs.
        Elsevier 2018; pp. 1–23.

[11]   Rashid S, Rashid S. Classification of cancer. In: Cancer and chemoprevention: An
        overview. Springer, Singapore 2017; pp. 15–16.

[12]   Bukhtoyarov Oleg V, Samarin DM. Pathogenesis of cancer: Cancer reparative trap. J
        Cancer Ther 2015; 6:399–412.

[13]   Cullen JM, Breen M. An overview of molecular cancer pathogenesis, prognosis, and
        diagnosis. Tumors Domest Anim 2016; 1–26.

[14] Rather RA, Bhagat M. Cancer chemoprevention and piperine: Molecular mechanisms and therapeutic opportunities. Front. Cell Dev Biol 2018; 6:10.

[15] Basu AK. DNA damage, mutagenesis and cancer. Int J Mol Sci 2018; 19: 970.

[16] Siddiqui IA, Sanna V, Ahmad N, et al. Resveratrol nanoformulation for cancer prevention and therapy. Ann N Y Acad Sci 2015; 1348(1):20–31.

[17] Kolat D, Kaluzinska Z, Bednarek AK, Pluciennik E. The biological characteristics of transcription factors AP-2α and AP-2γ and their importance in various types of cancers. Biosci Rep 2019; 39**:** BSR20181928.

[18] Siemann DW, Horsman MR. Modulation of the tumor vasculature and oxygenation to improve therapy. Pharmacol Ther 2015; 153: 107–124.

[19] Harman Saman SSR, Rasul SU and K. Inducing angiogenesis, a key step in cancer vascularization, and treatment approaches. Cancers (Basel) 2020; 12:1172.

[20] Zuazo-Gaztelu I, Casanovas O. Unraveling the role of angiogenesis in cancer ecosystems. Front Oncol 2018; 2(8):248.

[21] An W, Lai H, Zhang Y, et al. Apoptotic pathway as the therapeutic target for anticancer traditional Chinese medicines. Front Pharmacol 2019; 10:758.

[22] Hassan M, Watari H, AbuAlmaaty A, et al. Apoptosis and molecular targeting therapy in cancer. Biomed Res 2014; 2014:150845.

[23] Bell RAV, Megeney LA. Evolution of caspase-mediated cell death and differentiation: Twins separated at birth. Cell Death Differ 2017; 24:1359–1368.

[24] Pfeffer CM, Singh ATK. Apoptosis: A target for anticancer therapy. Int J Mol Sci 2018; 19(2).

[25] Namura S. Neuroprotectants: Cell-Death based. In: Primer on cerebrovascular diseases: Second Edition, Elsevier Inc 2017; pp. 189–92.

[26] Kale J, Osterlund EJ, Andrews DW. BCL-2 family proteins: Changing partners in the dance towards death. Cell Death Differ 2018; 25; 65–80.

[27] Peña-Blanco A, García-Sáez AJ. Bax, Bak and beyond — mitochondrial performance in apoptosis. FEBS J 2018; 285(3):416–31.

[28]   Wong RS. Apoptosis in cancer: from pathogenesis to treatment. J Exp Clin Cancer Res 2011; 30(1):87.

[29]   Campbell KJ, Tait SWG. Targeting BCL-2 regulated apoptosis in cancer. Open Biol 2018; 8(5):180002.

[30]   McIlwain DR, Berger T, Mak TW. Caspase functions in cell death and disease. Cold Spring Harb Perspect Biol Cold Spring Harbor Laboratory Press 2013; 5(4):1–28.

[31]   McComb S, Chan PK, Guinot A, et al. Efficient apoptosis requires feedback amplification of upstream apoptotic signals by effector caspase-3 or -7. Sci Adv American Association for the Advancement of Science 2019; 5(7): eaau9433.

[32]   Algeciras-Schimnich A, Barnhart BC, Peter ME. Apoptosis dependent and independent functions of caspases. In: Madame Curie Bioscience Database Austin (TX): Landes Bioscience; 2000- 2013. https://www.ncbi.nlm.nih.gov/books/NBK6198/

[33]   Xu X, Lai Y, Hua ZC. Apoptosis and apoptotic body: disease message and therapeutic target potentials. Biosci Rep 2019; 39(1): BSR20180992.

[34]   Lee J, Park SH, Lee J, et al. Differential effects of luteolin and its glycosides on invasion and apoptosis in MDA-MB-231 triple-negative breast cancer cells. EXCLI J Leibniz Research Centre for Working Environment and Human Factors 2019; 18:750–63.

[35]   Fulda S, Debatin K-M. Caspase activation in cancer therapy Landes Bioscience 2013; In: Madame Curie Bioscience Database [Internet]. Austin (TX): Landes Bioscience; 2000-2013. Available from: https://www.ncbi.nlm.nih.gov/books/NBK6027/

[36]   Jan R, Chaudhry G e. S. Understanding apoptosis and apoptotic pathways targeted cancer therapeutics. Adv Pharm Bull 2019; 9(2): 205-218.

[37]   Baig S, Seevasant I, Mohamad J, et al. Potential of apoptotic pathway-targeted cancer therapeutic research: Where do we stand? Cell Death Dis 2016; 7(1): e2058.

[38]   Mohammad RM, Muqbil I, Lowe L, et al. Broad targeting of resistance to apoptosis in cancer. Semin Cancer Biol 2015; 35: S78–S103.

[39]   Um HD. Bcl-2 family proteins as regulators of cancer cell invasion and metastasis: A review focusing on mitochondrial respiration and reactive oxygen species. Oncotarget 2016; 7(5).

[40] Inao T, Iida Y, Moritani T, et al. Bcl-2 inhibition sensitizes triple-negative human breast cancer cells to doxorubicin. Oncotarget 2018; 9(39):25545–56.

[41] Zhou QM, Sun Y, Lu YY, et al. Curcumin reduces mitomycin C resistance in breast cancer stem cells by regulating Bcl-2 family-mediated apoptosis. Cancer Cell Int BioMed Central Ltd 2017; 17(1):84.

[42] Wen M, Deng Z, Jiang S, et al. Identification of a novel Bcl-2 inhibitor by ligand-based screening and investigation of its anti-cancer effect on human breast cancer cells. Front Pharmacol 2019; 10:391.

[43] Perri M, Yap JL, Fletcher S, et al. Therapeutic potential of bcl-xl/mcl-1 synthetic inhibitor jy-1-106 and retinoids for human triple-negative breast cancer treatment. Oncol Lett 2018; 15(5):7231–36.

[44] Fernald K, Kurokawa M. Evading apoptosis in cancer. Trends Cell Biol 2013; 23(12): 620–633.

[45] Peng Y, Croce CM. The role of microRNAs in human cancer. Transduct Target Ther 2016; 1:15004.

[46] Jayamohan S, Kannan M, Moorthy RK, et al. Dysregulation of miR-375/AEG-1 Axis by human papillomavirus 16/18-E6/E7 promotes cellular proliferation, migration, and invasion in cervical cancer. Front Oncol 2019; 9:847.

[47] Weber TS, Jaehnert I, Schichor C, et al. Quantifying the length and variance of the eukaryotic cell cycle phases by a stochastic model and dual nucleoside pulse labelling. PLoS Comput Biol Public Library of Science 2014; 10(7): e1003616.

[48] Introduction to the cell cycle. In: Cell Biology. Elsevier 2017; pp. 697–711.

[49] Orth JD, Loewer A, Lahav G, et al. Prolonged mitotic arrest triggers partial activation of apoptosis, resulting in DNA damage and p53 induction. Mol Biol Cell American Society for Cell Biology 2012; 23(4):567–76.

[50] Surova O, Zhivotovsky B. Various modes of cell death induced by DNA damage. Oncogene 2013; 32(33):3789-97.

[51] Mills CC, Kolb EA, Sampson VB. Development of chemotherapy with cell-cycle inhibitors for adult and pediatric cancer therapy. Cancer Res 2018; 78(2):320-325.

[52] Benarba B, Elmallah A, Pandiella A. *Bryonia dioica* aqueous extract induces apoptosis and G2/M cell cycle arrest in MDA-MB 231 breast cancer cells. Mol Med Rep 2019; 20(1):73–80.

[53] Kwan YP, Saito T, Ibrahim D, et al. Evaluation of the cytotoxicity, cell-cycle arrest, and apoptotic induction by *Euphorbia hirta* in MCF-7 breast cancer cells. Pharm Biol 2015; 54(7):1–14.

[54] Liu S min, Ou S yi, Huang H hua. Green tea polyphenols induce cell death in breast cancer MCF-7 cells through induction of cell cycle arrest and mitochondrial-mediated apoptosis. J Zhejiang Univ Sci B Zhejiang University Press 2017; 18(2):89–98.

[55] Wu H, Chen L, Zhu F, et al. The cytotoxicity effect of resveratrol: Cell cycle arrest and induced apoptosis of breast cancer 4T1 Cells. Toxins (Basel) MDPI AG 2019; 11(12):731.

[56] Si W, Shen J, Zheng H, et al. The role and mechanisms of action of microRNAs in cancer drug resistance. Clin Epigenet 2019; 11:25.

[57] Su Z, Yang Z, Xu Y, et al. MicroRNAs in apoptosis, autophagy and necroptosis. Oncotarget 2015; 6(11):8474-90.

[58] Loh HY, Norman BP, Lai KS, et al. The regulatory role of microRNAs in breast cancer. Int. J Mol Sci 2019; 20(19):4940.

[59] Hemmatzadeh M, Mohammadi H, Jadidi-Niaragh F, et al. The role of oncomirs in the pathogenesis and treatment of breast cancer. Biomed Pharmacother 2016; 78:129–39.

[60] Zhang L, Liao Y, Tang L. MicroRNA-34 family: A potential tumor suppressor and therapeutic candidate in cancer. J Exp Clin Cancer Research 2019; 38:53.

[61] Zhang L, Zhou L, Shi M, et al. Downregulation of miRNA-15a and miRNA-16 promote tumor proliferation in multiple myeloma by increasing CABIN1 expression. Oncol Lett 2018; 15(1):1287–96.

[62] M. JR. Functions and epigenetic aspects of miR-15/16: Possible future cancer therapeutics. Gene Reports 2018;12: 149-164.

[63] Luo Q, Li X, Li J, et al. MiR-15a is underexpressed and inhibits the cell cycle by targeting CCNE1 in breast cancer. Int J Oncol 2013; 43(4):1212–18.

[64] Huang N, Wu J, Qiu W, et al. MiR-15a and miR-16 induce autophagy and enhance chemosensitivity of Camptothecin. Cancer Biol Ther 2015; 16(6):941–48.

[65] Jiang X, Liu Y, Zhang G, et al. Aloe-Emodin induces breast tumor cell apoptosis through upregulation of miR-15a/miR-16-1 that suppresses BCL2. Evid Based Complement Alternat Med 2020; 51082982020.

[66] Zeng Z, Chen X, Zhu D, et al. Low expression of circulating microRNA-34c is associated with poor prognosis in triple-negative breast cancer. Yonsei Med J Yonsei University College of Medicine 2017; 58(4):697–702.

[67] Zhao K, Cheng J, Chen B, et al. Circulating microRNA-34 family low expression correlates with poor prognosis in patients with non-small cell lung cancer. J Thorac Dis 2017; 9(10):3735–46.

[68] Gang L, Qun L, Liu WD, et al. MicroRNA-34a promotes cell cycle arrest and apoptosis and suppresses cell adhesion by targeting DUSP1 in osteosarcoma. Am J Transl Res 2017; 9(12):5388–99.

[69] Park EY, Chang ES, Lee EJ, et al. Targeting of miR34a-NOTCH1 axis reduced breast cancer stemness and chemoresistance. Cancer Res American Association for Cancer Research Inc 2014; 74(24):7573–82.

[70] Sharma S, Patnaik PK, Aronov S, et al. ApoptomiRs of breast cancer: Basics to clinics. Front Genet 2016; 7:175.

[71] Zadeh MM, Motamed N, Ranji N, et al. Silibinin-induced apoptosis and downregulation of microRNA-21 and MicroRNA-155 in MCF-7 human breast cancer cells. J Breast Cancer Korean Breast Cancer Society 2016; 19(1):45–52.

[72] Eliyatkin N, Yalcin E, Zengel B, et al. Molecular classification of breast carcinoma:from traditional, old-fashioned way to a New Age, and a New Way. J Breast Heal 2015; 11(2):59–66.

[73] Harbeck N, Gnant M. Breast cancer. The Lancet Seminar 2017; 389(10074)1134-1150.

[74] Al-thoubaity FK. Molecular classification of breast cancer: A retrospective cohort study. Ann Med Surg 2020; 49:44–48.

[75] Harbeck N, Penault-Llorca F, Cortes J, et al. Breast cancer. Nat Rev Dis Prim 2019; 5(1):1–31.

[76] Kalli S, Semine A, Cohen S, et al. American Joint Committee on cancer's staging system for breast cancer, Eighth Edition: What the Radiologist needs to know. RadioGraphics Radiological Society of North America Inc 2018; 38(7):1921–33.

[77] Dimitropoulos K, Barmpoutis P, Zioga C, et al. Grading of invasive breast carcinoma through Grassmannian VLAD encoding. PLoS One 2017; 12(9): e0185110.

[78] Murad H, Hawat M, Ekhtiar A, et al. Induction of G1-phase cell cycle arrest and apoptosis pathway in MDA-MB-231 human breast cancer cells by sulfated polysaccharide extracted from Laurencia papillosa. Cancer Cell Int 2016; 16:39.

[79] Liu W, Xu J, Wu S, et al. Selective anti-proliferation of HER2-positive breast cancer cells by anthocyanins identified by High-Throughput Screening. PLoS One 2013; 8(12): e81586.

[80] WHO | Breast cancer. WHO World Health Organization 2018; https://www.who.int/cancer/prevention/diagnosis-screening/breast-cancer/en/

[81] Momenimovahed Z, Salehiniya H. Epidemiological characteristics of and risk factors for breast cancer in the world. Breast Cancer: Targets and Therapy. Dov Med Press 2019; 11:151–164.

[82] Xiang Y, Guo Z, Zhu P, et al. Traditional Chinese medicine as a cancer treatment: Modern perspectives of ancient but advanced science. Cancer Med 2019; 8(5):19581975.

[83] Dare AJ, Anderson BO, Sullivan R, et al. Surgical services for cancer care. The International Bank for Reconstruction and Development / The World Bank 2015; https://www.ncbi.nlm.nih.gov/books/NBK343623/ doi: 10.1596/978-1-4648-0349-9_ch13

[84] Bellavance EC, Kesmodel SB. Decision-making in the surgical treatment of breast cancer: Factors influencing women's choices for mastectomy and breast conserving surgery. Front Oncol 2016; 6:74.

[85] Fajdic J, Djurovic D, Gotovac N, et al. Criteria and procedures for breast conserving surgery. Acta Inform Medica The Academy of Medical Sciences of Bosnia and Herzegovina 2013; 21(1):16–19.

[86] Nounou MI, Elamrawy F, Ahmed N, et al. Breast cancer: Conventional diagnosis and treatment modalities and recent patents and technologies supplementary issue: Targeted therapies in breast cancer treatment. Breast Cancer Basic Clin Res 2015; 9:17–34.

[87] Tohme S, Simmons RL, Tsung A. Surgery for cancer: A trigger for metastases. Cancer Res 2017; 77(7):1548-1552.

[88] Hu Q, Sun W, Wang C, et al. Recent advances of cocktail chemotherapy by combination drug delivery systems. Adv Drug Deliv Rev 2016; 98:19-34.

[89] Hosseinzadeh E, Banaee N, Nedaie HA. Cancer and treatment modalities. Curr Cancer Ther Rev 2017; 13(1).

[90] Jarosz-Biej M, Smolarczyk R, Cichoń T, Kułach N. Tumor microenvironment as a "Game Changer" in cancer radiotherapy. Int J Mol Sci 2019; 20(13):3212.

[91] Huang C-Y, Ju D-T, Chang C-F, et al. A review on the effects of current chemotherapy drugs and natural agents in treating non–small cell lung cancer. BioMedicine EDP Sciences 2017; 7(4):23.

[92] Abbas Z, Rehman S. An overview of cancer treatment modalities. In: Neoplasm. InTech 2018; DOI: 10.5772/intechopen.76558.

[93] Moo T, Sanford R, Dang C, et al. Overview of breast cancer therapy. PET Clin 2018; 13(3):339–54.

[94] Wang F, Porter M, Konstantopoulos A, et al. Preclinical development of drug delivery systems for paclitaxel-based cancer chemotherapy. J Control Release 2017; 267:100–18.

[95] Sak K. Chemotherapy and dietary phytochemical agents. Chemother Res Pract 2012; 2012:11.

[96] Habtemariam S, Lentini G. Plant-derived anticancer agents: Lessons from the pharmacology of geniposide and its aglycone, genipin. Biomedicines 2018; 6(2):39.

[97] Liu W, Yang B, Yang L, et al. Therapeutic effects of ten commonly used chinese herbs and their bioactive compounds on cancers. 2019; DOI: 10.1155/2019/6057837

[98] Alves-Silva JM, Romane A, Efferth T, et al. North African medicinal plants traditionally used in cancer therapy. Front Pharmacol 2017; 8:383.

[99] Osafo N, Boakye YD, Agyare C, et al. African plants with antiproliferative properties. In: Natural products and cancer drug discovery. InTech 2017; DOI:

10.5772/intechopen.68568.

[100] Pucci C, Martinelli C, Ciofani G. Innovative approaches for cancer treatment: Current perspectives and new challenges. Ecancermedicalscience 2019; 13:961.

[101] Shanmugam M, Rane G, Kanchi M, et al. The multifaceted role of curcumin in cancer prevention and treatment. Molecules MDPI 2015; 20(2):2728–69.

[102] Zhang C, Sheng J, Li G, et al. Effects of berberine and its derivatives on cancer: A systems pharmacology review. Front Pharmacol 2019; 10:1461.

[103] Liu C, Li P, Qu Z, et al. Advances in the antagonism of epigallocatechin-3-gallate in the treatment of digestive tract tumors. Molecules MDPI AG 2019; 24(9).

[104] Dayem AA, Choi HY, Yang GM, et al. The anti-cancer effect of polyphenols against breast cancer and cancer stem cells: Molecular mechanisms. Nutrients 2016; 8(9).

[105] Chang H, Mi M, Ling W, et al. Structurally related cytotoxic effects of flavonoids on human cancer cells in vitro. Arch Pharm Res 2008; 31(9):1137–44.

[106] Menezes JCJMDS, Orlikova B, Morceau F, et al. Natural and synthetic flavonoids: Structure–activity relationship and chemotherapeutic potential for the treatment of leukemia. Crit Rev Food Sci 2016; 56: S4–28.

[107] Zhang J, Wu Y, Zhao X, et al. Chemopreventive effect of flavonoids from Ougan (Citrus reticulata cv. Suavissima) fruit against cancer cell proliferation and migration. J Funct Foods 2014; 10:511–19.

[108] Sudhakaran M, Sardesai S, Dose AI. Flavonoids: New frontier for immuno-regulation and breast cancer control. Antioxidants 2019; 8(4):103.

[109] Obakan-Yerlikaya P, Arisan ED, Coker-Gurkan A, et al. Breast cancer and flavonoids as treatment strategy. In: Breast cancer - From biology to medicine. InTech 2017; DOI: 10.5772/66169

[110] Ye Q, Liu K, Shen Q, et al. Reversal of multidrug resistance in cancer by multifunctional flavonoids. Front Oncol 2019; 9:487.

[111] Park SH, Ham S, Kwon TH, et al. Luteolin induces cell cycle arrest and apoptosis through extrinsic and intrinsic signaling pathways in MCF-7 breast cancer cells. J Environ Pathol Toxicol Oncol 2014; 33(3):219–31.

[112] Liu R, Ji P, Liu B, et al. Apigenin enhances the cisplatin cytotoxic effect through p53modulated apoptosis. Oncol Lett 2017; 13(2):1024–30.

[113] Erdogan S, Turkekul K, Serttas R, et al. The natural flavonoid apigenin sensitizes human CD44+ prostate cancer stem cells to cisplatin therapy. Biomed Pharmacother 2017; 88:210–17.

[114] Seo HS, Ku JM, Choi HS, et al. Apigenin overcomes drug resistance by blocking the signal transducer and activator of transcription 3 signaling in breast cancer cells. Oncol Rep 2017; 38(2):715–24.

[115] Cirmi S, Ferlazzo N, Lombardo G, et al. Chemopreventive agents and inhibitors of cancer hallmarks: May citrus offer new perspectives? Nutrients MDPI AG 2016; 8(11):698.

[116] Aggarwal V, Tuli HS, Thakral F, et al. Molecular mechanisms of action of hesperidin in cancer: Recent trends and advancements. Exp Biol Med 2020; 245(5):486-497.

[117] Pandey P, Sayyed U, Tiwari RK, et al. Hesperidin induces ROS-mediated apoptosis along with cell cycle arrest at G2/M phase in human gallbladder carcinoma. Nutr Cancer Routledge 2019; 71(4):676–87.

[118] Rahim RA, Jayusman PA, Muhammad N, et al. Recent advances in nanoencapsulation systems using PLGA of bioactive phenolics for protection against chronic diseases. Int J Environ Res Public Health 2019; 16(24).

[119] Khan H, Ullah H, Martorell M, et al. Flavonoids nanoparticles in cancer: Treatment, prevention and clinical prospects. Semin Cancer Biol 2019; S1044-579X (19):30182-8.

[120] Din FU, Aman W, Ullah I, et al. Effective use of nanocarriers as drug delivery systems for the treatment of selected tumors. Int J Nanomedicine 2017; 12:7291–7309.

[121] Sun T, Zhang YS, Pang B, et al. Engineered nanoparticles for drug delivery in cancer therapy. Angewandte Chemie - International Edition 2014,Wiley-VCH Verlag 2014; DOI:10.1002/anie.201403036

[122] Schaaf MB, Garg AD, Agostinis P. Defining the role of the tumor vasculature in antitumor immunity and immunotherapy article. Cell Death Dis 2018; 9:115.

[123] Feng L, Dong Z, Tao D, et al. The acidic tumor microenvironment: a target for smart cancer nano-theranostics. Natl Sci Rev 2018; 5:269–86.

[124] Wakaskar RR. Role of nanoparticles in drug delivery encompassing cancer therapeutics. Int J Drug Dev Res 2017; 93(93):3–4.

[125] Suk JS, Xu Q, Kim N, et al. PEGylation as a strategy for improving nanoparticle-based drug and gene delivery. Adv Drug Deliv Rev 2016; 99(Pt A):28.

[126] Yoo J, Park C, Yi G, et al. Active targeting strategies using biological ligands for nanoparticle drug delivery systems. Cancers (Basel) MDPI AG 2019; 11(5).

[127] Attia MF, Anton N, Wallyn J, et al. An overview of active and passive targeting strategies to improve the nanocarriers efficiency to tumour sites. J Pharm Pharmacol 2019; 71(8):1185–98.

[128] Upponi JR, Torchilin VP. Passive vs. Active targeting: An update of the EPR role in drug delivery to tumors. In: Alonso M., Garcia-Fuentes M. (eds) Nano-Oncologicals. Advances in Delivery Science and Technology. Springer, Cham. 2014; pp. 3–45.

[129] Sanna V, Singh CK, Jashari R, et al. Targeted nanoparticles encapsulating (-) epigallocatechin-3-gallate for prostate cancer prevention and therapy. Sci Rep 2017; 7(1):1–15.

[130] Niazvand F, Orazizadeh M, Khorsandi L, et al. Effects of Quercetin-loaded nanoparticles on MCF-7 human breast cancer cells. Med MDPI AG 2019; 55(4).

[131] Colombo M, Figueiró F, Fraga Dias A de, et al. Kaempferol-loaded mucoadhesive nanoemulsion for intranasal administration reduces glioma growth in vitro. Int J Pharm 2018; 543(1–2):214–23.

[132] Merle H, Verdeguer M, Blázquez MA, et al. Chemical composition of the essential oils from *Eriocephalus africanus* L. var. africanus populations growing in Spain. Flavour Fragr J 2007; 22(6):461–64.

[133] Catarino MD, Silva AMS, Saraiva SC, et al. Characterization of phenolic constituents and evaluation of antioxidant properties of leaves and stems of *Eriocephalus africanus*. Arab J Chem 2018; 11(1):62–69.

[134] Mohamed TA, Habib AM, ELzefzafy MM, et al. *In vitro* culture and evaluation some phytochemical compounds of *Eriocephalus africanus* L. plant. Eur Pharm Med Res 4(1):46-56.

[135] Behiry SI, EL-Hefny M, Salem MZM. Toxicity effects of *Eriocephalus africanus* L. leaf essential oil against some molecularly identified phytopathogenic bacterial strains. Nat Prod Res 2019; DOI: 10.1080/14786419.2019.1566824

[136] Panda SK, Luyten W. Antiparasitic activity in Asteraceae with special attention to ethnobotanical use by the tribes of Odisha, India. Parasite 2018; 25.

[137] Bakar F, Bahadir Acikara Ö, Ergene B, et al. Antioxidant activity and phytochemical screening of some Asteraceae plants. Turk J Pharm Sci 2015; 12(2), 123-132.

2. CHAPTER TWO: MANUSCRIPT ONE

2.1 Phytochemical constituents and *in vitro* anticancer screening of isolated compounds from *Eriocephalus africanus*

In the search for new, safe and alternative plant-derived therapeutics for the treatment and management of cancer, the study in this chapter explores the anticancer potential of the plant species, *Eriocephalus africanus*, belonging to the family Asteraceae. Literature demonstrated Asteraceae to possess numerous phytocompounds with anticancer activities; however, there are no scientific reports on the anticancer activity of this species, despite belonging to the same family. Therefore, this chapter presents a detailed investigation on the phytochemical constituents of *E. africanus* from extraction, isolation, characterisation and identification, and *in vitro* screening for anticancer potential of the extracts and isolated phytocompounds.

This chapter is formatted according to the journal specifications.

Phytochemical constituents and *in vitro* anticancer screening of isolated compounds from *Eriocephalus africanus*

Judie Magura[a], Roshila Moodley[b*], Kaminee Maduray[a] and Irene Mackraj[a]

[a]*School of Laboratory Medicine and Medical Sciences, University of KwaZulu–Natal, Durban, South Africa* [b]*School of Chemistry and Physics, University of KwaZulu–Natal, Durban, South Africa*

Abstract

This study investigated the *in vitro* anticancer potential of phytochemical constituents isolated from the methanolic extract of *Eriocephalus africanus*. One flavanone (hesperidin) and two flavones (luteolin and apigenin) were isolated for the first time from the plant using column chromatography. Standard MTT assay was used to evaluate the effect of the constituents on cell viability in MCF-7, A549, HepG2 and normal HEK 293 cell lines. The flavonoids decreased cell viability in a dose-dependent manner in all tested cell lines. Hesperidin and luteolin were more sensitive against MCF-7, with EC_{50} values of 62.57 µg/mL and 70.34 µg/mL, respectively and apigenin showed the most potent activity against HepG2 (EC_{50} = 11.93 µg/mL). The results revealed *E. africanus* to be a rich source of flavonoids and natural anticancer agents, which could potentially be used in the development of new therapeutics for cancer treatment.

Graphical Abstract
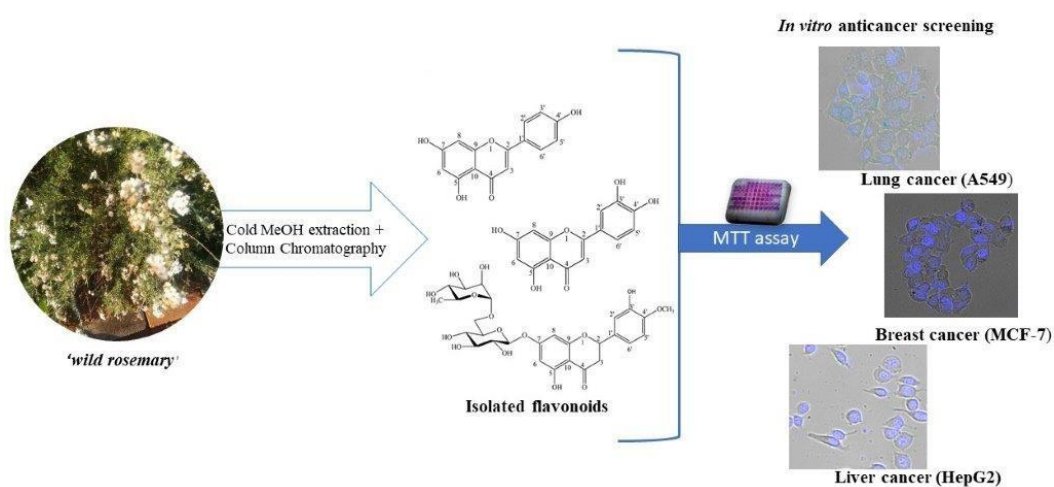
Keywords: Flavonoids; apigenin; hesperidin; luteolin; HepG2; natural products.

1. Introduction

Plant-derived 'natural' compounds have made a significant impact on modern medicine as a source for novel drug development. Currently, natural products and their derivatives account for more than half of the Food and Drug Administration (FDA) approved anticancer drugs (Sofi and Nabi 2018). These anticancer agents have reduced cell toxicity, minimized side effects and improved treatment efficacy compared to conventional methods of treatment, which include surgery, radiation, and chemotherapy (Rayan et al. 2017). Drugs of natural origin in clinical use for the treatment of various cancers include paclitaxel derived from *Taxus brevifolia* L. (pacific yew tree), Vincristine derived from *Catharanthus roseus* (L.) G. Don. (periwinkle) and epigallacotechin-3-gallate, a phenolic catechin from green tea (Cragg and Pezzuto 2016). The plant kingdom hosts a wide and diverse variety of compounds that have shown to exert anticancer activities by inducing apoptosis or autophagy, inhibiting tumour angiogenesis, and enhancing antioxidant activity (Wang et al. 2012).

Eriocephalus africanus is commonly known as '*wild rosemary*', derived from its leaf morphology, which is similar in appearance to that of rosemary (*Rosmarinus officinalis* L.); however, it is from the family Asteraceae (Merle et al. 2007). Traditionally, it is used to treat heart disease, inflammation and dermal conditions. A few studies have reported *E. africanus* to have antioxidant and antibacterial activities (Mohamed et al. 2017; Behiry et al. 2019). However, despite these preliminary reports and its use in ethnomedicine, there is still a lack of scientific knowledge regarding its chemical constituents and biological activities. This study, therefore, aims to isolate the major secondary metabolites from *E. africanus* and screen for their anticancer potential (*in vitro*) against human carcinomas namely, breast cancer (MCF-7), lung cancer (A549) and liver cancer (HepG2).

2. Results and Discussion

2.1 Characterisation of isolated compounds

The isolated compounds were identified based on spectral data (Supplementary material, Figures S1-S21) and by comparison to literature (Lahmer et al. 2015; Mohamed et al. 2015; Jadeja et al. 2017). Compound **1** identified as hesperidin (Supplementary material, Figure S22); HR-ESI-MS *m/z* 609.18 [M-H] $^+$ corresponding to $C_{28}H_{34}O_{15}$. Compound **2**, luteolin (Supplementary material, Figure S22) was obtained as a yellow powder; HR-ESI-MS *m/z*

285.04 [M-H] $^{+}$ corresponds to $C_{15}H_{10}O_6$. Compound **3** was identified as apigenin (Supplementary material, Figure S22)**,** HR-ESI-MS *m/z* 269.04 [M-H] $^{+}$ corresponds to

$C_{15}H_{10}O_5$.

2.2 Anticancer activity

The *in vitro* anticancer activity screening *via* the MTT assay showed that the ethyl acetate fraction (EtOAc) of MeOH extract prepared from *E. africanus* and their isolated compounds reduced significantly cell viability in a dose-dependent manner, with moderate cytotoxicity against the normal human embryonic kidney cell line (HEK 293) (Supplementary material, Figure S23(a)-(d)). Hesperidin and luteolin were more sensitive against MCF-7 (EC$_{50}$ of 62.57 µg/mL and 70.34 µg/mL, respectively) than HepG2 and A549. Moreover, the EtOAc showed the highest effect against MCF-7 with EC$_{50}$ of 45.47 µg/mL proving the synergistic effect of the compounds. Apigenin showed the strongest anticancer effects against HepG2 (EC$_{50}$ of 11.93 µg/mL) and reduced cell viability to at least 23% against A549 at higher concentrations (200 µg/mL). Previously, anticancer activity of natural flavonoids including apigenin, against human carcinomas, have been reported (Yan et al. 2017), and these have been consistent with this study for apigenin against HepG2.

The activity of flavonoids has been proposed to be partly linked to their structure, which consists of two benzene rings (A and B) linked by a 3-carbon heterocyclic ring (C). Previous studies have demonstrated the influence of substitution on the B-ring on the function of flavonoids as ERβ (estrogen receptor β) agonists, where the absence of substitution increased potency while substitution reduced potency (Huang et al. 2010). In another study by Krych and Gebicka (2013), it was observed that OH$^-$ substitution on the B-ring at position 4′ and 5′ enhanced the inhibitory activity of catalase enzymes (enzymes belonging to the antioxidant defence system of a cell) whereas, substitution on the B-ring at position 3′ decreased the activity. In our study, although not all the activity can be fully attributed to positional structure, significant differences in activity between hesperidin (with position 3′ substitution) and apigenin (without position 3′ substitution) were observed. Further investigation is required to conclusively investigate the effect of structure on anticancer activity in flavonoids. The anticancer activity of hesperidin, luteolin and apigenin has previously also been attributed to induction of DNA fragmentation, promotion of caspase-3 and 9 cleavage, and cell cycle arrest

at the G2/M phase through elevated levels of reactive oxygen species, respectively (Abotaleb et al. 2019).

3. Conclusion

This study revealed, for the first time, that the methanol extract of *E. africanus* was a rich source of natural flavonoids which could be potential anticancer agents, as they exhibited a significant reduction in cell viability for all the tested cancer cell lines. Furthermore, apigenin isolated from *E. africanus* produced remarkable anticancer activity against HepG2 which suggests its possible use in the development of new therapeutics against liver cancer.

Conflict of interest

The author(s) confirm that this article content has no conflict of interest.

Acknowledgements

References

Abotaleb M, Samuel SM, Varghese E, Varghese S, Kubatka P, Liskova A, Büsselberg D. 2019. Flavonoids in cancer and apoptosis. Cancers (Basel). 11.

Behiry SI, EL-Hefny M, Salem MZM. 2019. Toxicity effects of *Eriocephalus africanus* L. leaf essential oil against some molecularly identified phytopathogenic bacterial strains. Nat Prod Res. DOI: 10.1080/14786419.2019.1566824

Cragg GM, Pezzuto JM. 2016. Natural products as a vital source for the discovery of cancer chemotherapeutic and chemopreventive agents. Med. Princ. Pract. 25(suppl 2):41-59.

Huang Z, Fang F, Wang J, Wong C. 2010. Structural activity relationship of flavonoids with estrogen-related receptor gamma. FEBS Letters. 584:22-26.

Jadeja YS, Kapadiya KM, Jebaliya HJ, Shah AK, Khunt RC. 2017. Dihedral angle study in Hesperidin using NMR Spectroscopy. Magn. Reson. Chem.55:589-594.

Krych J, Gebicka L. 2013. Catalase is inhibited by flavonoids. Int. J. Biol. Macromol. 58:148153.

Lahmer N, Belboukhari N, Cheriti A, Sekkoum K. 2015. Hesperidin and hesperitin preparation and purification from *Citrus sinensis* peels. Der. Pharma. Chemica. 7(2):1-4.

Merle H, Verdeguer M, Blázquez MA, Boira H. 2007. Chemical composition of the essential oils from *Eriocephalus africanus* L. var. africanus populations growing in Spain. Flavour Fragr. J. 22:461-464.

Mohamed AAA, Melati K, Wong Keng C. 2015. Chemical constituents and antioxidant activity of *Teucrium barbeyanum* Aschers. Rec. Nat. Prod.9(1):159-163.

Mohamed TAD, Sayed Habib AME, ELzefzafy MM, Gouda T, Dawoud M, Soliman AIE. 2017. *In vitro* culture and evaluation some phytochemical compounds of *Eriocephalus africanus* L plant. Eur.Pharm. Med.Res. 4(1):46-56.

Rayan A, Raiyn J, Falah M. 2017. Nature is the best source of anticancer drugs: Indexing natural products for their anticancer bioactivity. PLoS ONE.12(11): e0187925.

Sofi MS, Nabi S. 2018. The role of phytocompounds in cancer treatment: A current review. J. Med. Plant. Stud. 6(4):83-93.

Wang H, Khor TO, Shu L, Su Z, Fuentes F, Jong-Hun L, Kong AT. 2012. Plants against cancer: A review on natural phytochemicals in preventing and treating cancers and their druggability. Anticancer Agents Med Chem. 12(10):1281-1305.

Yan X, Qi M, Li P, Zhan Y, Shao H. 2017. Apigenin in cancer therapy: anti-cancer effects and mechanisms of action. Cell Biosci.7:50.

SUPPLEMENTARY MATERIAL

Phytochemical constituents and *in vitro* anticancer screening of isolated compounds from *Eriocephalus africanus*

Judie Magura [a], Roshila Moodley [b*], Kaminee Maduray [a] and Irene Mackraj [a]

[a] *School of Laboratory Medicine and Medical Sciences, University of KwaZulu–Natal, Durban, South Africa* [b] *School of Chemistry and Physics, University of KwaZulu–Natal, Durban, South Africa*

Abstract

This study investigated the *in vitro* anticancer potential of phytochemical constituents isolated from the methanolic extract of *Eriocephalus africanus*. One flavanone (hesperidin) and two flavones (luteolin and apigenin) were isolated for the first time from the plant using column chromatography. Standard MTT assay was used to evaluate the effect of the constituents on cell viability in MCF-7, A549, HepG2 and normal HEK 293 cell lines. The flavonoids decreased cell viability in a dose-dependent manner in all tested cell lines. Hesperidin and luteolin were more sensitive against MCF-7, with EC_{50} values of 62.57 µg/mL and 70.34 µg/mL, respectively and apigenin showed the most potent activity against HepG2 (EC_{50} = 11.93 µg/mL). The results revealed *E. africanus* to be a rich source of flavonoids and natural anticancer agents, which could potentially be used in the development of new therapeutics for cancer treatment.

Keywords: Flavonoids; apigenin; hesperidin; luteolin; HepG2; natural products.

Experimental

General procedures

Infrared (IR) spectra were recorded on a Perkin Elmer Spectrum 100 FT-IR spectrometer accessorized with a universal attenuated total reflectance (ATR). Nuclear magnetic resonance (NMR) spectra (^{1}H, ^{13}C and 2D) were recorded in deuterated DMSO (Merck, Darmstadt, Germany) at room temperature on a 600 MHz spectrometer (AVANCE III, Bruker, Rheinstetten, Germany). High resolution mass spectra (HR-MS) were recorded using a timeof-flight mass spectrometer (LCT Premier TOF-MS, Waters Micro-mass, Milford, MA, USA). Column chromatography was performed using silica gel (Kieselgel 60, 0.063-0.200 mm, Merck, Darmstadt, Germany) and Sephadex LH-20 (25-100 µm bead size, Sigma-Aldrich, Germany). Thin layer chromatography (TLC) was carried out on TLC plates (Merck silica gel 60, 20× 20 cm F254 aluminum sheets), which were developed in 10% H_2SO_4 in methanol (MeOH) and viewed under an ultraviolet lamp (254 nm). Cells for seeding were counted using the Countess II FL automated cell counter (Thermofisher, Waltham, MA USA). All reagents including 3-(4,5-dimethylthiazolyl)-2,5-diphenyl-tetrazolium bromide (MTT), 2,2-diphenyl-1picrylhydrazyl (DPPH) and 5-fluorouracil (5FU) were of analytical grade and they were purchased from Sigma-Aldrich, Germany.

Plant material

Plant material was collected from St Thomas` Anglican Musgrave, Durban (Latitude 29.846514, Longitude 31.000609) during summer and was identified as *Eriocephalus africanus* by the botanist, Sandra Dell from Botanical Society of South Africa - KZN Coastal Branch. A voucher specimen (No. Magura 01) was deposited in the ward herbarium at UKZN. The collected aerial parts of the plant (leaves and stems) were initially washed using tap water then double-distilled water and allowed to air dry (during summer temperatures range from 27 $^{\text{o}}$C to 32 $^{\text{o}}$C). The dried sample was crushed into powder form using a home blender (Braun JB 5160, Kronberg im Taunus, Germany).

Preparation of the ethyl acetate from MeOH (EtOAc) extract

The dry powdered sample (1.8 kg) was successively extracted with MeOH (3 × 2500 mL) at 25 $^{\text{o}}$C for 72 h using an orbital shaker and evaporated using a rotary evaporator at 65 $^{\text{o}}$C to obtain a crude extract. The crude extract (approximately 100 mL) was dissolved in water (300 mL) and partitioned twice with an equal volume of 100 mL of ethyl acetate (EtOAc). The

obtained EtOAc fraction from the MeOH extract was evaporated to dryness using a rotary evaporator to yield 10 g then subjected to preliminary bioactivity screening *via* antioxidant assays, Figure S24.

Antioxidant activity of the ethyl acetate fraction from the methanol extract

Three assays were used to evaluate the antioxidant activity namely, DPPH radical scavenging activity, reducing power activity, and nitric oxide radical scavenging activity. The EtOAc fraction from the MeOH extract showed strong antioxidant activity (Figure S24) and was then subjected to column chromatography for the isolation of compounds. The isolated compounds were characterised using NMR, IR and HR-MS.

Isolation of phytocompounds

Guided by the antioxidant screening, the EtOAc fraction from the MeOH extract (4 g) was redissolved in MeOH and filtered using a Whatman No 8-filter paper; the residue gave compound **1** (200 mg). The filtrate was subjected to column chromatography using silica gel (Merck Kieselgel 60, 0.063-0.200 mm, 70-230 mesh ASTM) as the stationary phase and EtOAc: MeOH (10:0, 9:1, 8:2 and 7:3, v/v) as the mobile phase. Thereafter, Sephadex LH-20 was used, and elution was effected with 100% MeOH. TLC was used to monitor collected fractions and those with similar profiles were combined and recrystallised. The Sephadex column afforded compound **2** (60 mg). Compound **3** (36 mg) was obtained from fractions (21-23) eluted from the silica gel column.

Compound **1**, Figure S1-S7:

^{1}H-NMR (600 MHz, DMSO, δ_H ppm), ^{1}H-NMR (600 MHz, DMSO, δ ppm), 11.96 (s, 1H, 5OH), 6.93 (d, J = 4.20 Hz, 1H, H-2'), 6.90 (dd, J = 8.60, 4.20 Hz, 1H, H-6'), 6.89 (d, J = 8.60 Hz 1H, H-5'), 6.13(d, J = 2.41 Hz, 1H, H-8), 6.12 (s, 1H, H-6), 5.49 (dd, J = 8.60, 3.15 Hz,1H, H-2), 4.94 (d, J = 7.72 Hz, 1H, H-1"), 4.52 (d, J = 1.79 Hz, 1H, H-1'''), 3.80 (s, 3H, -OCH3), 3.20–3.60 (6H, m, H-2" to H-6"), 3.20–3.60 (3H, m, H-2''' to H-6'''), 3.31 (dd, J = 17.23, 8.52 Hz 1H, H-3a), 2.78 (dd, J =17.16, 3.00 Hz,1H, H-3b), 1.08 (d, J = 6.0 Hz, 3H, H-6''').

^{13}C NMR (600 MHz, DMSO- δ_C ppm): 197.41 (C-4), 165.52 (C-7), 163.41 (C-5), 162.8 9 (C9), 148.43 (C-4'), 146.80 (C-3'), 131.23(C-1'), 118.52(C-6'), 114.48 (C-2'), 112.51 (C-5'),

103.81(C-10), 100.90 (C-1'''), 99.89 (C-1''), 96.88 (C-6), 96.06 (C-8), 78.78 (C-2), 76.61 (C5''), 75.91 (C-2''), 73.38 (C-4'''), 72.32 (C-3''), 71.10 (C-4''), 70.66 (C-3'''), 70.06 (C-2'''), 68.72 (C-5'''), 66.39 (C-6''), 56.16 (-OCH3), 42.36 (C-3), 18.14 (-CH$_3$).

Compound **2**, Figure S8-S14:

^{1}H-NMR (600 MHz, DMSO, δ_H ppm), 12.97 (s, 1 H, 5-OH), 7.42 (d, J = 2.33 Hz, 1H, H-2'), 7.41(dd, J = 9.01, 2.33 Hz, 1H, H-6') 6.91 (d, J = 8.72 Hz, 1 H, H-5'), 6.67 (s, 1 H, H-3), 6.46 (d, J = 2.21 Hz, 1H, H-8), 6.20 (d, J = 2.25 Hz, 1H, H-6).

^{13}C NMR (600 MHz, DMSO- δ_C ppm): 182.09 (C-4), 164.99 (C-7), 164.35 (C-2), 161.88 (C-5), 157.78 (C-9), 150.38 (C-4'), 146.29 (C-3'), 121.81 (C-1'), 119.42 (C-2'), 116.53 (C-5'), 113.77 (C-6'), 103.99(C-10), 103.20(C-3), 99.40 (C-6), 94.41(C-8).

Compound **3**, Figure S15-S21:

 ^{1}H-NMR (600 MHz, DMSO, δ_H ppm), 12.87 (s, 1 H, 5-OH), 7.89 (d, J = 8.00 Hz, 2H, H-2', 6'), 6.94 (d, J = 8.80 Hz, 2H, H-3', 5'), 6.69 (d, J = 2.37 Hz,1H, H-6), 6.47 (d, J = 1.85 Hz, 1H, H-8), 6.17 (s, 1H, H-3).

^{13}C NMR (600 MHz, DMSO- δ_C ppm): 182.11 (C-4), 165.28 (C-7), 164.28 (C-2),161.74 (C5), 161.15 (C-4'), 157.86 (C-9), 128.92 (C-2', 6'), 121.63 (C-1'), 116.53 (C-3', 5'), 103.84 (C-10), 103.14 (C-6); 99.55 (C-3), 94.67 (C-8).

Anticancer activity or cytotoxicity screening

Human MCF 7, A549, HepG2 and HEK 293, originally procured from the American Tissue Culture Collection (ATCC) (Virginia, USA) were cultured in Dulbecco's modified Eagle's medium (DMEM, Biowest, USA) supplemented with 10% fetal bovine serum (FBS) and 1% penicillin or streptomycin at 37 ^{o} C and 5% CO$_2$. For the MTT assay, cells were seeded in 96well microtiter plates at 5×10^3 cells/well in 100 µL of supplemented DMEM and incubated (37 ^{o}C, 5% CO$_2$), for 16 h. The medium was removed and the test compounds, prepared by dissolving in DMSO and diluting with supplemented media to give concentration ranges of 20200 µg/mL, were added to each well (100 µL final volume). The final concentration of DMSO in each well was less than 0.5%. The wells receiving only medium served as the blank, untreated cells in supplemented DMEM as the negative control and 5-FU was used as a positive control. After 24 h of incubation with the test compounds, the medium was removed and 100 µL of fresh medium was added, followed by 20 µL of MTT (5mg/mL in PBS). The plates were

incubated for 4 h. Thereafter, the purple formazan crystals that formed were dissolved by adding 100 µL of DMSO to each well. The absorbance was measured at 560 nm using a microplate reader (SPECTROstar Nano, BMG Germany). All experiments were done in triplicate and repeated at least once for reproducibility.

Statistical analysis

Statistical analysis was carried out using the ANOVA test and the significant difference between means was tested by Tukey`s post hoc at $p < 0.05$. Measurements were conducted in triplicate and expressed as mean $\pm$ SD. The Statistical Package for the Social Sciences (PASW Statistics 24, IBM Corporation, Cornell, N.Y.) was used. The EC_{50} values were calculated using the non-linear regression dose versus response curves (GraphPad Software, La Jolla CA).

Spectral data for hesperidin, luteolin and apigenin
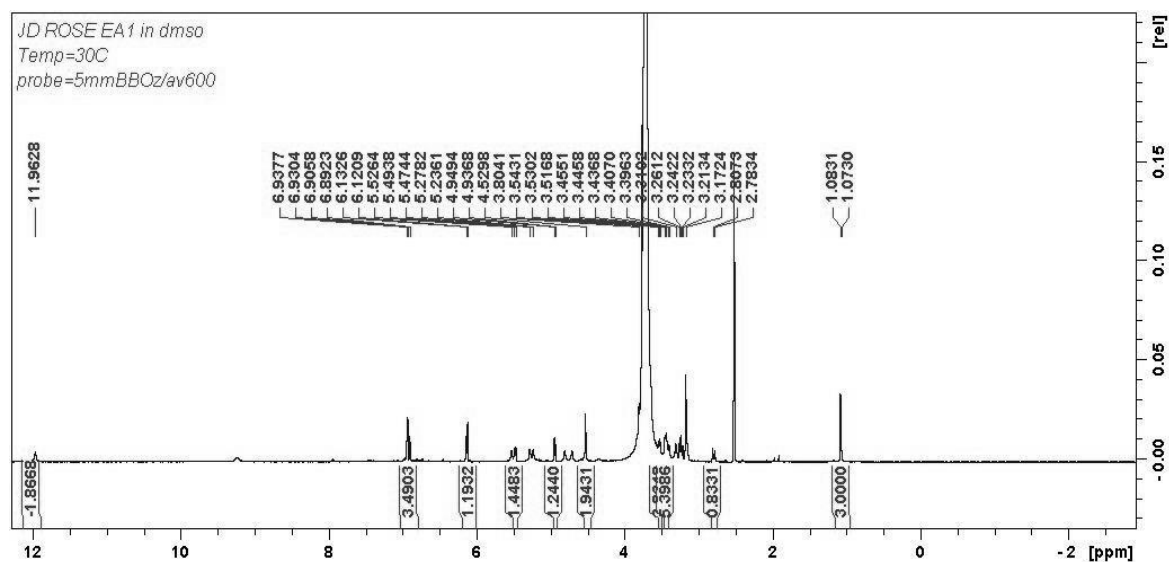
Figure S1. ^{1}H-NMR spectrum for hesperidin (**1**)
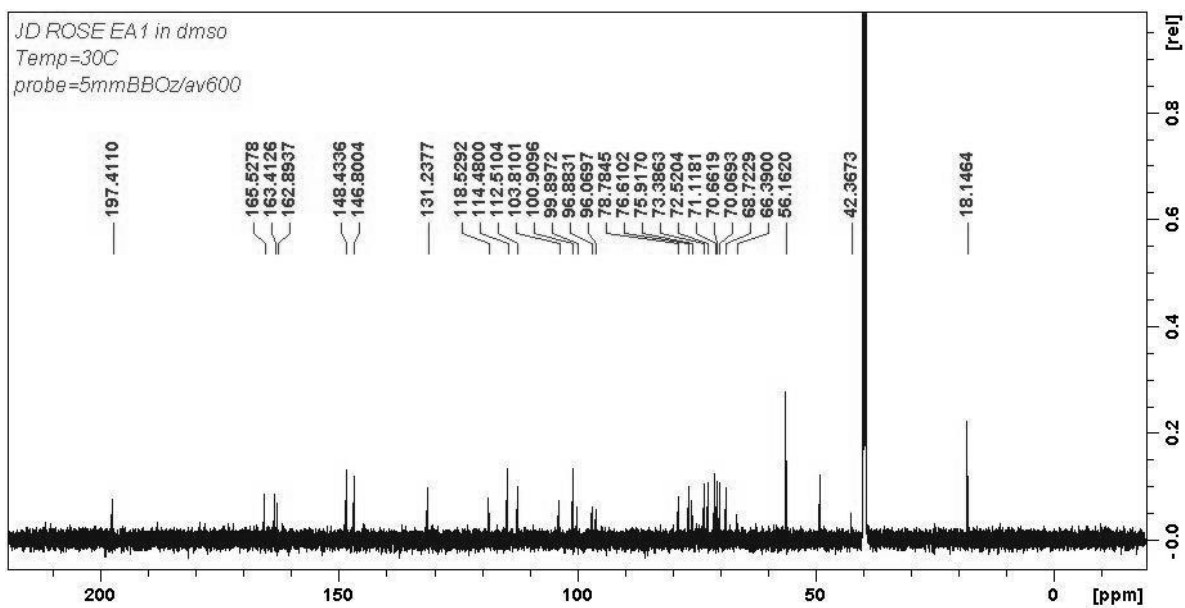
Figure S2. ^{13}C-NMR spectrum for hesperidin (**1**)
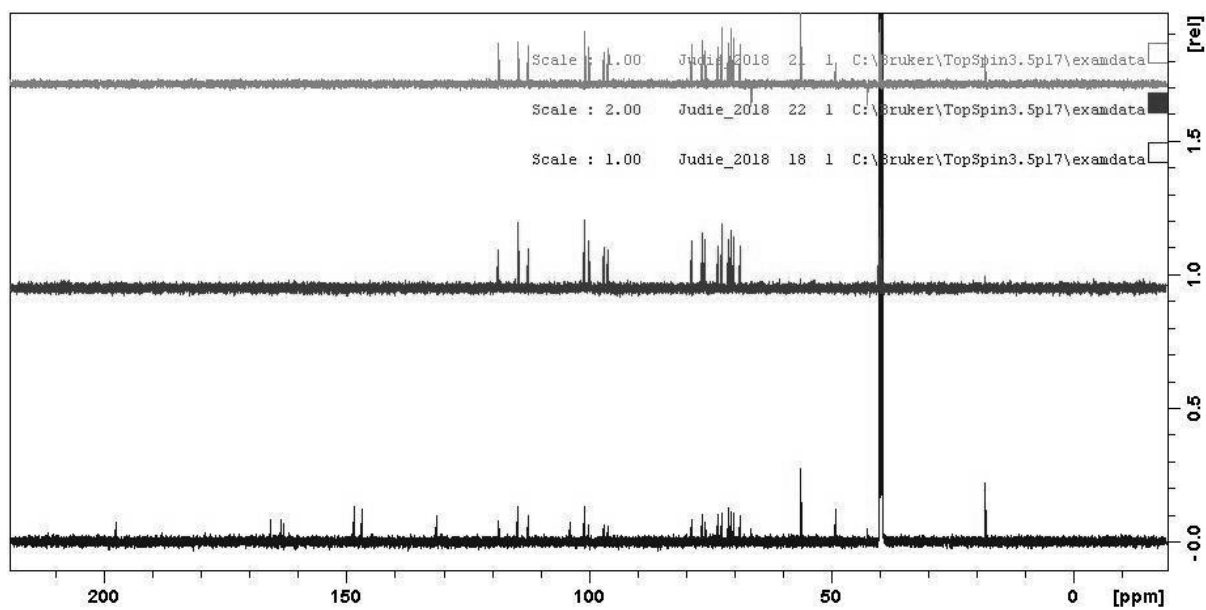
Figure S3. DEPT spectrum for hesperidin (**1**)
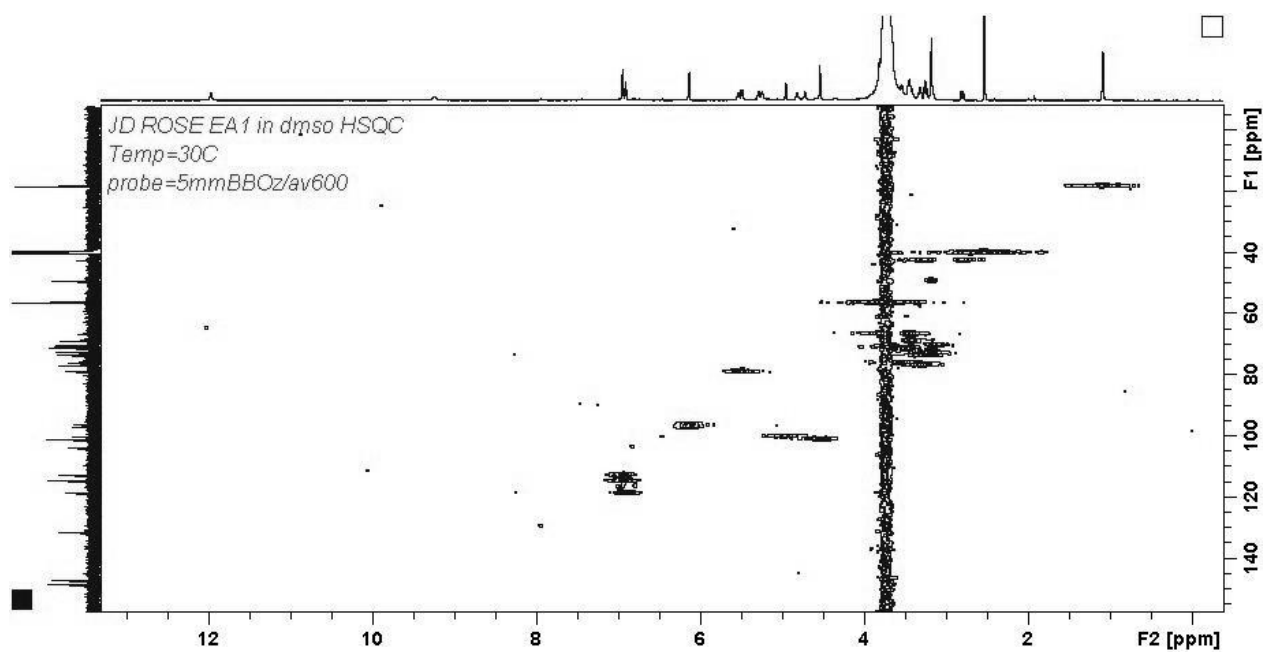
Figure S4. HSQC spectrum for hesperidin (**1**)
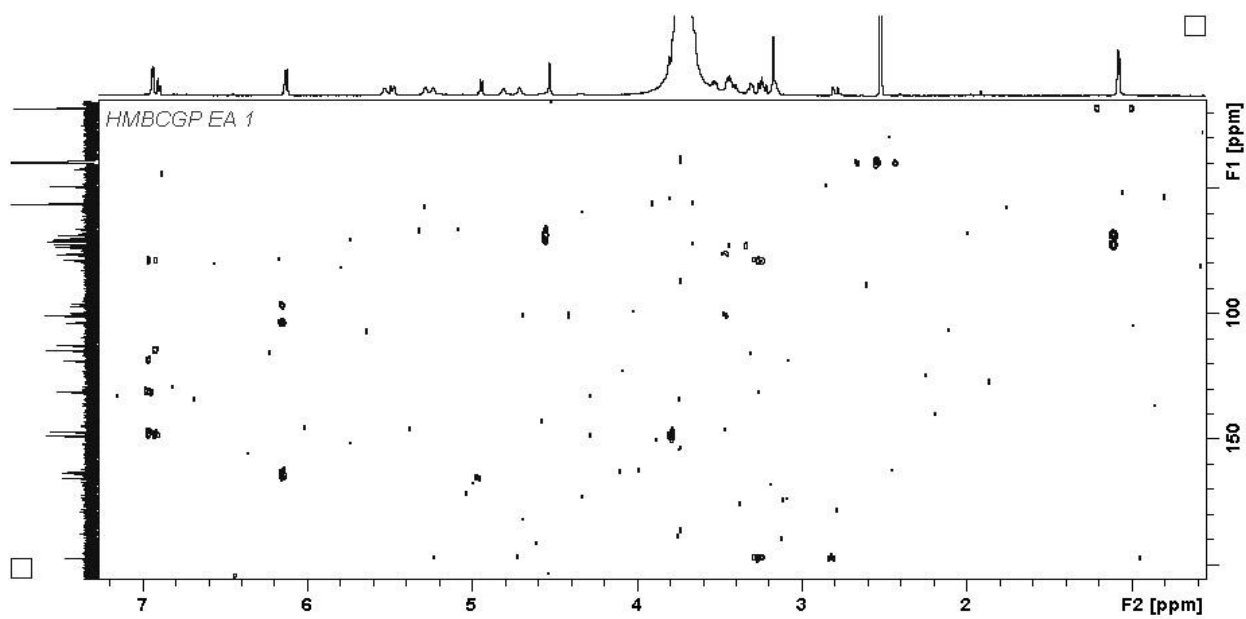
Figure S5. HMBC spectrum for hesperidin (**1**)

Single Mass Analysis
Tolerance = 5.0 PPM   /   DBE: min = -1.5, max = 500.0
Element prediction: Off
Number of isotope peaks used for i-FIT = 2

Monoisotopic Mass, Even Electron Ions
1 formula(e) evaluated with 1 results within limits (all results (up to 1000) for each mass)
Elements Used:
C: 25-30   H: 30-35   O: 10-15
EA1 2 (0.034) Cm (1:61)
TOF MS ES-

1.87e+005

Mass	Calc. Mass	mDa	PPM	DBE	i-FIT	i-FIT (Norm)	Formula
Minimum:				-1.5			
Maximum:		5.0	5.0	500.0			
609.1815	609.1819	-0.4	-0.7	12.5	12.8	0.0	C28 H33 O15
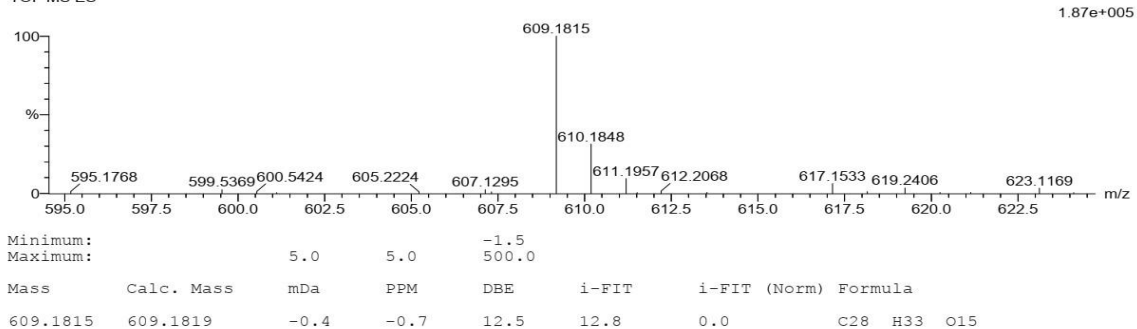
Figure S6. Mass spectrum for hesperidin (**1**)
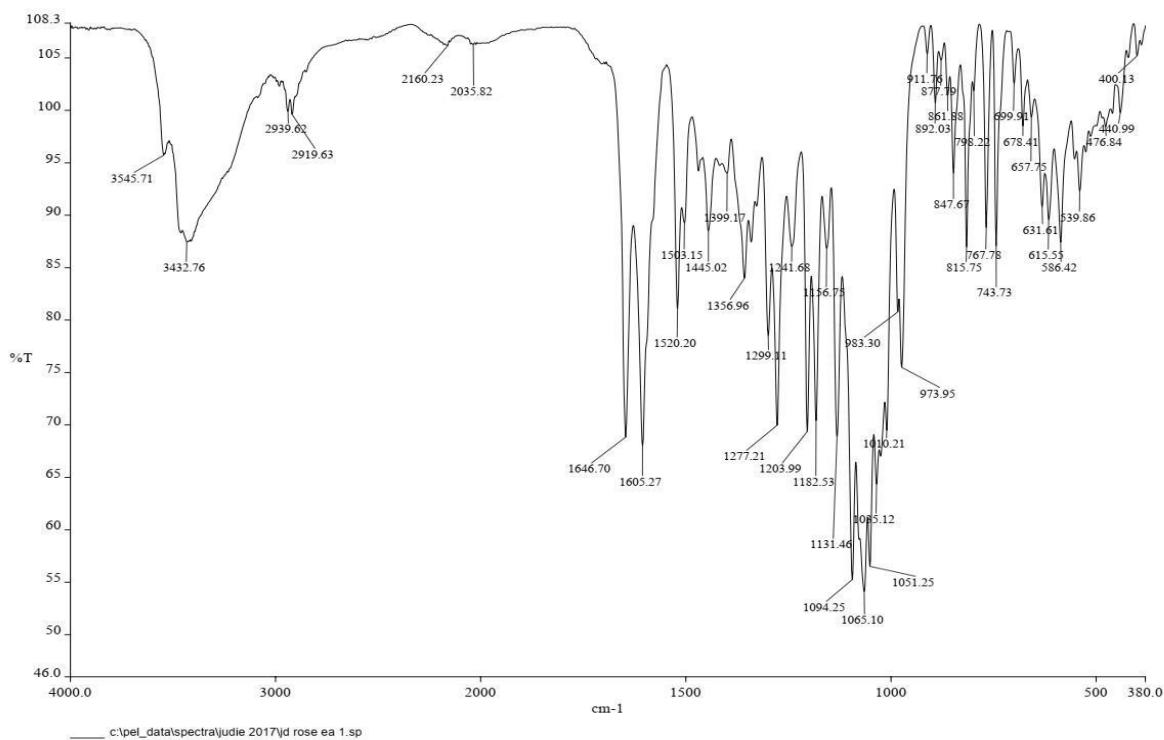
Figure S7. IR spectrum for hesperidin (**1**)
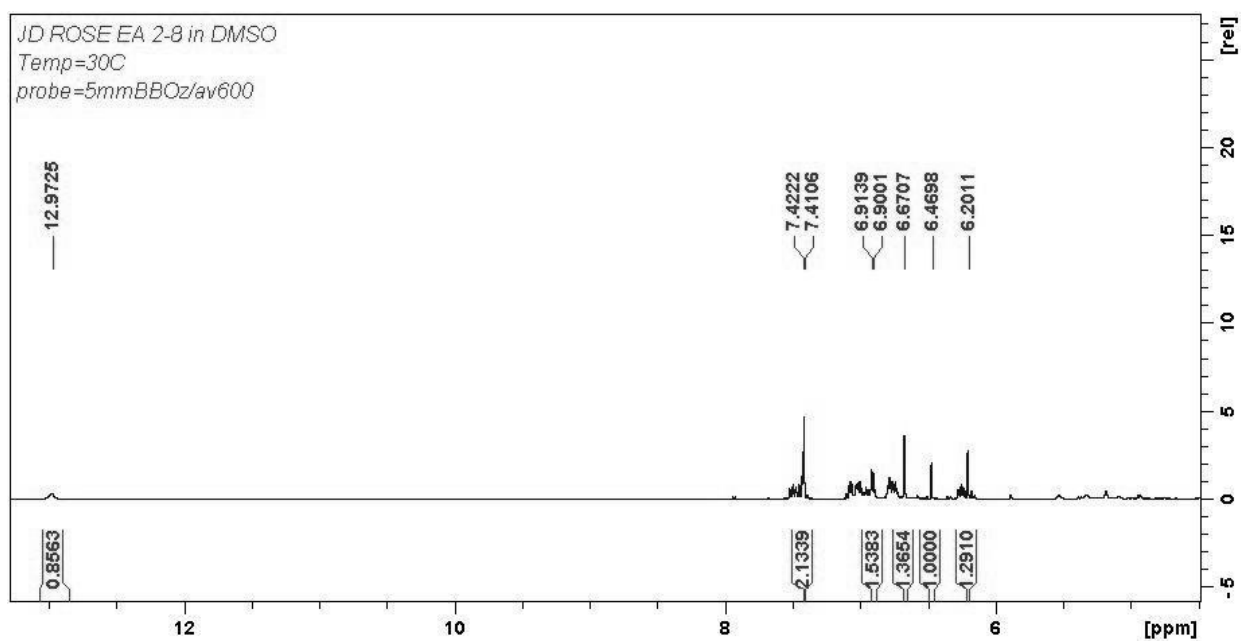
Figure S8. ^{1}H-NMR spectrum for luteolin (**2**)
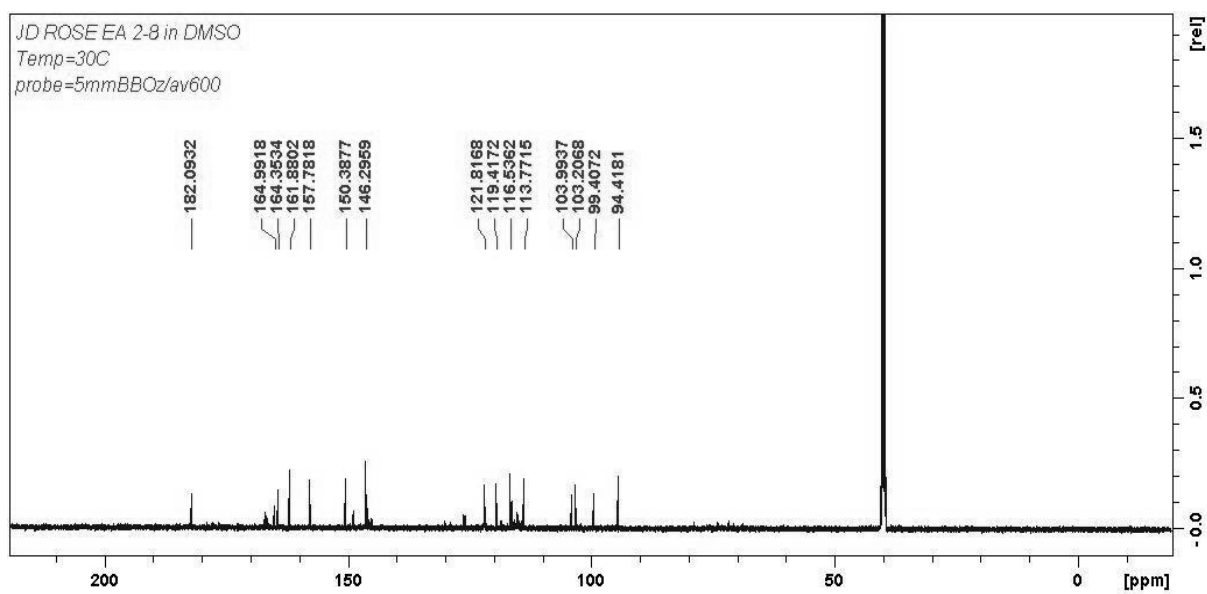
Figure S9. ^{13}C-NMR spectrum for luteolin (**2**)

53
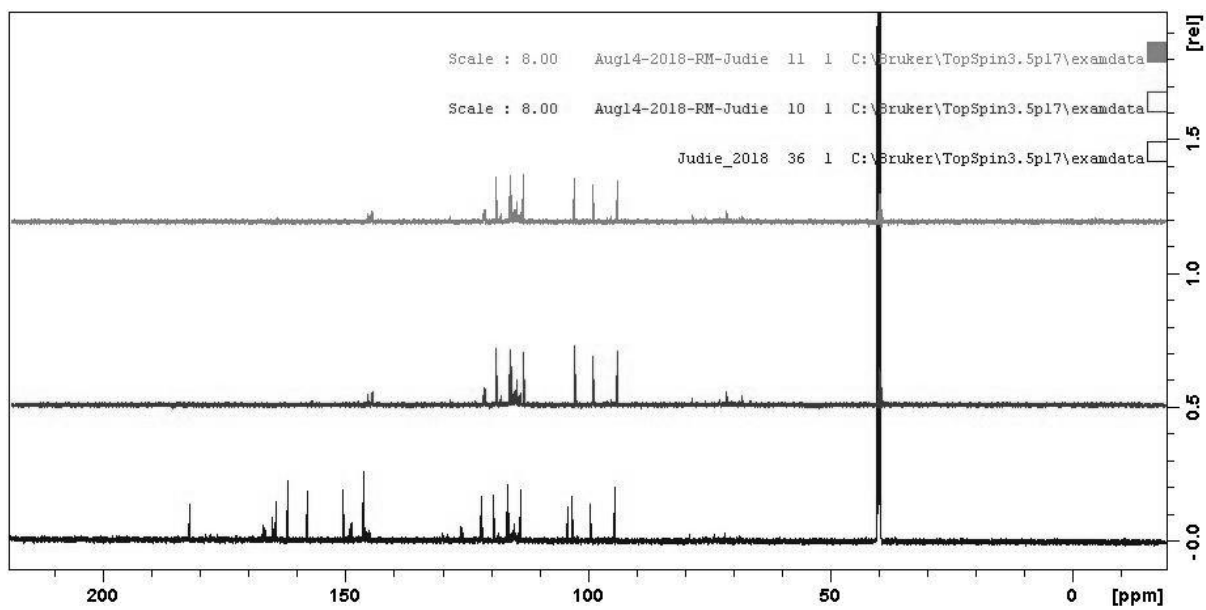
Figure S10. DEPT spectrum for luteolin (**2**)

Rose EA 2-8 HSQC
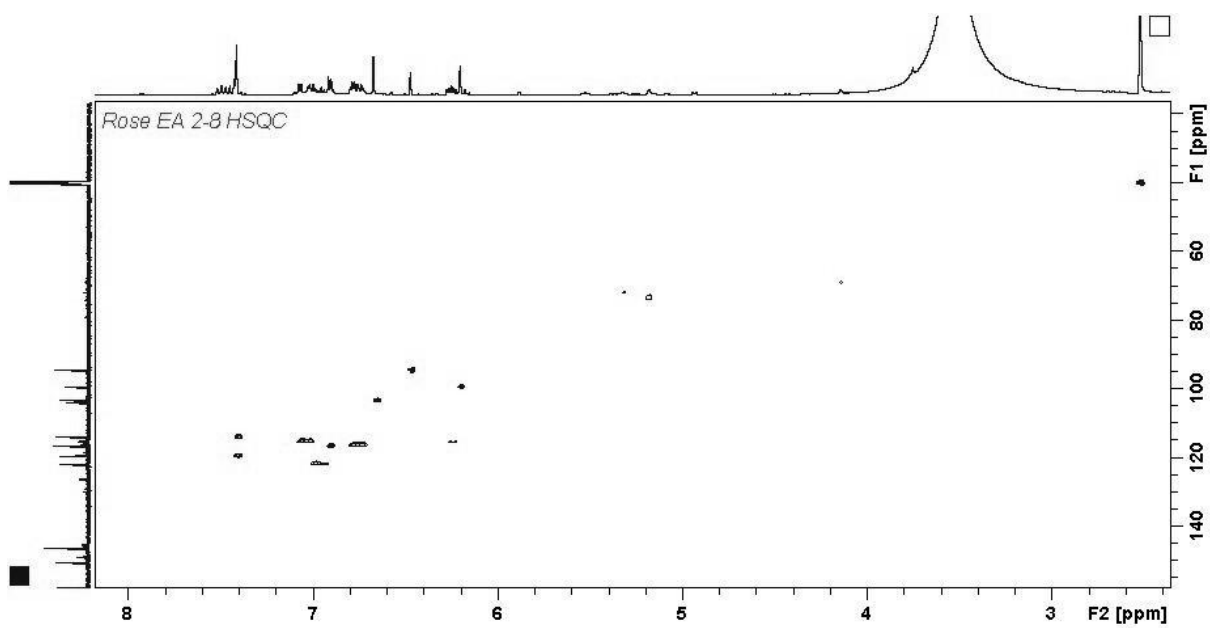
Figure S11. HSQC spectrum for luteolin (**2**)
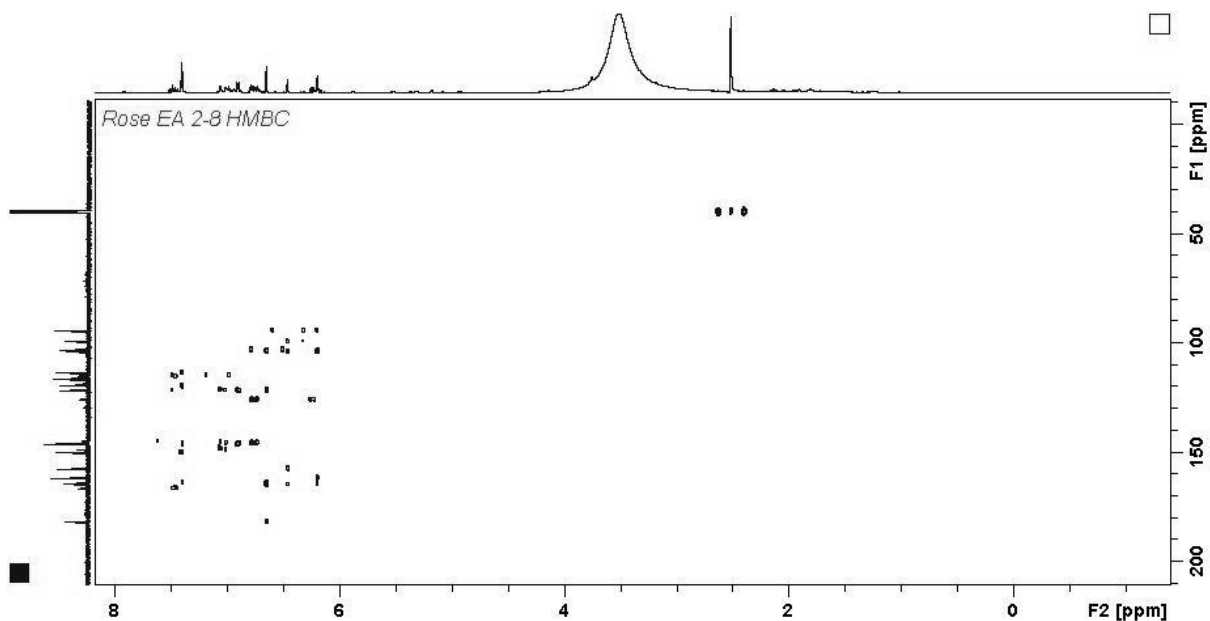
Figure S12. HMBC spectrum for luteolin (**2**)

Elemental Composition Report   Page 1

Single Mass Analysis
Tolerance = 5.0 PPM   /   DBE: min = -1.5, max = 500.0
Element prediction: Off
Number of isotope peaks used for i-FIT = 2

Monoisotopic Mass, Even Electron Ions
4 formula(e) evaluated with 1 results within limits (all results (up to 1000) for each mass)
Elements Used:
C: 10-15   H: 5-10   O: 5-10
EA2-8 4 (0.102) Cm (1:61)
TOF MS ES-   6.44e+004
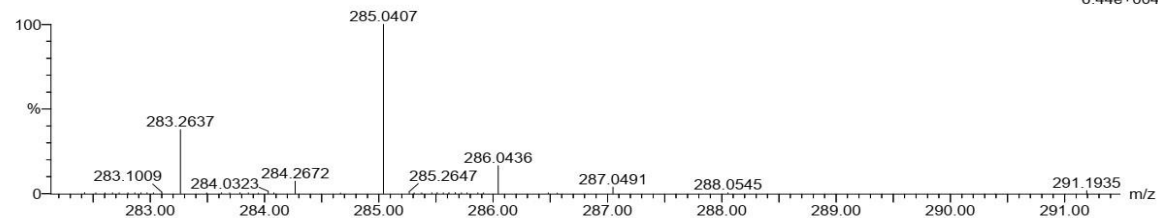
Minimum:				-1.5			
Maximum:		5.0	5.0	500.0			
Mass	Calc. Mass	mDa	PPM	DBE	i-FIT	i-FIT (Norm)	Formula
285.0407	285.0399	0.8	2.8	11.5	157.4	0.0	C15 H9 O6

Figure S13. Mass spectrum for luteolin (**2**)
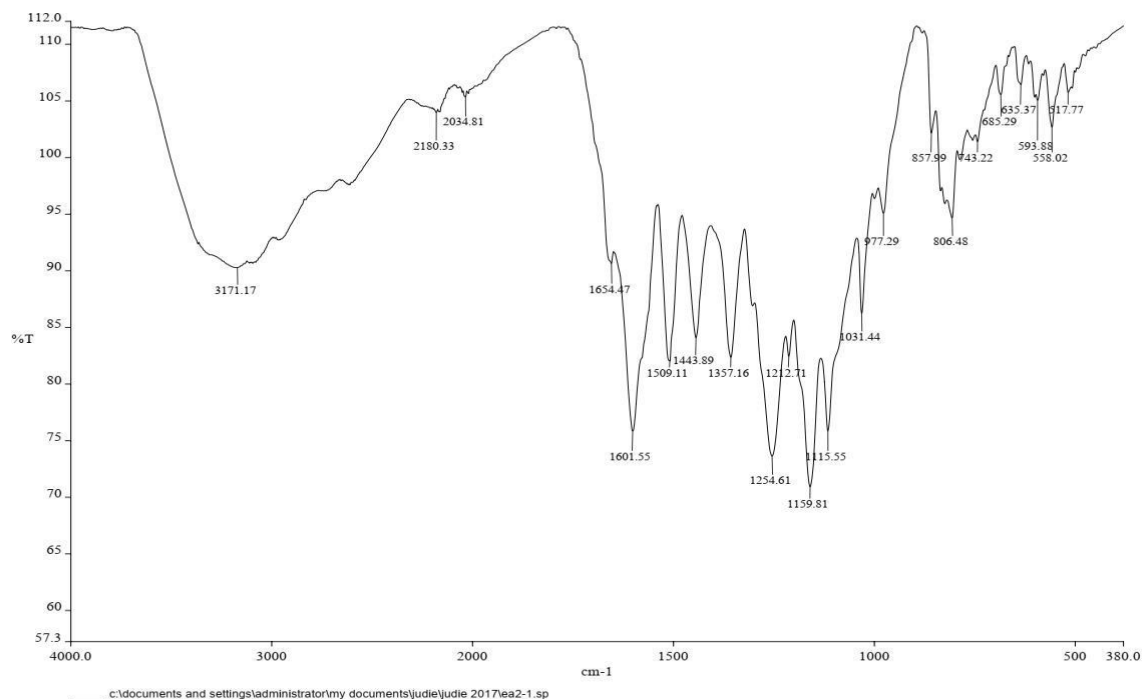
Figure S14. IR spectrum for luteolin (**2**)
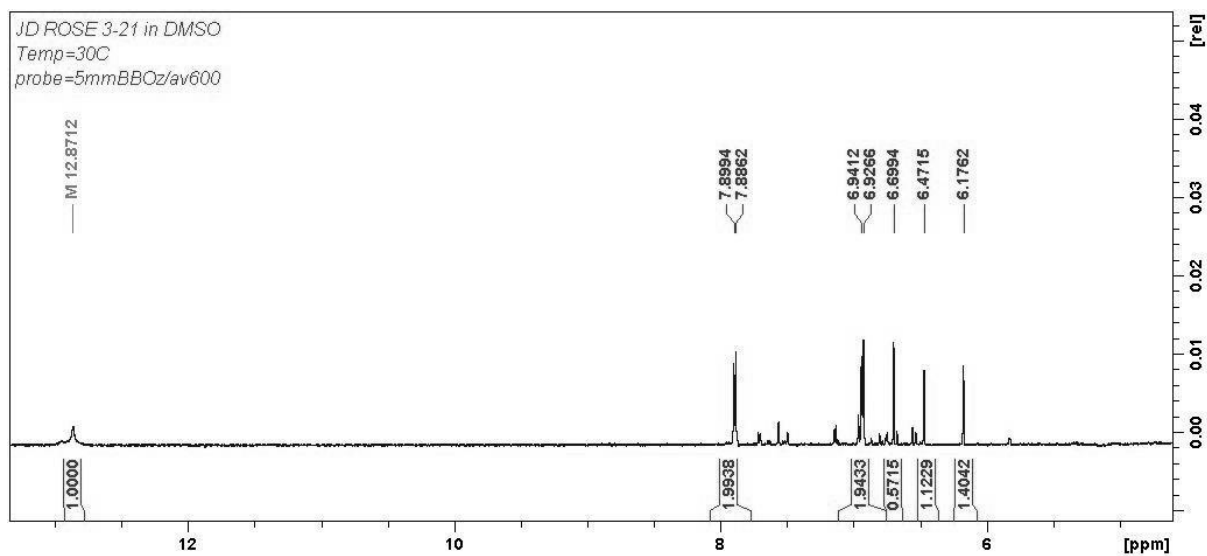
Figure S15. ¹H-NMR spectrum for apigenin (**3**)
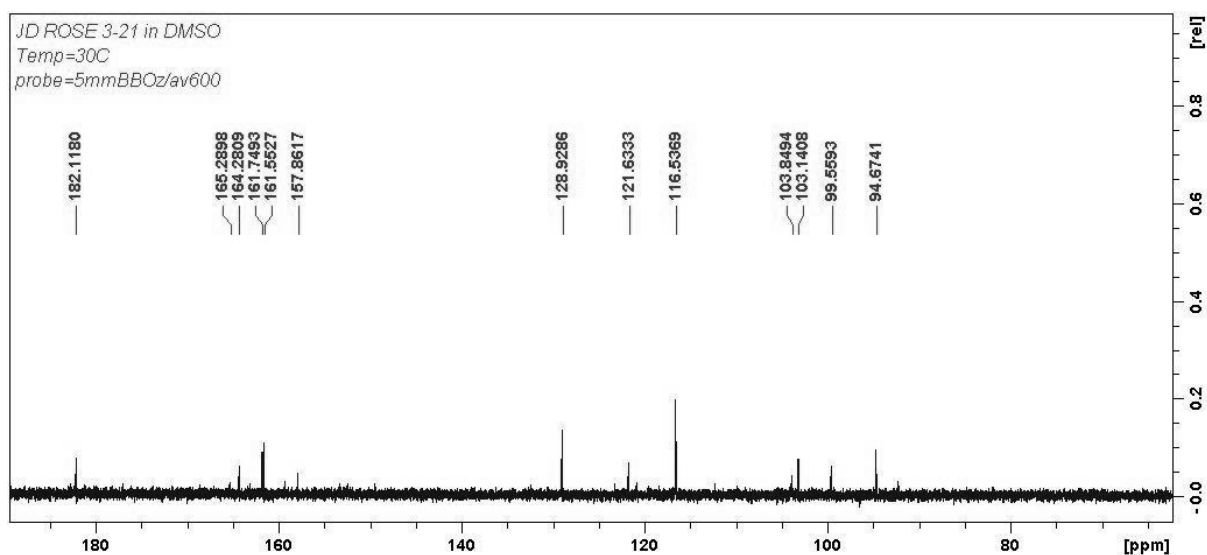
Figure S16. ^{13}C-NMR spectrum for apigenin (**3**)
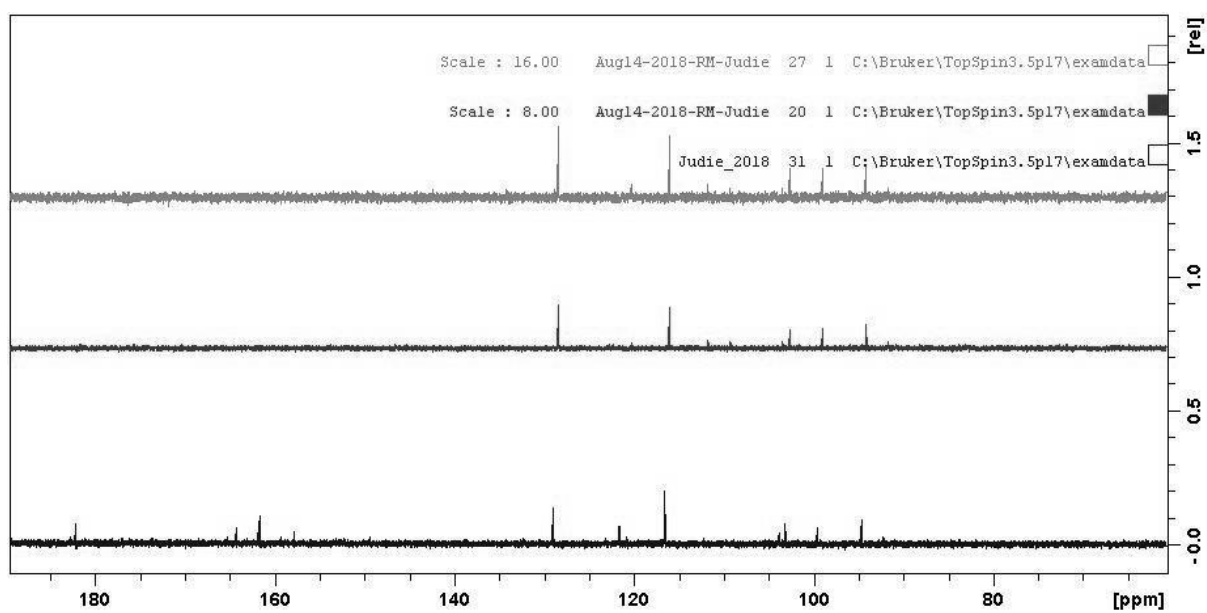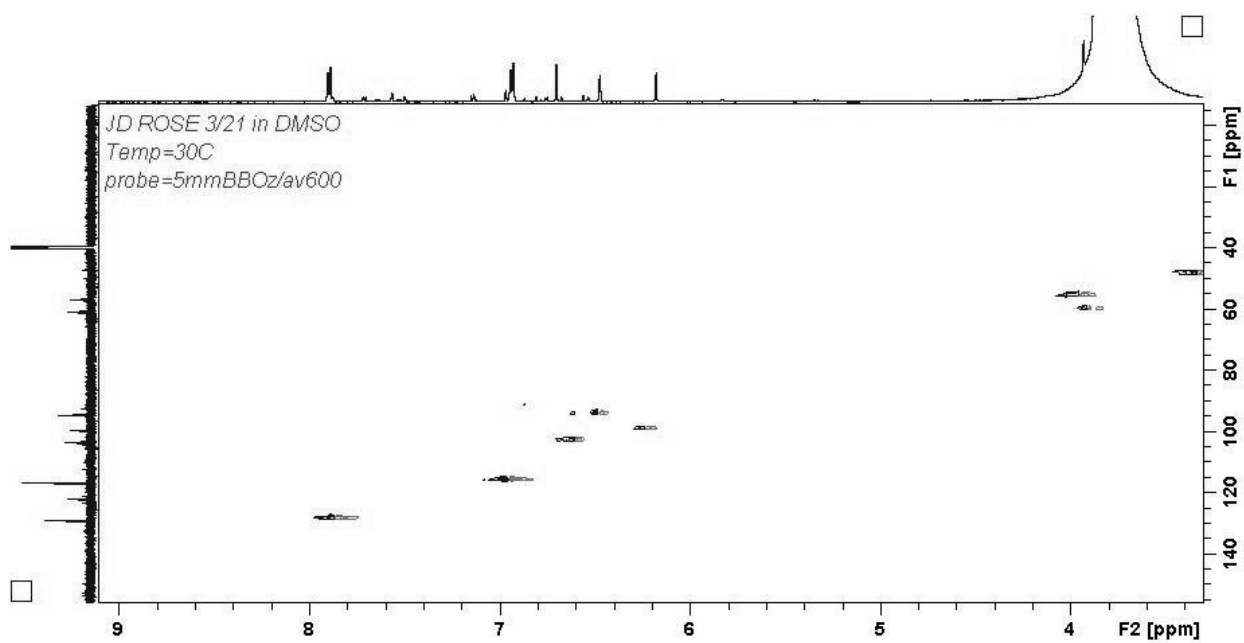

Figure S17. DEPT spectrum for apigenin (**3**)
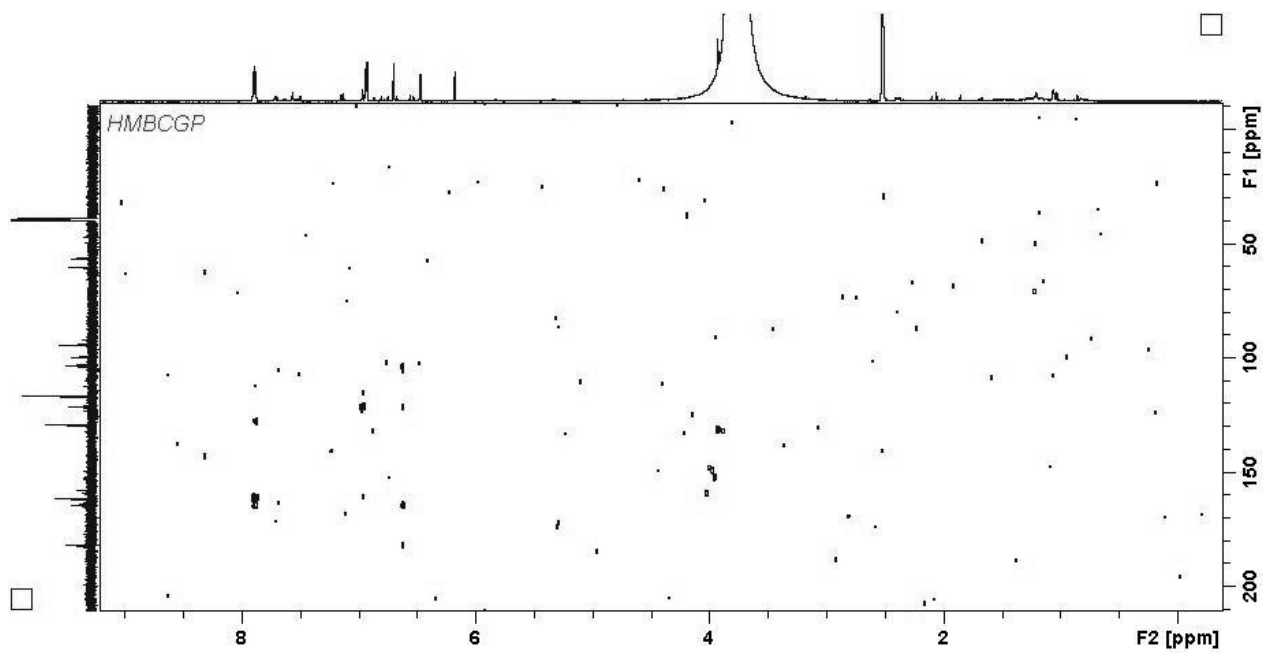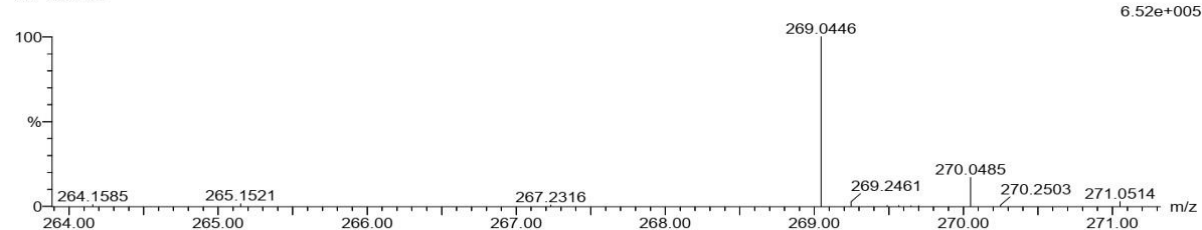
Figure S18. HSQC spectrum for apigenin (**3**)

Figure S19. HMBC spectrum for apigenin (**3**)

Single Mass Analysis
Tolerance = 5.0 PPM   /   DBE: min = -1.5, max = 500.0
Element prediction: Off
Number of isotope peaks used for i-FIT = 2

Monoisotopic Mass, Even Electron Ions
4 formula(e) evaluated with 1 results within limits (all results (up to 1000) for each mass)
Elements Used:
C: 10-15   H: 5-10   O: 0-5
JD-3_21 2 (0.034) Cm (1:61)
TOF MS ES-

6.52e+005

Mass	Calc. Mass	mDa	PPM	DBE	i-FIT	i-FIT (Norm)	Formula
Minimum:				-1.5			
Maximum:		5.0	5.0	500.0			
269.0446	269.0450	-0.4	-1.5	11.5	107.8	0.0	C15 H9 O5

Figure S20. Mass spectrum for apigenin (**3**)
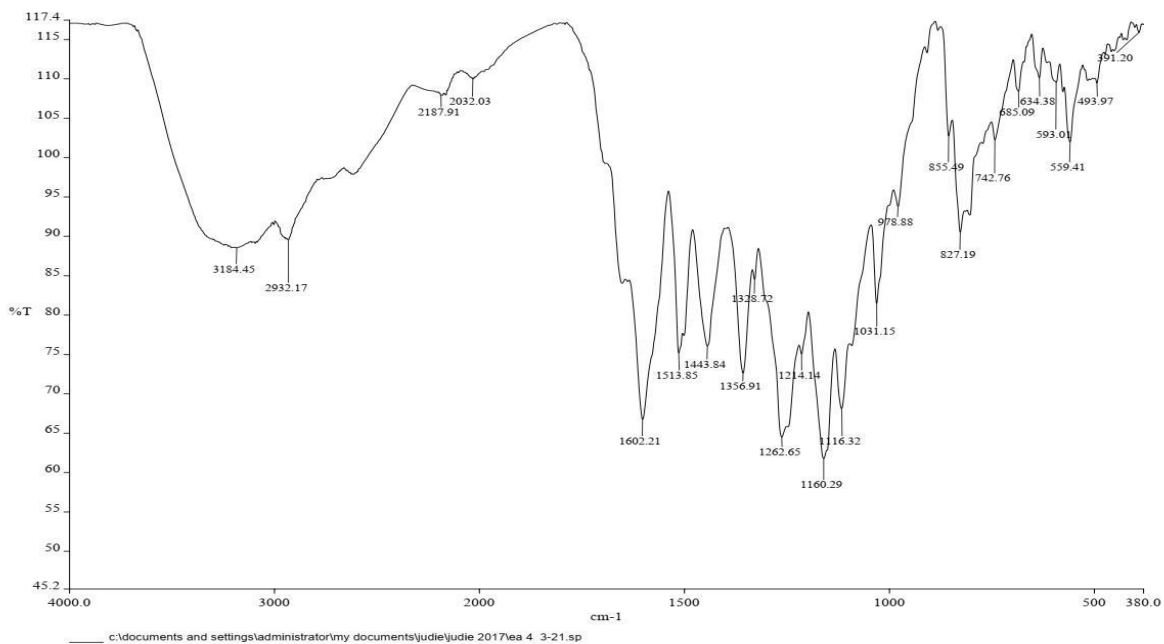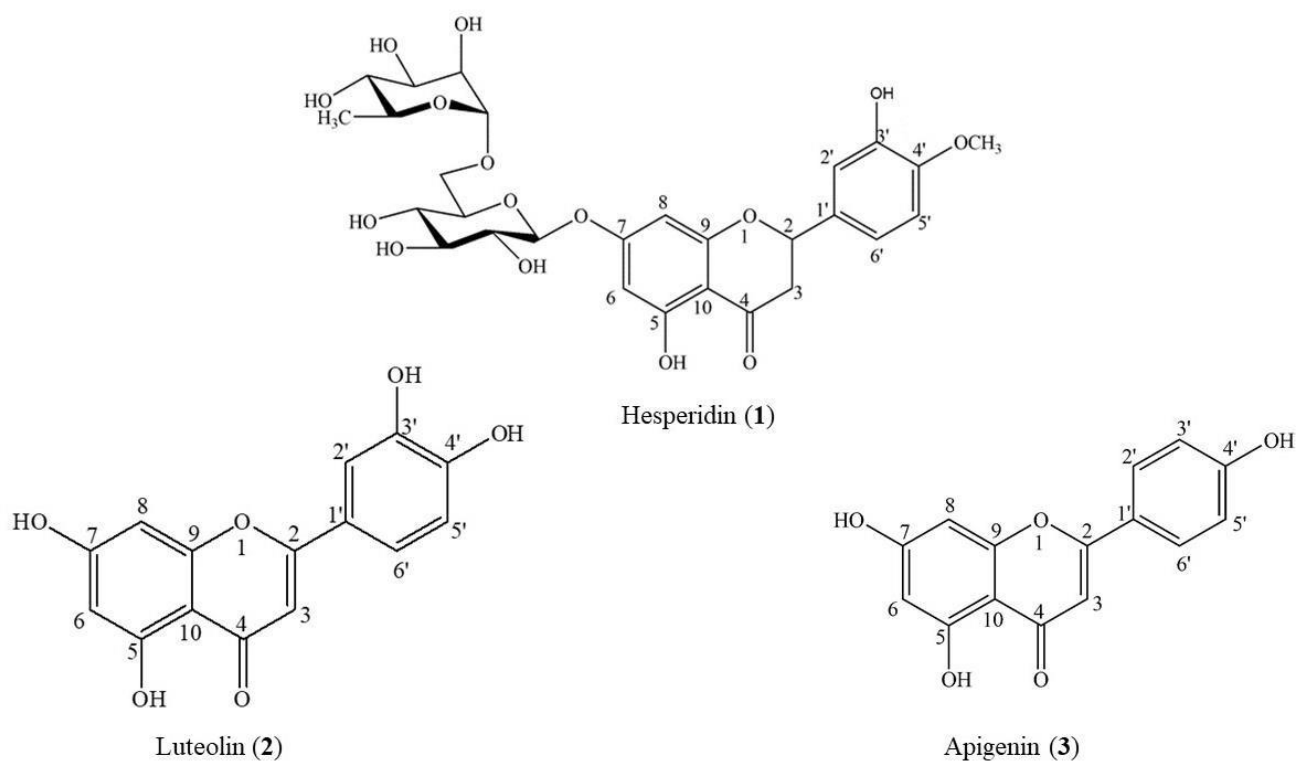
Figure S21. IR spectrum for apigenin (**3**)

59

Figure S22. Chemical structures of the compounds isolated from *Eriocephalus africanus*, hesperidin (**1**), luteolin (**2**), and apigenin (**3**).
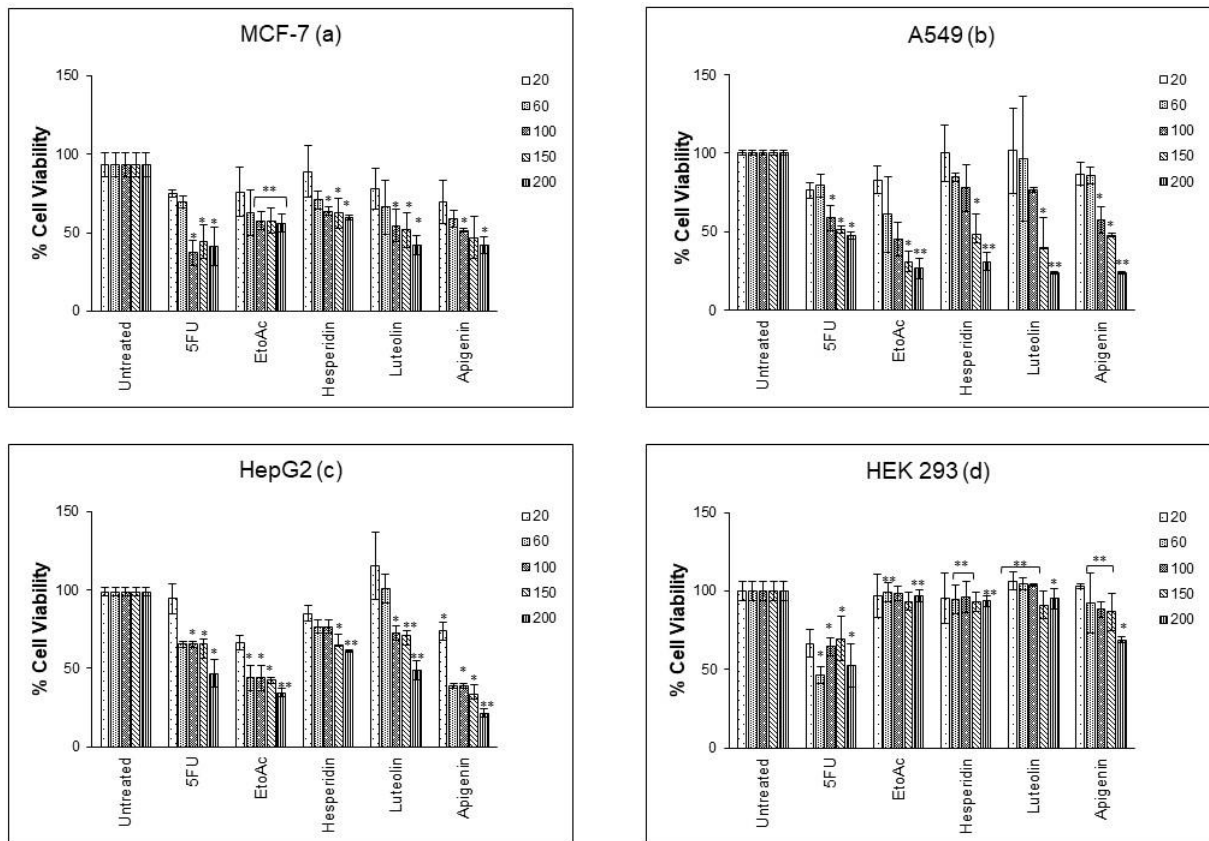
Figure S23. Cell viability of the ethyl acetate (EtOAc) fraction from the methanol (MeOH) extract of *E. africanus* and isolated compounds (hesperidin, luteolin, and apigenin) against (a) MCF-7, (b) A549, (c) HepG2 and (d) HEK 293 as determined by the MTT assay. Values are given as mean ± SD (n =3), *p < 0.05 from untreated cells, – **p < 0.05 from the positive control, 5- fluorouracil (5FU).
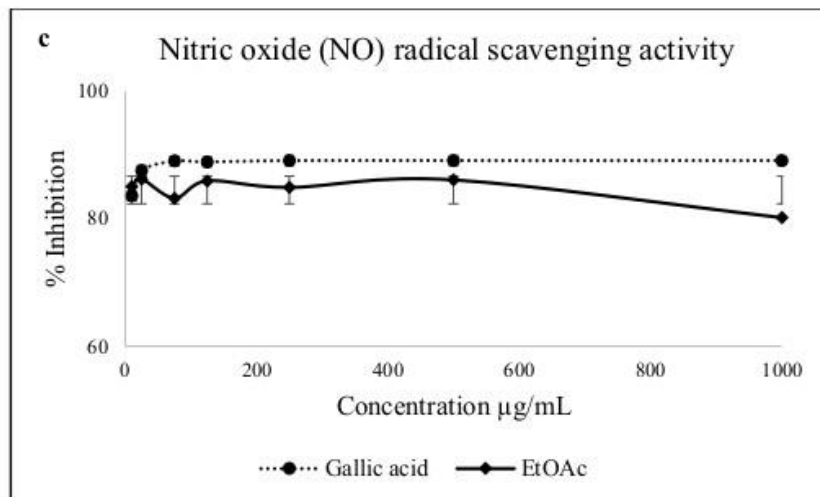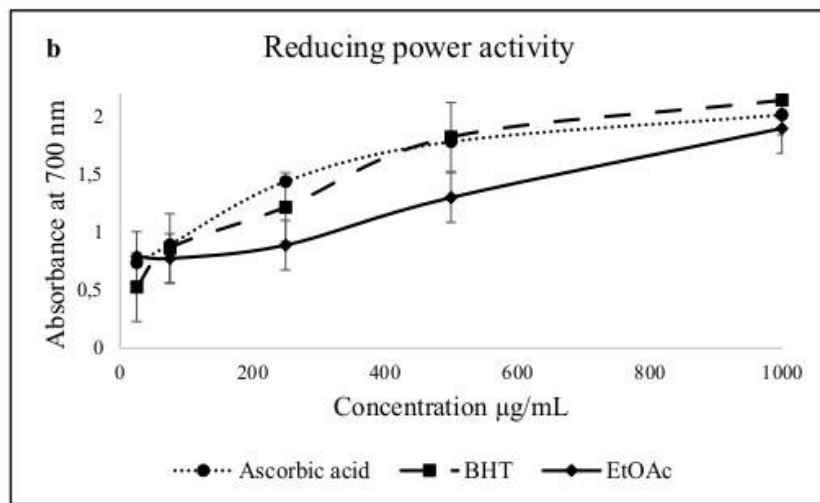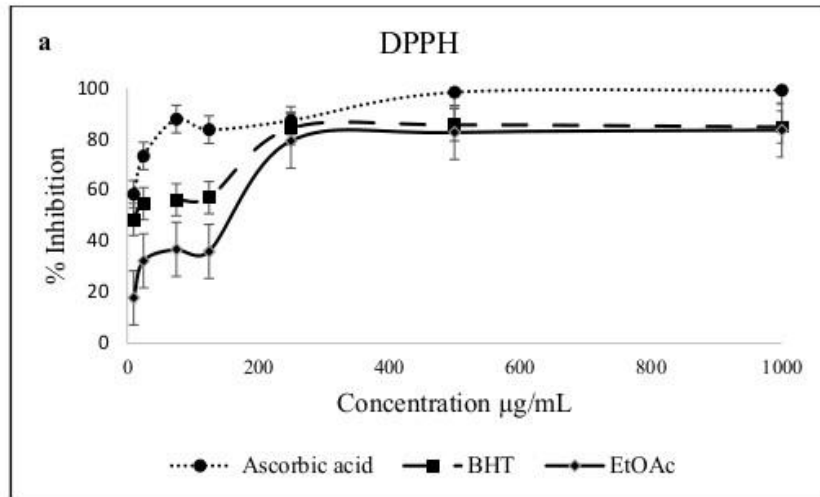
Figure S24. DPPH (a), reducing power scavenging activity (b), and nitric oxide (NO) radical scavenging activity (c) of the ethyl acetate (EtOAc) fraction from the methanol (MeOH) extract of *Eriocephalus africanus*. Values are given as mean ± SD, n =3.

3. CHAPTER THREE: MANUSCRIPT TWO

3.1 The effect of hesperidin and luteolin isolated from *Eriocephalus africanus* on apoptosis, cell cycle and miRNA expression in MCF-7

Submitted to: Journal of Biomolecular Structure and Dynamics (currently being considered for publication, corrections submitted).

The phytochemical analysis of the methanolic extracts of *E. africanus* in chapter two, revealed *E. africanus* to be a rich source of flavonoids, which, upon exposure to MCF-7 cells, caused a significant dose-dependent decrease in cell viability. Subsequently, this chapter evaluates the molecular mechanisms implicated in the observed decrease in cell viability. Particularly, this chapter pays special attention to the effect of the isolated flavonoids on the apoptotic pathway. Dysregulated apoptotic function is a hallmark of cancer and it has been implicated in the pathogenesis of various types of cancer, including breast cancer. In this regard, identifying bioactive compounds inducing or restoring apoptotic function is a highly active and major approach in the search for alternative treatments for cancer.

This chapter is formatted according to the journal specifications.

The effect of hesperidin and luteolin isolated from *Eriocephalus africanus* on apoptosis, cell cycle and miRNA expression in MCF-7

Judie Magura[a], Roshila Moodley[b*], Irene Mackraj[a]

[a]School of Laboratory Medicine and Medical Sciences, University of KwaZulu–Natal, Durban, South Africa

[b]School of Chemistry and Physics, University of KwaZulu–Natal, Durban, South Africa

Abstract

This study investigates the molecular mechanisms underlying the anticancer activity of hesperidin and luteolin, isolated from *Eriocephalus africanus,* in the human breast carcinoma cell line (MCF-7). The viability of MCF-7 cells, upon treatment with hesperidin and luteolin, was evaluated using the 3-[4,5-dimethylthiazole-2-yl]-2,5-diphenyltetrazolium bromide (MTT) cytotoxicity assay; apoptotic activity and effect on cell cycle progression were analysed by flow cytometry; effect on expression of key apoptotic regulatory genes (caspase-3, -8, -9, Bcl-2 and Bax) and apoptotic microRNAs (-16, -21 and -34a) were evaluated using quantitative real-time PCR. Hesperidin and luteolin reduced cell viability in a dose and time-dependent manner, caused a significant accumulation of apoptotic cells into the G0/G1 and sub-G1 cell cycle phases, induced apoptosis through the intrinsic and extrinsic pathways, down-regulated anti-apoptotic, *Bcl-2*, and upregulated pro-apoptotic, *Bax*. In addition, hesperidin and luteolin significantly downregulated the expression of miR-21 and upregulated that of miR-16 and 34a in MCF-7. Pearson's analysis revealed a positive correlation between *Bcl-2* and miR-21 and negative correlation between *Bcl-2*, miR-16 and -34a. Findings from this study provide new

evidence on the molecular basis of the anticancer activity of luteolin and hesperidin in breast cancer cell lines.

1. Introduction

Cancer is one of the major causes of death worldwide and the number of cancer patients are continuously rising, with an estimated global increase of 26 million new cancer cases and 17 million cancer deaths per year by 2030, according to the American Association for Cancer Research Report 2014 (Arteaga et al. 2014). To date, about 200 different types of cancers have been identified, with breast cancer being the most prevalent cancer among women, accounting for 1.5 million new cases per year, making it a global health threat (Hussain et al. 2019). Breast cancer is a complex heterogeneous disease; its progression and development are strongly linked to loss of cellular apoptotic function that is associated with accumulated alterations in genetic and epigenetic control (Abotaleb et al. 2019; Loh et al. 2019). Current evidence indicates that targeting the apoptotic pathway may be the most effective non-surgical treatment to combat breast cancer (Pfeffer & Singh 2018).

Apoptosis, a genetic cell death mechanism, which serves to eliminate unwanted cells, is executed through two distinct pathways; the mitochondrial (intrinsic) pathway and death receptor (extrinsic) pathway (Venkatadri et al. 2016). The extrinsic pathway involves the cell surface binding of death receptors such as Fas, to death ligands (FasL), leading to caspase-8mediated cell death. In contrast, the intrinsic pathway involves permeabilization of the mitochondrial outer membrane, mediated by Bcl-2 family proteins, leading to release of proapoptotic factors such as cytochrome *c* and subsequently caspase-9 initiated cell death (Green & Llambi 2015). After activation of the initiator caspases (-8 and -9), the two pathways converge on the effector caspases (-3 and -7), leading to apoptotic cell death with characteristic

biochemical and morphological changes (Pfeffer & Singh 2018). Several *in vitro* studies indicate that cellular death, induced by different stimuli in human breast cancer, is initiated through the mitochondrial pathway by the activation of caspase-3 and -9, and is often accompanied by the up-regulation of pro-apoptotic Bcl-2 family proteins (*Bax, Bak* and *Bad*), down-regulation of anti-apoptotic Bcl-2 family proteins (*Bcl-2* and *Bcl-xL*), the release of cytochrome *c*, production of mitochondrial ROS and cell cycle arrest (Shahali et al. 2018; Sun et al. 2018; Jin et al. 2019). While the role of *Bcl-2* in breast cancer is well known, recently microRNAs (miRNAs) have taken a central role in carcinogenesis and as therapeutic agents. Apoptosis-related miRNAs (apoptomiRs) post-transcriptionally regulate gene expression by binding with target mRNAs, generally in the 3′ untranslated region (3′ UTR), and control translation *via* degradation or repression (Sharma et al. 2016).

To date, several miRNAs (including miR-15/16, -34a and -21) have been implicated in regulation of apoptosis and chemoresistance in breast cancer, through targeting key proteins (such as the Bcl-2 family) involved in cell death mechanisms (Loh et al. 2019). MiR-15 induced G1 cell cycle arrest and apoptosis through downregulation of the anti-apoptotic gene (*Bcl -2*) expression in breast cancer cell lines (Mei et al. 2015). Upregulation of miR-15 and 16, induced apoptosis in aloe-emodin treated MCF-7, via *Bcl-2* repression (Jiang et al. 2020), and re-sensitised breast cancer cells to tamoxifen treatment (Loh et al. 2019). Inactivation of miR21, a key oncomir in carcinogenesis and *Bcl-2* regulator, also induced apoptosis, inhibited tumour progression and reversed doxorubicin resistance in breast cancer cells (Wang et al. 2011; Srivastava et al. 2015; Sharma et al. 2016). Moreover, upregulation of miR-34a inhibited cell proliferation in breast cancer cell lines (Imani et al. 2018; Cui & Placzek 2018) and altered docetaxel resistance of breast cancer cells through downregulation of *Bcl-2* (Hu et al. 2018).

Despite the advances in the current apoptosis targeting chemotherapies, toxicity and chemoresistance are drawbacks often observed in these therapies (Mohammad et al. 2015).

Hence, over the last two decades, there have been extensive studies on the use of naturally derived compounds as alternative apoptotic inducing, anticancer agents. Natural products account for over 50% of the drugs currently in clinical use, and globally, 80% of the population still utilize plant-derived medicines to alleviate their health problems (Millimouno et al. 2014). Moreover, studies suggest that natural phytocompounds could be more effective in cancer treatment than conventional treatments due to minimal side effects, their chemo-sensitising effects and their ability to target multiple cellular signalling pathways (Aung et al. 2017). Flavonoids are a group of natural polyphenolic metabolites comprising of two phenyl rings (A and B) joined by a heterocyclic ring C, which are widely distributed in plants (Dayem et al. 2016). Structurally, flavonoids possess variations in the number and position of substituent groups across these rings, and a few studies have suggested that these structural variances may influence their biological activities, including anticancer properties (Tu et al. 2015; Menezes et al. 2016). These variations in substituents classify them into subgroups, including flavonols, flavones, flavanones and flavanols (Venkatarame et al. 2017). Hesperidin, a flavanone glycoside with a 7-O glycoside moiety and luteolin, a flavone aglycone with a 2,3-double bond, have both been shown to have anticancer, antitumor and antiproliferative activities in various human cancer cell models, *in-vitro* (Xia et al. 2018; Jang et al. 2019; Huang et al. 2019).

The anticancer molecular mechanisms of action of hesperidin and luteolin in breast cancer is not well understood, and the correlation between apoptotic-related miRNAs and their target mRNA in hesperidin or luteolin-induced cell death against breast cancer is unknown. In this study, we investigate the anticancer activity of hesperidin and luteolin against MCF-7 cells by evaluating their effect on cell viability, cell cycle progression and expression of key apoptotic genes, such as *Bcl-2, Bax* and caspases, and apoptotic-related miRNAs, miR-16, -21 and -34a. We also investigated the influence of flavonoid structure on cytotoxicity and the correlation between the expression of miRNAs-and their target gene, *Bcl-2*.

2. Materials and Methods

2.1. Chemicals

All reagents used in this study were of analytical grade. Flavonoids, quercetin, apigenin, taxifolin, eriodictyol, hesperetin and chrysin, and positive the control (5-fluorouracil) were purchased from Sigma-Aldrich, Germany. Hesperidin and luteolin were previously isolated from *Eriocephalus africanus* (Magura et al. 2020). Hoechst 33342 and propidium iodide were obtained from ThermoFischer Scientific, USA.

2.2. Cell culture

Human MCF-7 cell lines obtained from American Tissue Culture Collection (ATCC) (Virginia, USA), were cultured in DMEM supplemented with 10% FBS and 1% penicillin/streptomycin (Biowest, USA). Cells were maintained at 37 $^{\circ}$C and 5% CO_2 under humidified conditions.

2.3. Cytotoxicity and analysis of structure-influence of flavonoids

The cytotoxicity of hesperidin and luteolin on MCF-7 cell lines was evaluated using the standard MTT assay. In addition, to evaluate the influence of structure on cytotoxicity, a comparative study on the cytotoxic effect of flavonoids with slight differences in their structure to hesperidin and luteolin, namely, quercetin, apigenin, taxifolin, eriodictyol, chrysin and hesperetin, in MCF-7 cells, was also performed. Briefly, cells at 5×10^3 cells/well were seeded into 96-well plates (100 µL total medium volume) and allowed to attach overnight, then treated with concentrations of 20, 60, 100 and 140 µg/mL (in triplicate) of the tested flavonoids for 24 h and 48 h. Untreated cells served as the negative control (control) and cells treated with 5fluorouracil (5-FU) served as the positive control. After incubation, cell viability was measured *via* the MTT assay, and the absorbance was recorded at 560 nm using a microplate

reader (SPECTROstar Nano, BMG Germany). Data was presented as percentage cell viability relative to the untreated cells.

2.4. Annexin V and PI staining

Annexin V Apoptosis Kit 1 (BD Pharmingen™, California San Jose, USA) and flow cytometry were used to assess the apoptotic effects of hesperidin and luteolin in MCF-7 cells. Briefly, cells were seeded in 6-well plates and following overnight attachment, they were treated with flavonoids for 48 h at concentration of 100 µg/mL. Thereafter, cells were harvested using Accutase™ (ThermoFischer Scientific, USA) and collected by centrifugation at 2000 rpm for 5 min. The collected cells were re-suspended in binding buffer, and an aliquot of 100 µL was treated with 5 µL of both Annexin V and PI and incubated for 15 min in the dark. Thereafter, 400 µL of binding buffer was added to each tube and analysed by flow cytometry within an hour.

2.5. Morphology changes using Hoechst staining

For the Hoechst staining, cells were seeded into 4-well glass slides (Lab-Tek® II, Chamber slide™) and treated with 100 µg/mL of hesperidin or luteolin for up to 48 h. Thereafter, cells were stained with 10 µg/mL of Hoechst and incubated for 30 min at room temperature. Subsequently, images were captured using the Floid® Cell Imaging Station under an excitation wavelength of 390/40 nm and an emission wavelength of 446/33nm for blue fluorescence.

2.6. Cell cycle analysis

For all treatments at 48 h incubation, the cell cycle analysis was carried out according to the manufacturer`s protocol (BD Pharmigen™ FITC BrdU Flow Kit). Data was recorded in triplicate using a BD FACSCanto™ II flow cytometer and analysed with Kaluza 2.1 (Beckman Coulter) analysis software.

2.7. Expression of mRNA using quantitative Real Time-PCR

Total RNA was extracted from untreated and treated MCF-7 cells using a Quick-RNA MiniPrep kit (Zymo Research, CA, USA) according to the manufacturer`s protocol. The purified mRNA was transcribed into cDNA using reverse transcription and cDNA synthesis kit (SensiFast™, Bioline USA). The expression of the genes of interest were analysed using real-time PCR and LightCycler® FastStart DNA Master SYBR Green (Roche Diagnostics, IN, USA). β-Actin was used as the reference gene to normalise the Cq values. The primer sequences used in this experiment are illustrated in Table 1. The cycling program was set as follows: DNA polymerase was activated for 10 min at 95 °C followed by 45 cycles consisting of a denaturing step for 15 s at 95 °C, and annealing/extension step for 30 s at 60 °C and 72°C for 30 s (Fani et 2016). The $2^{-\Delta\Delta Cq}$ comparative method was used to calculate the fold change in gene expression in response to treatment with luteolin and hesperidin (Schmittgen & Livak 2008; Xie et al. 2018).

Table 1. Primer sequences for quantitative Real Time-PCR

Gene	Forward	Reverse	References
β-actin	5′-GCACCACACCTTCTACAATG -3′	5′-TGCTTGCTGATCCACATCTG-3′	Khan et al. 2016
Bcl-2	5′-GGCTGGGATGCCTTTGTG-3′	5′-CAGCCAGGAGAAATCAAACAGA-3′	Khan et al. 2016
Bax	5′-TGCTTCAGGGTTTCATCCAG-3′	5′-GGCGGCAATCATCCTCTG -3′	Khan et al. 2016
Caspase-3	5′- CAGAACTGGACTGTGGCATTG-3′	5′-GCTTGTCGGCATACTGTTTCA-3′	Khan et al. 2016
Caspase-8	5′-CATCCAGTCACTTTGCCAGA-3′	5′-GCATCTGTTTCCCCATGTTT-3′	Pilco-Ferreto & Calaf 2016
Caspase-9	5′-CCAGAGATTGCGAAACCAGAGG-3′	5'-GAGCACCGACATCACCAAATTC-3'	Pilco-Ferreto & Calaf 2016

2.8. Quantitative Real-Time –PCR analysis of miRNA expression

MiRNAs were isolated from the treated and untreated cells using the PureLink miRNA isolation kit according to the manufacturer's protocol. Complementary DNA (cDNA) was synthesised using the SensiFast™ cDNA synthesis kit (Bioline, USA), after which, the miRNA expression was determined using real-time PCR and SYBR green master mix (Roche Diagnostics, IN, USA). U6 was used to normalise the Cq values and as the reference gene. Specific miRNA primers used in this experiment were as follows: miR-16, Forward; 5′TAGCAGCACGTAAATATTGGCG-3′, Reverse; 5'-CCAGTATTGACTGTGCTGCTGA-3', miR-21, Forward; 5′- GGGGATTTCTTGGTTTGTGAA-3′ and Reverse 5′ATACAGCTAGAAAAGTCCCTGAAAA-3′ and miR-34a, Forward; 5′-GCGGCCAATCAGCAAGTATACT-3′, Reverse; 5′-GTGCAGGGTCCGAGGT-3′ (Zhou et

al. 2018; L. Zhang et al. 2018). The miRNAs expression was calculated using the $2^{-\Delta\Delta Cq}$ comparative method.

2.9. Statistical Analysis

All experiments were carried out in triplicate and data was expressed as mean ± standard deviation. For statistical significance, the one-way analysis of variance (ANOVA) with Tukey`s post hoc at $p < 0.05$ was performed, using GraphPad Prism software (La Jolla, CA). The Pearson's correlation test was computed using Microsoft Excel Data Analysis ToolPak to evaluate the correlation between miRNAs and their target mRNA.

3. Results

3.1. Cytotoxicity of hesperidin and luteolin, and structure-influence of flavonoids on cytotoxicity.

MCF-7 cells treated with hesperidin and luteolin at concentrations 20, 60, 100 and 140 µg/mL for 24 h and 48 h showed decreased cell viability in a dose and time-dependent manner (Figure 1). Treatment with 100 or 140 µg/mL effectively reduced cell viability to approximately 36% for hesperidin and 15% for luteolin after 48 h. Since no statistically significant difference ($p < 0.05$) was observed for treatments at both concentrations, 100 µg/mL at 48 h was selected for proceeding experiments. The MTT structure-influence analysis confirmed that the cytotoxic activity of flavonoids is influenced by structure with activity at 100 µg/mL for 48 h increasing in the order of taxifolin < eriodictyol < chrysin < quercetin < hesperidin ≈ hesperetin < apigenin ≈ luteolin (Supplementary Figure 1(a)-(d)).
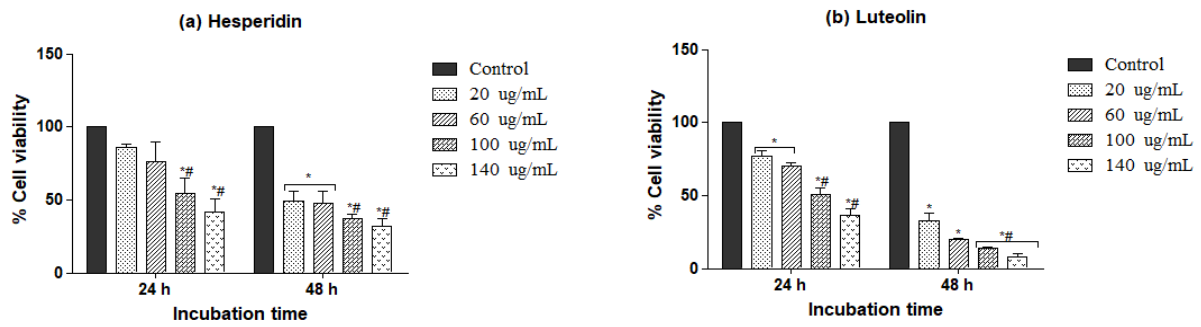
Figure 1. Cytotoxicity of (a) hesperidin and (b) luteolin at 24 h and 48 h in MCF-7. The results are represented as mean ± SD of three experimental replicates, * significant difference at $p < 0.05$ from the control and # from the 20 and 60 µg/mL group, at $p < 0.05$.

3.2. Annexin V-FITC and PI staining

To establish whether the cell death observed after treating MCF-7 with hesperidin and luteolin, was due to apoptosis or necrosis, Annexin V-FITC and PI staining followed by flow cytometric analysis was performed. The results show a significant increase in apoptotic cell populations for both hesperidin (56 ± 3.14%) and luteolin (83.6 ±0.71%) treated cells, in contrast to the control (0.04 ± 0.00%) (Figure 2).
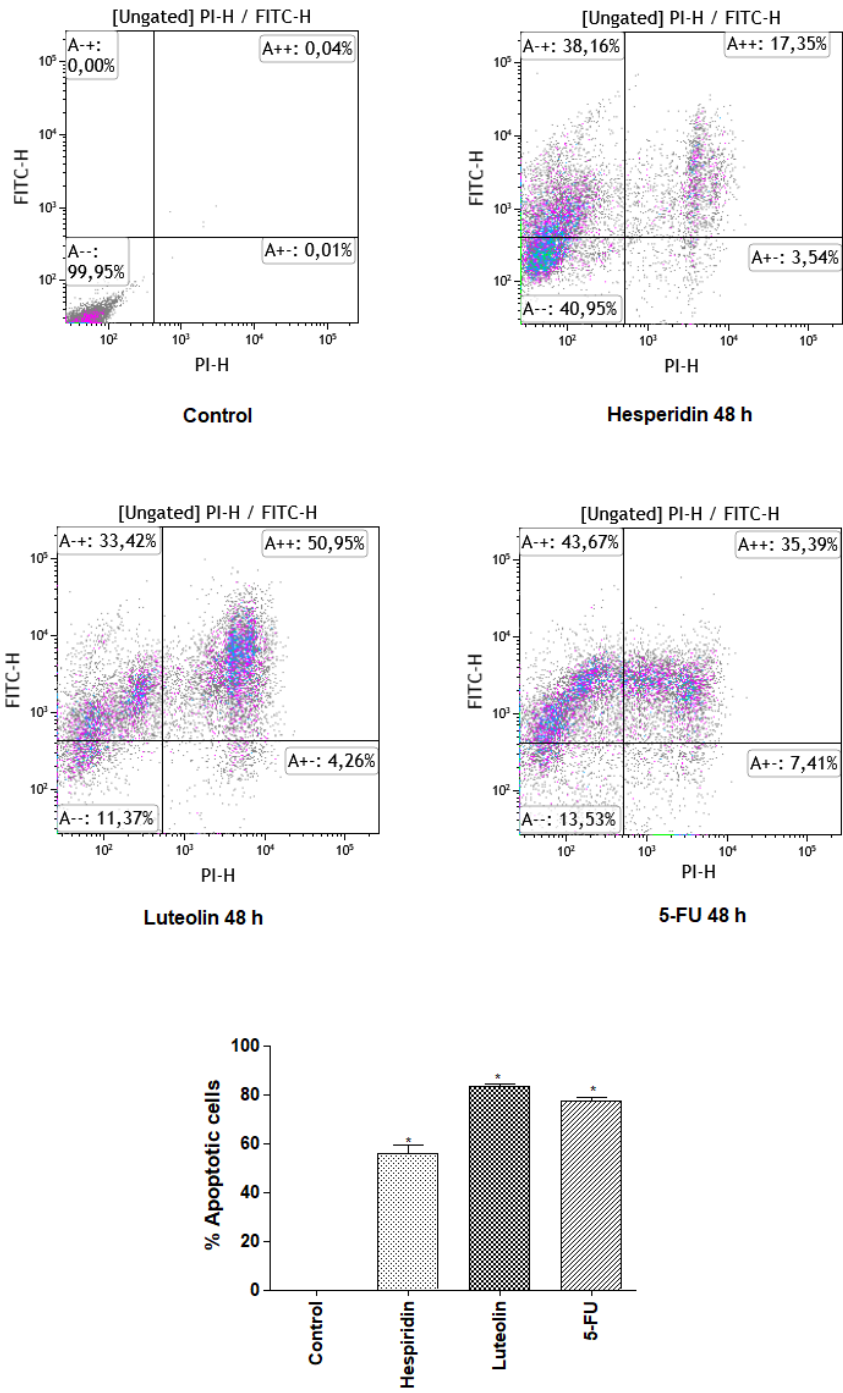
Figure 2. Apoptotic effects of hesperidin, luteolin and 5-fluorouracil (5-FU) on MCF-7 48 h post-treatment. The bar graph represents total percentage of apoptotic cells in quadrants A-+, early apoptotic and A++, late apoptotic. Values are represented as mean ± SD of three independent experiments, * statistically significant difference from the control (untreated cells) at p < 0.05.

3.3. Morphological changes

To further confirm the apoptotic effect of hesperidin and luteolin, hesperidin and luteolin treated cells were stained with Hoechst 33342 and examined microscopically using Floid® Live Cell Imaging Station. Hoechst 33342 is a cell permeable dye which emits blue fluorescence when bound to DNA, allowing the visualisation of the cell nuclei and identification of apoptotic makers. Apoptotic morphological changes were observed in hesperidin and luteolin treated MCF-7 cells, as illustrated in Figure 3.
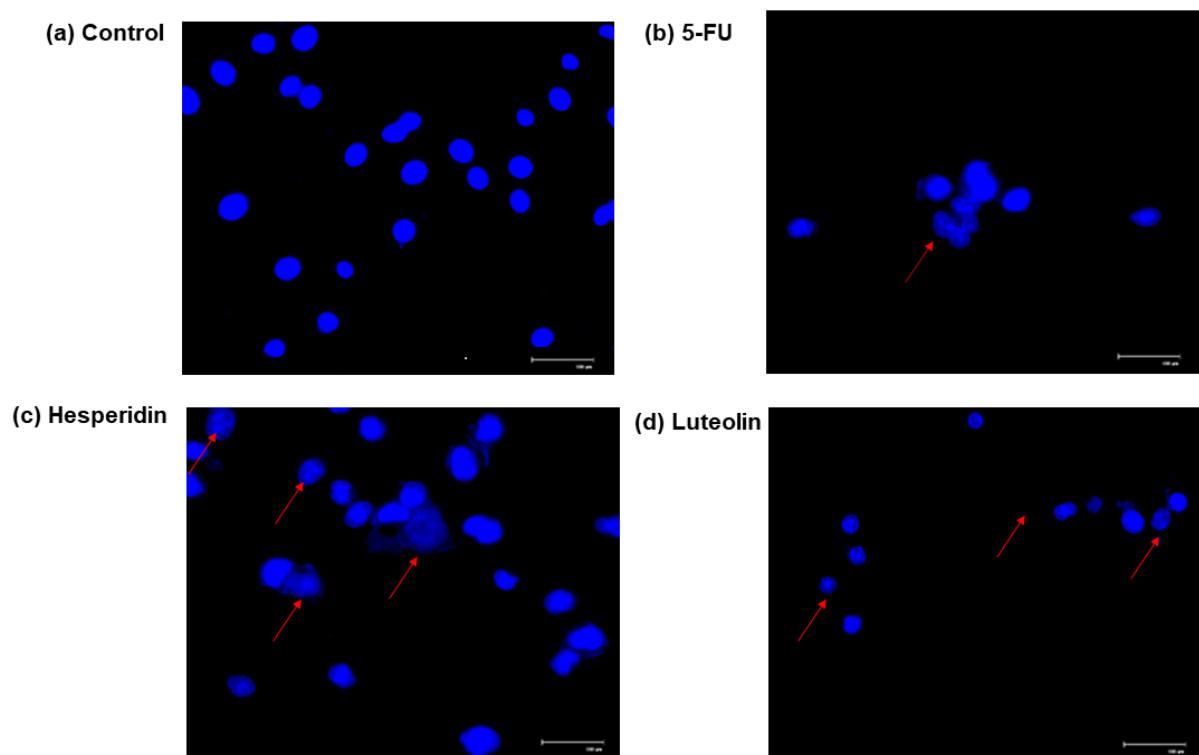
Figure 3. Morphological changes in hesperidin and luteolin treated MCF-7 cells at 100 µg/mL for 48 h, 5-fluorouracil (5-FU) and control (untreated cells). Hoechst 33342 was used for staining and micrographs were captured using Floid® Live Cell Imaging Station. The red arrows indicate nuclear fragmentation and condensation.

3.4. Cell cycle analysis

To assess if the apoptotic effect was subsequently due to cell cycle arrest, the changes in the cell cycle upon treatment with hesperidin or luteolin at 100 ug/mL for 48 h were investigated.
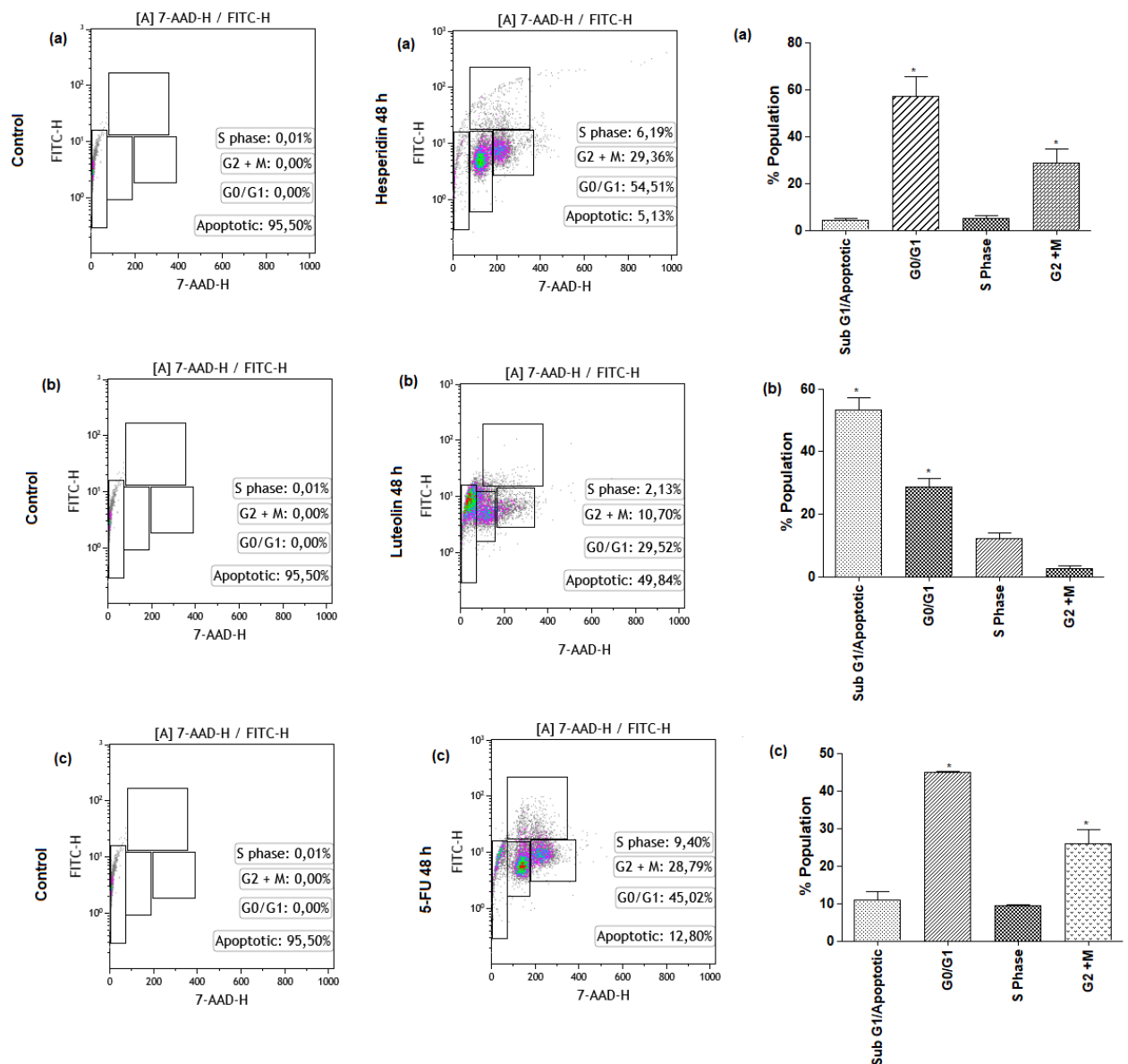

Figure 4. Cell cycle analysis after treatment with (a) hesperidin, (b) luteolin and (c) 5fluorouracil (5-FU) at 100 ug/mL for 48 h. The bar graphs represent the total percent cell population in different phases. Values are shown as mean ± SD of experimental triplicates, * significant difference at $p < 0.05$.

Hesperidin treatment resulted in a significant accumulation of cell population in the G0/G1 phase (50%), suggesting cell cycle arrest in the G0/G1 phase. Treatment with luteolin showed higher accumulation of cell populations in the apoptotic or sub G1 phase 53% vs. 28.6% in G0/G1, 3.3% in S phase and 8.9% in the G2+M phase (Figure 4).

3.5. Changes in apoptotic gene expression on hesperidin and luteolin treatment

To establish the molecular pathway of the hesperidin and luteolin-induced apoptosis in MCF7 cells, the expression of caspase-9 (intrinsic) and caspase-8 (extrinsic) were analysed using real-time PCR, 48 h post-treatment. Since the intrinsic and extrinsic pathways converge (Pfeffer & Singh 2018), increased levels of caspase-3 have also been associated with activation of both apoptotic pathways; therefore, the expression of caspase-3 was also evaluated. The results showed an increase in the expression of caspase-3 and -9 in hesperidin treated cells and an increase in expression of both caspase-9 and -8 in luteolin treated cells (Figure 5a). Additionally, an increase in the expression of pro-apoptotic proteins *Bax* and decrease in antiapoptotic proteins *Bcl-2*, were observed (Figure 5b).
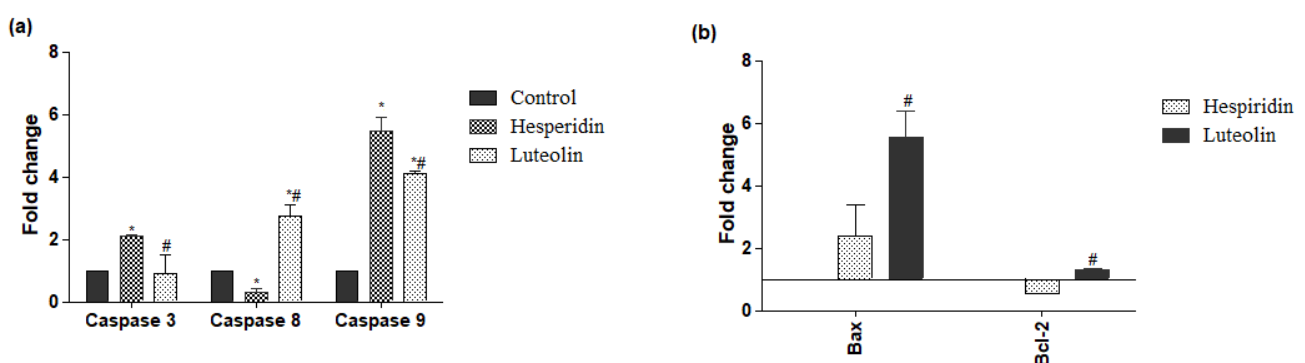

Figure 5. Expression of (a) caspase-3, -8 and -9 and (b) *Bax* and *Bcl-2* in hesperidin and luteolin treated MCF-7 cells at 100 ug/mL for 48 h. Data is represented as mean ± SD, * significant difference at $p < 0.05$ vs control and # at $p < 0.05$ vs hesperidin treated.

3.6. Effect of hesperidin and luteolin on miRNA expression

To further evaluate the molecular pathway of hesperidin and luteolin, expression levels of miR16, -21, and -34a were assessed in hesperidin and luteolin treated MCF-7 cells. The quantitative analysis showed a significant increase, relative to the control, in the expression levels of miR16 and -34a, and downregulation of miR-21 in hesperidin treated cells (Figure 6). Treatment with luteolin showed an approximately 2.4-fold increase in both miR-16 and -34a expression (Figure 6), and a decrease in the expression of miR-21, 48 h post-treatment.
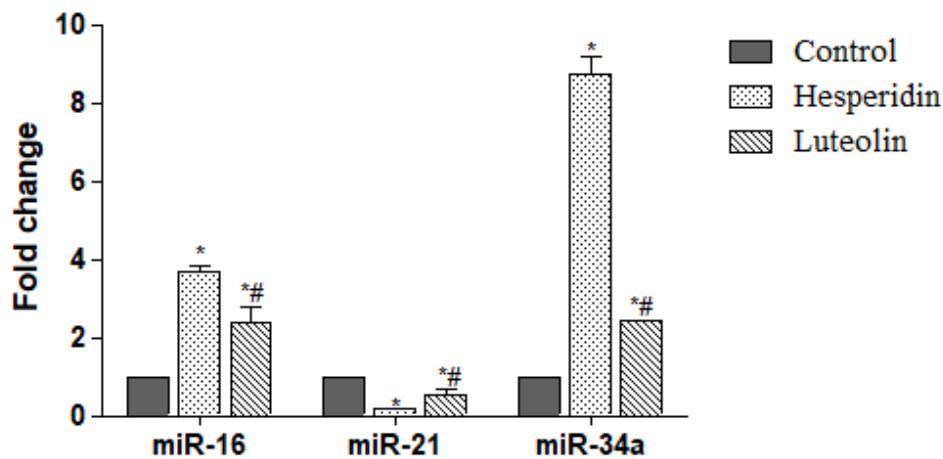

Figure 6. Expression of miR-16, -21 and -34a in hesperidin and luteolin treated MCF-7 cells at 100 ug/mL for 48 h. Values represented as mean ± SD, * significant difference at $p < 0.05$ vs control and [#] significant different at $p < 0.05$ vs hesperidin treated.

3.7. Correlation analysis of miRNAs and their target mRNA

The correlations among miR-16, -21, -34a, and mRNA, *Bcl-2* were evaluated using the Pearson correlation test. The Pearson`s test showed a negative correlation between the expression of miR-16, -34a and target *Bcl-2*, r (2) = -0.73, $p < 0.05$, two-tailed and a strong positive correlation between miR-21 and *Bcl-2*, r (2) =1, with no significant difference, p = ns,

twotailed. Overall, an increase in expression of miR-16 and -34a was correlated with a decrease in expression of *Bcl-2*, whereas, a decrease in miR-21 was associated with a decrease in *Bcl-2* as well.

4. Discussion

Evasion of apoptosis is a hallmark of cancer, hence, induction or reactivation of apoptosis by cytotoxic anticancer agents, is a key approach in the development of novel, promising therapeutic strategies for cancer treatment (Jaudan et al. 2018). Many reports on natural product-derived flavonoids, have shown that they inhibit proliferation and induce apoptosis in cancer cells. For example, Zhang et al. (2018) demonstrated that flavonoids, isorhamnetin, genkwanin and acacetin, isolated from *Tephroseris kirilowii*, inhibited cell proliferation through the induction of apoptotic cell death and G2/M phase cell cycle arrest. Similarly, catechin, also a plant-derived flavonoid, reduced cell proliferation and induced apoptosis in murine lymphoma cells LB02 *via* modulation of antiapoptotic proteins (Papademetrio et al. 2013).

In this study, two flavonoids, hesperidin and luteolin, which we previously isolated from *Eriocephalus africanus*, exhibited cytotoxicity against the breast cancer cell line (MCF-7) in a dose and time-dependent manner (Figure 1). In addition, flavonoid structure was shown to have an influence on cytotoxicity (Supplementary Figure 1(a)-(d)). The flavone (luteolin), with a 2,3-double bond and carbonyl at position 4 in the C-ring, presented higher cytotoxicity in comparison to the flavanone, eriodictyol, with no double bond in the C-ring. The additional hydroxyl group in the B-ring of luteolin compared to apigenin, did not influence the cytotoxicity of flavones; however, removal of the hydroxyl groups from the B-ring, as in chrysin, considerably reduced the cytotoxicity of the flavone. Addition of the hydroxyl group to position 3 of the C-ring, as in quercetin, reduced the cytotoxicity of the flavonol relative to luteolin. Similarly, addition of the hydroxyl group to position 3 of the flavanonol, taxifolin,

reduced cytotoxicity compared to eriodictyol. Replacement of a hydroxyl group in the B-ring of eriodictyol with a methoxy group, as in hesperetin, considerably increased cytotoxicity of the flavanone whilst further addition of a sugar moiety to position 7 of the A-ring, did not noticeably affect cytotoxicity, as is seen in the glycoside, hesperidin. The results indicate that flavonoid structures that present with a double bond in the C-ring and hydroxyl or methoxy substituents in the B-ring, positively influenced cytotoxicity whilst structures with a hydroxyl group at position 3 of the C-ring negatively affect cytotoxicity. Menezes et al. (2016), also demonstrated structural influences in several flavonoids for the treatment of leukaemia. A study on the cytotoxicity of flavonoids towards cultured normal human cells by Matsuo et al. (2005) suggested that, if flavonoids are efficiency incorporated into cells, they tend to generate more intracellular reactive oxygen species that then exert cytotoxicity on cells.

These findings suggest that factoring structural influences in anticancer activity, could be useful in developing effective drugs for treatment. Furthermore, the cytotoxicity of hesperidin and luteolin was confirmed to be apoptotic-induced, as demonstrated by the Annexin V/ PI and flow cytometric analysis (Figure 2), and treatment with both hesperidin and luteolin (100 ug/mL for 48 h) resulted in the accumulation of apoptotic cell populations of $56 \pm 3.14\%$ and $83.6 \pm 0.71\%$, respectively. Furthermore, microscopic evaluation (Figure 3) of hesperidin and luteolin treated cells exhibited typical morphological features of cells undergoing apoptosis, such as chromatin condensation and nuclear fragmentation, accompanied by reduction in cell population (Syed Abdul Rahman et al. 2013). Increasing evidence suggests that the induction of apoptosis, associated with cell cycle arrest, is a viable approach for anticancer agents (X. Li et al. 2018; Zhang et al. 2018). Flow cytometric analysis in this study revealed significant accumulation of MCF-7 cells in the G0/G1 and sub-G1 phases, 48 h post-treatment with hesperidin and luteolin, respectively. These results suggest that hesperidin induces cell cycle arrest in the G0/G1 phase, inhibiting the entry of DNA damaged cells into the S phase, and

possibly eliminating them through apoptosis. On the other hand, luteolin showed inhibition of cell cycle progression through sub-G1 arrest.

Disruption in mitochondrial function in response to apoptotic stimuli in the intrinsic pathway, results in activation of caspase-9 followed by effector caspase-3, leading to apoptotic cell death. This pathway is controlled by the Bcl-2 family proteins, including *Bax* and *Bid*, inducing apoptosis, and *Bcl-2* and *Bcl-xL* inhibiting apoptosis (Green & Llambi 2015). Thus, elevated expression levels of caspase-3 and -9 coupled with upregulation of pro-apoptotic *Bax* and downregulation *Bcl-2* (Figure 5), confirmed that hesperidin and luteolin-induced apoptosis in MCF-7, could be through the intrinsic apoptotic pathway. Interestingly, treatment with luteolin also resulted in significantly increased expression of caspase-8 (Figure 5a), suggesting that it could be multi-signalling and may induce apoptosis in MCF-7 through both the extrinsic and intrinsic pathways. Our observations pertaining to hesperidin and luteolin-induced apoptosis is in keeping with previous studies on the pro-apoptotic activity of hesperidin and luteolin in other cancer cells, including human NSCLC A549 *via* mitochondria-mediated apoptosis (Xia et al. 2018), MDA-MB-231 through novel downregulation of hTERT (Huang et al. 2019), and HeLa cells *via* a caspase-dependent pathway with G0/G1 cell cycle arrest (Wang et al. 2015).

There are no previous reports on the effect of flavonoids (hesperidin or luteolin) on apoptosis-related miRNAs and their correlation with their target genes. MicroRNAs have been implicated in several biological pathways, including apoptosis, cell cycle regulation, tumour progression, metastasis, cancer recurrence and chemo-resistance (Zadeh et al. 2016; Loh et al. 2019). In the present study, the expression of miR-16, -21, -34a, and their target gene *Bcl-2* was assessed 48 h post-treatment with 100 ug/mL of hesperidin or luteolin. Treatment with hesperidin and luteolin resulted in the upregulation of miR-16 and -34a, and downregulation of miR-21 and *Bcl-2* (Figure 5b and 6). Other studies demonstrated miR-16 and -34a as pro-apoptotic, negatively regulating anti-apoptotic *Bcl-2* genes and acting as tumour suppressors in breast

cancer cell lines (Sharma et al. 2016). Furthermore, upregulation of miR-16 and -34a was shown to promote apoptosis and cell cycle arrest in several *in vitro* studies (Momen-Heravi & Bala 2016; Mondal et al. 2019). On the other hand, miR-21 is an established, overexpressed oncomir in breast cancer, and various studies implicate its knockdown or downregulation with apoptosis induction, decreased cell proliferation, and re-sensitisation of cells to treatment (Du et al. 2017; Hu et al. 2018; F. Li et al. 2018; G. Li et al. 2018). Our results suggest that, in addition to modulation of key apoptosis related mRNA and activation of caspase, hesperidin and luteolin also induced apoptosis in MCF-7 through modulation of apoptotic miRNAs (*viz* miR-16, -21 and -34a). Modulation of the miRNAs could also have sensitised MCF-7 cells to hesperidin and luteolin treatment.

Furthermore, Pearson`s analysis revealed that the expression of miR-16 and -34a was inversely correlated with the expression of the target gene *Bcl-2*, as confirmed by the negative correlation. A positive correlation was observed between the expression of miR-21 and *Bcl-2*, indicating a co-downregulation of miR-21 and *Bcl-2*. It may be noted that cancer studies involving mRNA should include miRNA, as the modulators of these genes, thereby providing further anticancer targets. It is apparent from the correlations, that epigenetic control is a key aspect of cancer therapy.

5. Conclusion

This study demonstrated that the anticancer activity of natural polyphenolic flavonoids, hesperidin and luteolin, was mediated through the reduction of cell viability, inhibition of cell cycle progression, intrinsic and extrinsic apoptotic pathways with upregulation of proapoptotic *Bax* gene, and downregulation of the anti-apoptotic *Bcl-2* gene. Furthermore, this study provides new insights on the effect of hesperidin and luteolin on the expression of apoptotic

miRNAs and their relationship with their target genes, broadening the understanding of molecular mechanisms involved in flavonoid-induced cell death.

Conflict of interest

The author(s) confirm no conflict of interest.

References

Abotaleb M, Samuel SM, Varghese E, Varghese S, Kubatka P, Liskova A, Büsselberg D. 2019. Flavonoids in cancer and apoptosis. Cancers (Basel). 11.

Arteaga CL, Adamson PC, Engelman JA, Gaynor RB, Hilsenbeck SG, Limburg PJ, Lowe SW, Mardis ER, Ramsey SD, Rebbeck TR, et al. 2014. Cancer Progress Report 2014. Clin Cancer Res.: clincanres.2123.2014.

Aung T, Qu Z, Kortschak R, Adelson D, Aung TN, Qu Z, Kortschak RD, Adelson DL. 2017. Understanding the effectiveness of natural compound mixtures in cancer through their molecular mode of action. Int J Mol Sci. 18:656.

Cui J, Placzek WJ. 2018. Post-transcriptional regulation of anti-apoptotic BCL2 family members. Int J Mol Sci. 19.

Dayem AA, Choi HY, Yang GM, Kim K, Saha SK, Cho SG. 2016. The anti-cancer effect of polyphenols against breast cancer and cancer stem cells: Molecular mechanisms. Nutrients. 8.

Du G, Cao D, Meng L. 2017. MiR-21 inhibitor suppresses cell proliferation and colony formation through regulating the PTEN/AKT pathway and improves paclitaxel sensitivity in cervical cancer cells. Mol Med Rep. 15:2713–2719.

Green DR, Llambi F. 2015. Cell death signaling. Cold Spring Harb Perspect Biol. 7.

Hu WZ, Tan CL, He YJ, Zhang GQ, Xu Y, Tang JH. 2018. Functional miRNAs in breast cancer drug resistance. Onco Targets Ther. 11:1529–1541.

Huang L, Jin K, Lan H. 2019. Luteolin inhibits cell cycle progression and induces apoptosis of breast cancer cells through downregulation of human telomerase reverse transcriptase. Oncol Lett. 17:3842–3850.

Hussain S, Cevik E, Tombuloglu H, Farag K, Said O. 2019. miRNA profiling in MCF-7 breast cancer cells: Seeking a new biomarker. J Biomedical Sci.8(2):3.

Imani S, Wu R-C, Fu J. 2018. MicroRNA-34 family in breast cancer: from research to therapeutic potential. J Cancer. 9.

Jang CH, Moon N, Oh J, Kim JS. 2019. Luteolin shifts oxaliplatin-induced cell cycle arrest at g0/g1 to apoptosis in hct116 human colorectal carcinoma cells. Nutrients. 11:1–14.

Jaudan A, Sharma S, Malek SNA, Dixit A. 2018. Induction of apoptosis by pinostrobin in human cervical cancer cells: Possible mechanism of action.Hsieh Y-H, editor. PLoS One. 13: e0191523.

Jiang X, Liu Y, Zhang G, Lin S, Wu J, Yan X, Ma Y, Ma M. 2020. Aloe-emodin induces breast tumor cell apoptosis through upregulation of miR-15a/miR-16-1 that suppresses BCL2. Evid Based Complementary Altern Med. 11:1-10.

Jin H, Ko YS, Park SW, Chang KC, Kim HJ. 2019. 13-Ethylberberine induces apoptosis through the mitochondria-related apoptotic pathway in radiotherapy-resistant breast cancer cells. Molecules. 24.

Khan F, Ahmed F, Pushparaj PN, Abuzenadah A, Kumosani T, Barbour E, AlQahtani M, Gauthaman K. 2016. Ajwa Date (*Phoenix dactylifera* L.) extract inhibits human breast adenocarcinoma (MCF7) cells in vitro by inducing apoptosis and cell cycle arrest. PLoS One. 11:1-27.

Li F, Lv JH, Liang L, Wang J chao, Li CR, Sun L, Li T. 2018. Downregulation of microRNA21 inhibited radiation-resistance of esophageal squamous cell carcinoma. Cancer Cell Int. 18:39.

Li G, Song Y, Li Gangcan, Ren J, Xie J, Zhang Y, Gao F, Mu J, Dai J. 2018. Downregulation of microRNA-21 expression inhibits proliferation and induces G1 arrest and apoptosis via the PTEN/AKT pathway in SKM-1 cells. Mol Med Rep. 18:2771–2779.

Li X, Qiu Z, Jin Q, Chen G, Guo M. 2018. Cell cycle arrest and apoptosis in HT-29 cells induced by dichloromethane fraction from *Toddalia asiatica* (L.) Lam. Front Pharmacol. 9:629.

Loh HY, Norman BP, Lai KS, Rahman NMANA, Alitheen NBM, Osman MA. 2019. The regulatory role of microRNAs in breast cancer. Int J Mol Sci. 20.

Magura J, Moodley R, Maduray K, Mackraj I. 2020. Phytochemical constituents and *in vitro* anticancer screening of isolated compounds from *Eriocephalus africanus*. Nat Prod Res. DOI: 10.1080/14786419.2020.1744138

Matsuo M, Sasaki N, Saga K, Kaneko T. 2005. Cytotoxicity of flavonoids toward cultured normal human cells. Biol. Pharm. Bull. 28:253–259.

Mei Z, Su T, Ye J, Yang C, Zhang S, Xie C. 2015. The miR-15 family enhances the radiosensitivity of breast cancer cells by targeting G2 checkpoints. Radiat Res. 183:196–207.

Menezes JCJMDS, Orlikova B, Morceau F, Diederich M. 2016. Natural and synthetic flavonoids: structure–activity relationship and chemotherapeutic potential for the treatment of leukemia. Crit Rev Food Sci Nutr. 56: S4–S28.

Millimouno FM, Dong J, Yang L, Li J, Li X. 2014. Targeting apoptosis pathways in cancer and perspectives with natural compounds from mother nature. Cancer Prev Res. 7:1081–1107.

Mohammad RM, Muqbil I, Lowe L, Yedjou C, Hsu HY, Lin LT, Siegelin MD, Fimognari C,

Kumar NB, Dou QP, et al. 2015. Broad targeting of resistance to apoptosis in cancer. Semin Cancer Biol. 35: S78–S103.

Momen-Heravi F, Bala S. 2016. The miRNA and extracellular vesicles in alcoholic liver disease. In: Mol Asp Alcohol Nutr A Vol Mol Nutr Ser. [place unknown]: Elsevier Inc; p. 275–286.

Mondal I, Sharma S, Kulshreshtha R. 2019. MicroRNA therapeutics in glioblastoma: Candidates and targeting strategies. In: AGO-Driven Non-Coding RNAs. [place unknown]: Elsevier; p. 261–292.

Papademetrio DL, Trabucchi A, Cavaliere V, Ricco R, Costantino S, Wagner ML, Álvarez E. 2013. The catechin flavonoid reduces proliferation and induces apoptosis of murine lymphoma cells LB02 through modulation of antiapoptotic proteins. Brazilian J Pharmacogn. 23:455–463.

Pfeffer CM, Singh ATK. 2018. Apoptosis: A target for anticancer therapy. Int J Mol Sci. 19.

Pilco-Ferreto N, Calaf GM. 2016. Influence of doxorubicin on apoptosis and oxidative stress in breast cancer cell lines. Int J Oncol. 49.

Schmittgen TD, Livak KJ. 2008. Analyzing real-time PCR data by the comparative C(T) method. Nat Protoc. 3:1101–8.

Shahali A, Ghanadian M, Jafari SM, Aghaei M. 2018. Mitochondrial and caspase pathways are involved in the induction of apoptosis by nardosinen in MCF-7 breast cancer cell line. Res Pharm Sci. 13:12–21.

Sharma S, Patnaik PK, Aronov S, Kulshreshtha R. 2016. ApoptomiRs of breast cancer: Basics to clinics. Front Genet. 7.

Srivastava SK, Arora S, Averett C, Singh S, Singh AP. 2015. Modulation of micrornas by phytochemicals in cancer: Underlying mechanisms and translational significance. Biomed Res Int. 2015.

Sun X, Zhang H, Zhang Y, Yang Q, Zhao S. 2018. Caspase-dependent mitochondrial apoptotic pathway is involved in astilbin-mediated cytotoxicity in breast carcinoma cells. Oncol Rep. 40:2278–2286.

Syed Abdul Rahman SN, Abdul Wahab N, Abd Malek SN. 2013. In vitro morphological assessment of apoptosis induced by antiproliferative constituents from the rhizomes of *Curcuma zedoaria*. Evidence-based Complement Altern Med. 2013.

Tu B, Chen Z-F, Liu Z-J, Li R-R, Ouyang Y, Hu Y-J. 2015. Study of the structure-activity relationship of flavonoids based on their interaction with human serum albumin. RSC Adv. 5:73290–73300.

Venkatadri R, Muni T, Iyer AKV, Yakisich JS, Azad N. 2016. Role of apoptosis-related miRNAs in resveratrol-induced breast cancer cell death. Cell Death Dis. 7: e2104.

Venkatarame V, Saralamma G, Kim EH, Lee HJ, Raha S, Lee WS, Doo J. 2017. Flavonoids: A new generation molecule to stimulate programmed cell deaths in cancer cells. J Biomed Transl Res. 18:30–37.

Wang Y, Yu H, Zhang J, Gao J, Ge X, Lou G. 2015. Hesperidin inhibits HeLa cell proliferation through apoptosis mediated by endoplasmic reticulum stress pathways and cell cycle arrest. BMC Cancer 2015 151. 15:1–11.

Wang ZX, Lu B Bin, Wang H, Cheng ZX, Yin YM. 2011. MicroRNA-21 modulates chemosensitivity of breast cancer cells to doxorubicin by targeting PTEN. Arch Med Res. 42:281–290.

Xia R, Sheng X, Xu X, Yu C, Lu H. 2018. Hesperidin induces apoptosis and GO/G1 arrest in human non-small cell lung cancer A549 cells. Int J Mol Med. 41:464–472.

Xie X, Huang Y, Chen L, Wang J. 2018. miR-221 regulates proliferation and apoptosis of ovarian cancer cells by targeting BMF. Oncol Lett. 16:6697–6704.

Zadeh MM, Motamed N, Ranji N, Majidi M, Falahi F. 2016. Silibinin-induced apoptosis and downregulation of microRNA-21 and MicroRNA-155 in MCF-7 human breast cancer cells. J Breast Cancer. 19:45–52.

Zhang H-W, Hu J-J, Fu R-Q, Liu X, Zhang Y-H, Li J, Liu L, Li Y-N, Deng Q, Luo Q-S, et al.2018. Flavonoids inhibit cell proliferation and induce apoptosis and autophagy through downregalation of PI3Kγ mediated PI3K/AKT/mTOR/p70S6K/ULK in human breast cancer cells. Sci Rep. 8:11255.

Zhang L, Zhou L, Shi M, Kuang Y, Fang L. 2018. Downregulation of miRNA-15a and miRNA-16 promote tumor proliferation in multiple myeloma by increasing CABIN1 expression. Oncol Lett. 15:1287–1296.

Zhou Y, Ding BZ, Lin YP, Wang HB. 2018. MiR-34a, as a suppressor, enhance the susceptibility of gastric cancer cell to luteolin by directly targeting HK1. Gene. 644:56–65.

SUPPLEMENTARY MATERIAL

The effect of hesperidin and luteolin isolated from *Eriocephalus africanus* on apoptosis, cell cycle and miRNA expression in MCF-7

Judie Magura[a], Roshila Moodley[b*], Irene Mackraj[a].

[a]School of Laboratory Medicine and Medical Sciences, University of KwaZulu–Natal, Durban, South Africa

[b]School of Chemistry and Physics, University of KwaZulu–Natal, Durban, South Africa

*Corresponding author: Roshila Moodley; School of Chemistry and Physics, College of Agriculture, Engineering and Science, University of KwaZulu-Natal (Westville), P.O. Box: X54001, Durban, South Africa; Tel/Fax: +27 31 260 8127, +27 84 606 7710; E-mail: Moodleyrosh@ukzn.ac.za

1. Structural influence of flavonoids on cytotoxicity in MCF-7 cells

To evaluate the structural influence of flavonoids on cytotoxicity in MCF-7, the effect of flavonoids with slight differences in their moiety *viz*; hesperidin, luteolin, quercetin, apigenin, taxifolin, eriodictyol, chrysin and hesperetin, on MCF-7 cell viability was investigated using the MTT assay. The results are illustrated in Figure S1.
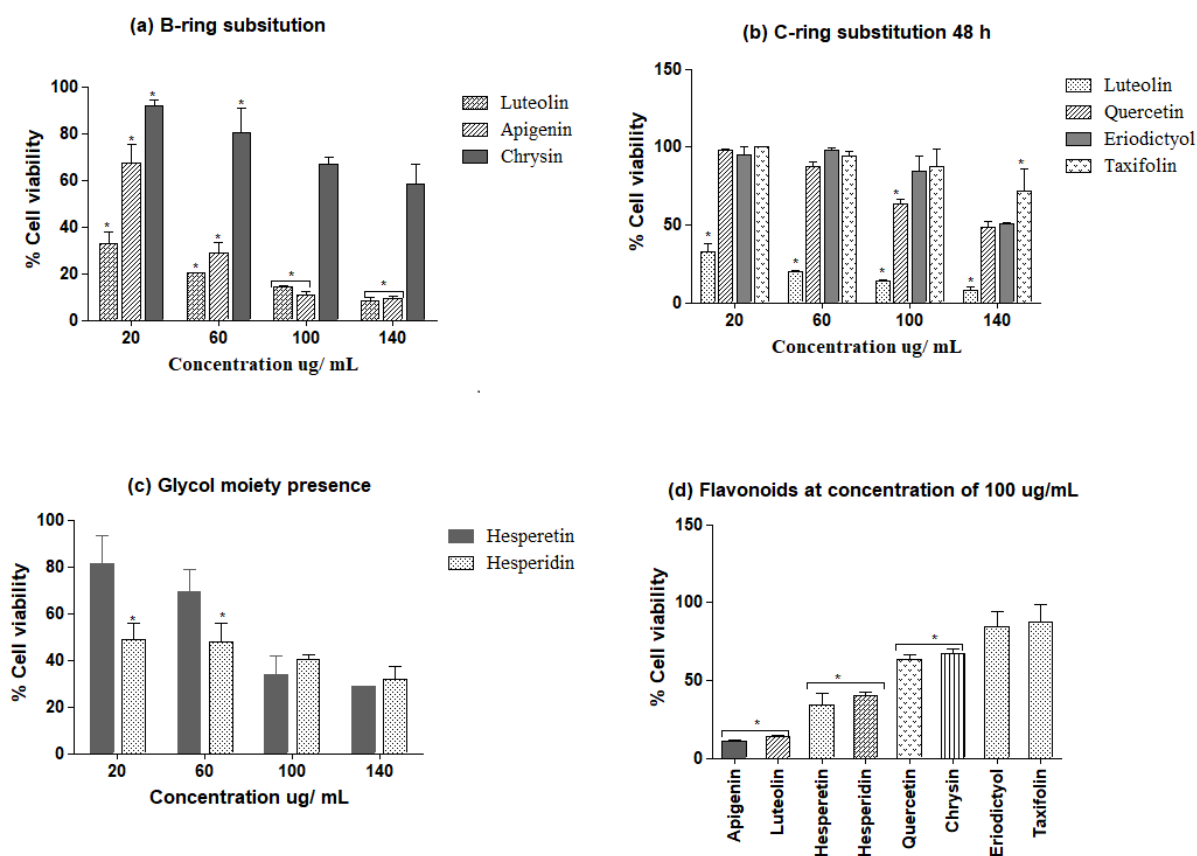

Figure S1. Cytotoxic activity of different flavonoids in MCF-7 at concentrations of 20 – 140 µg/mL and 48 h incubation. (a) represents comparative cytotoxicity among flavonoids with variation in -OH substitution in the B-ring, (b) flavonoids with or without a 2,3-double bond in the C-ring and -OH substitution, (c) flavonoids with or without a glycol moiety. Values are presented as mean ± SD of three experimental replicates, *, statistically significant difference at $p < 0.05$.
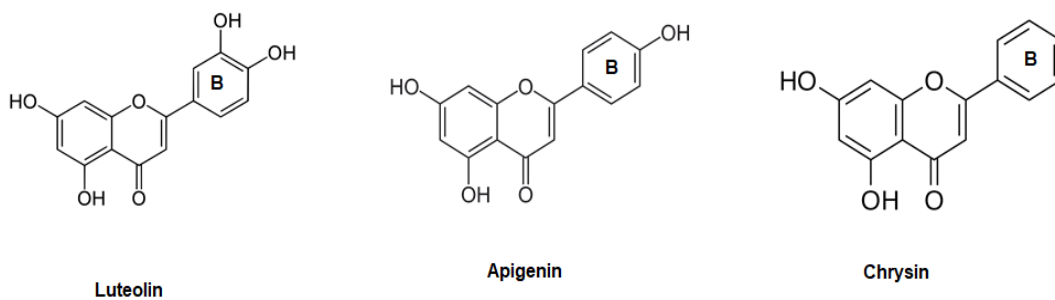
Luteolin   Apigenin   Chrysin

Figure S2. Molecular structures of flavonoids with varying -OH substitution in the B-ring

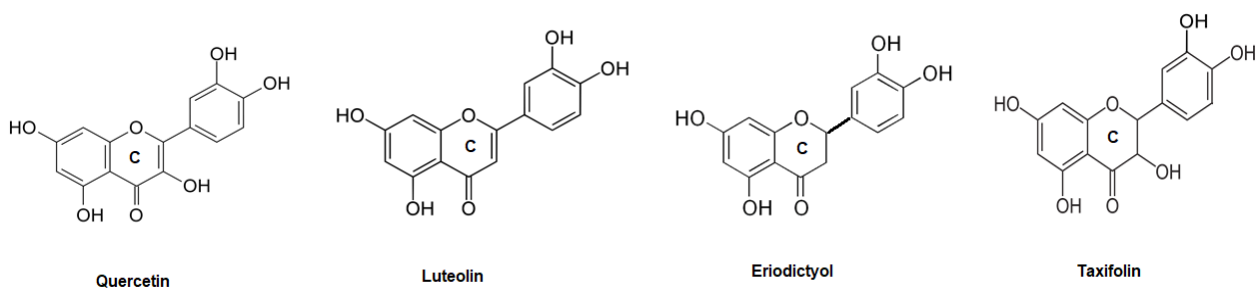Quercetin   Luteolin   Eriodictyol   Taxifolin

Figure S3. Molecular structures of flavonoids with or without the 2,3 double bond and varying -OH substitution in the C-ring

Hesperidin   Hesperitin
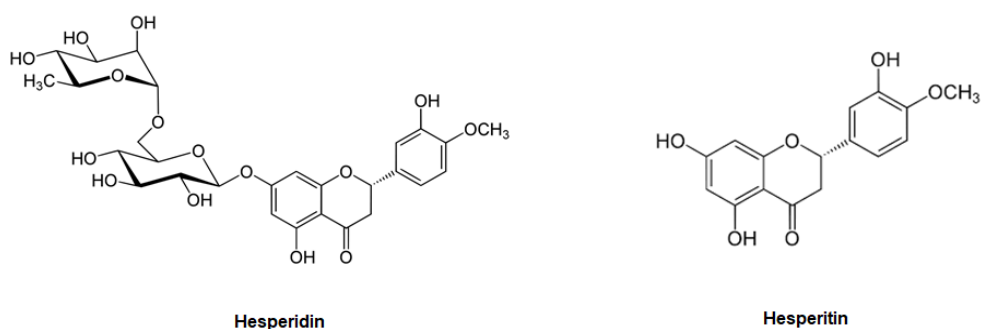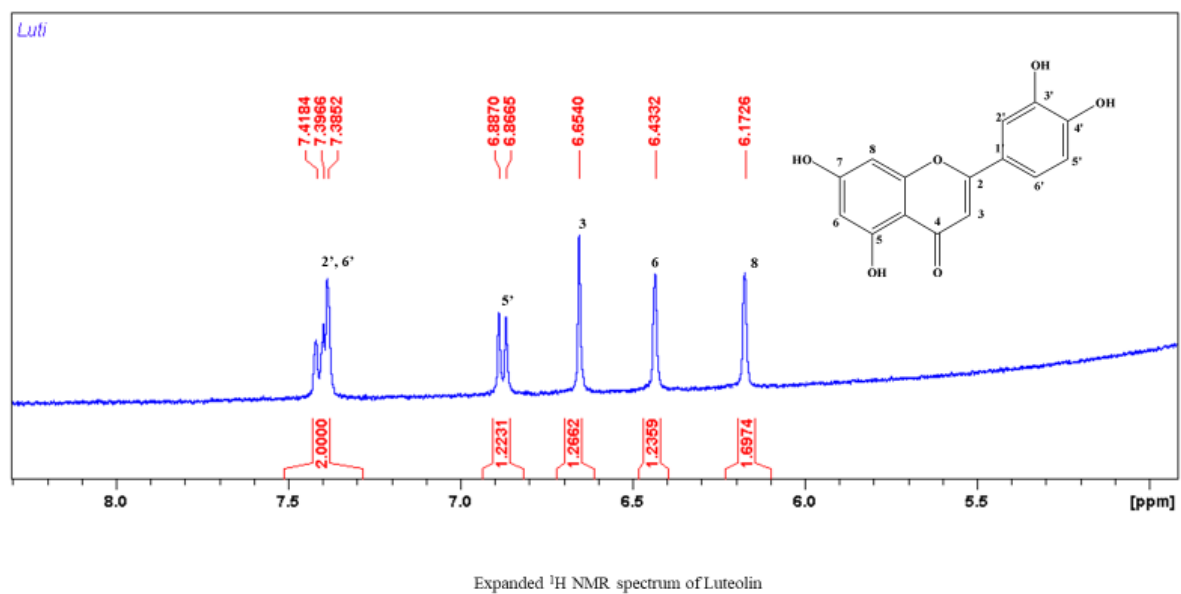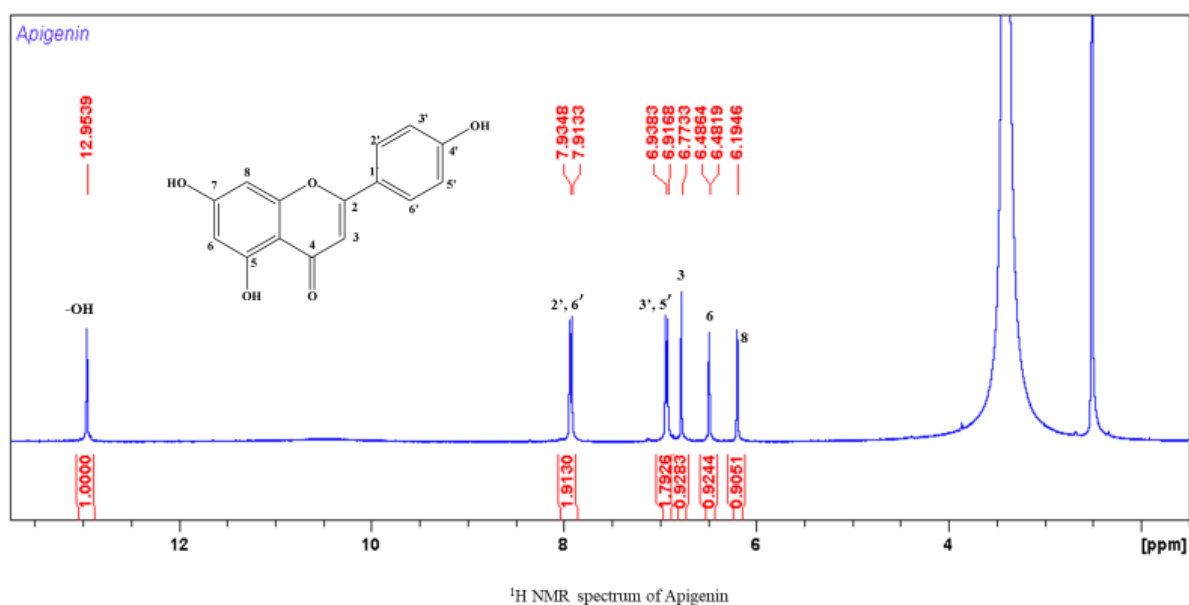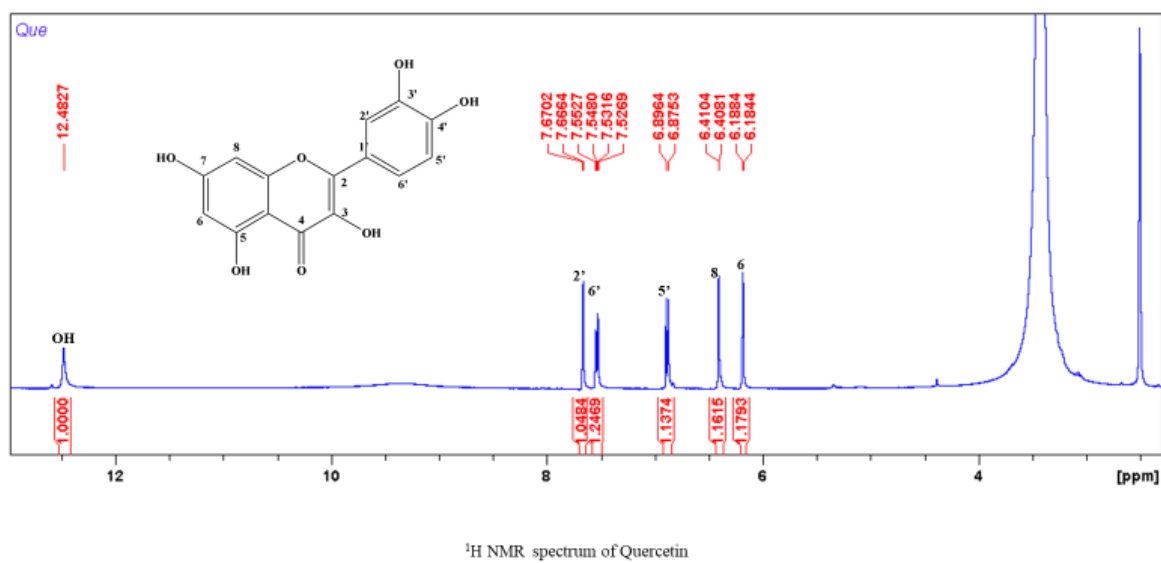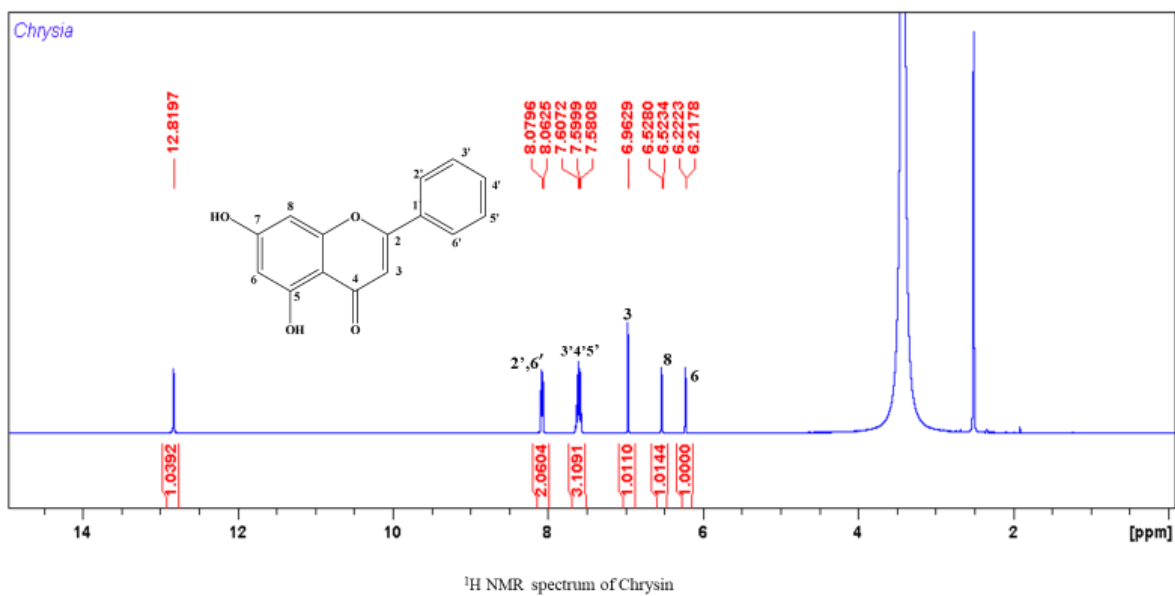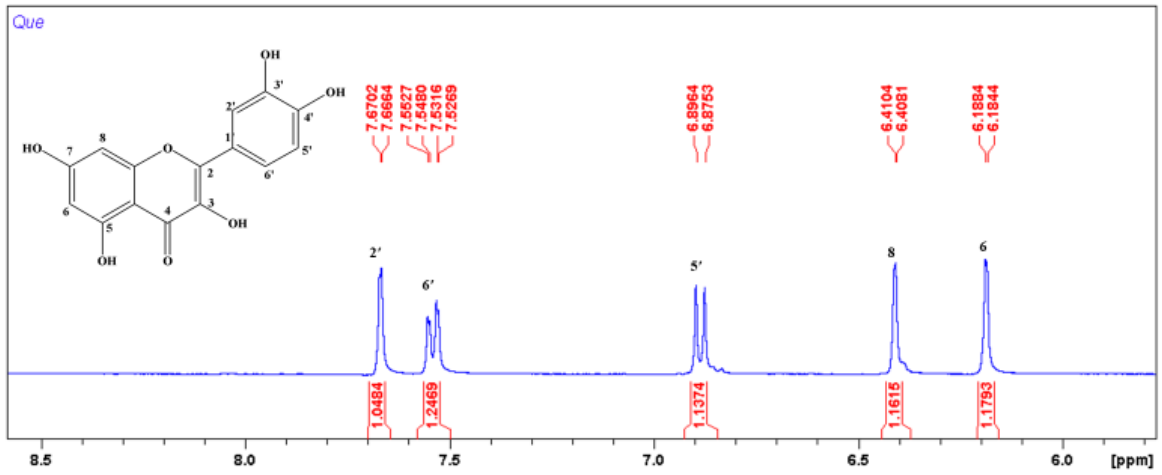
Figure S4. Molecular structures of flavonoids with or without the glycol moiety.
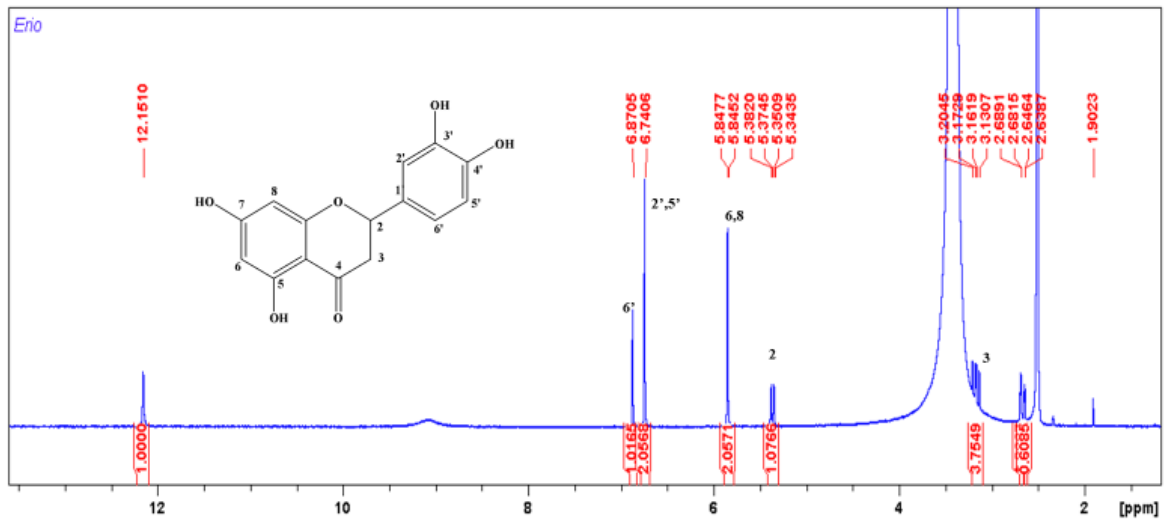
2. ^{1}H NMR spectra of the flavonoids

^{1}H NMR spectrum of Apigenin

Expanded ^{1}H NMR spectrum of Luteolin

93

¹H NMR spectrum of Chrysin
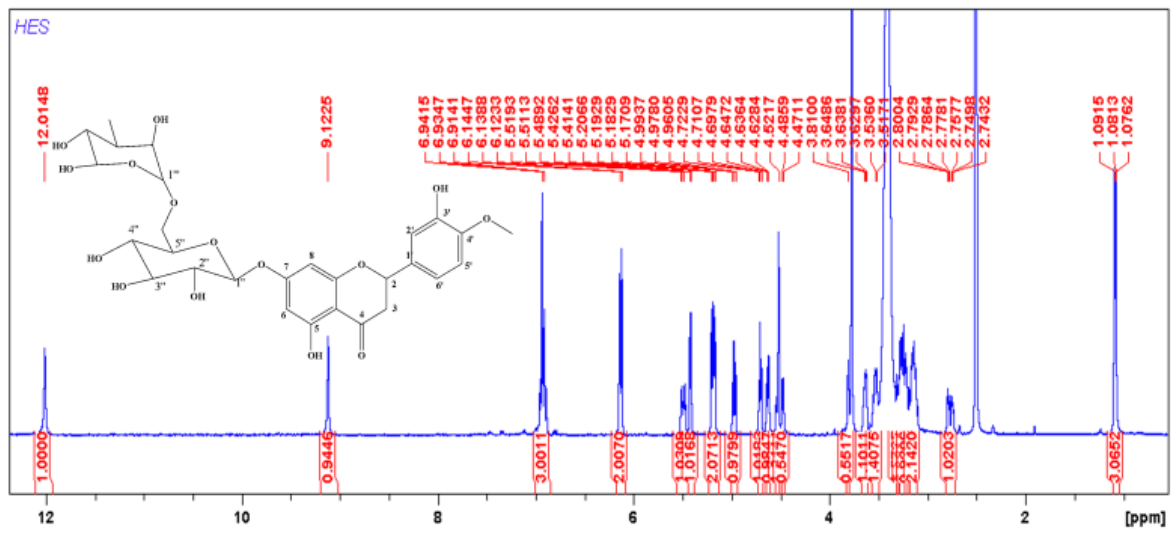

¹H NMR spectrum of Quercetin

Expanded ^{1}H NMR spectrum of Quercetin

^{1}H NMR spectrum of Eriodictyol
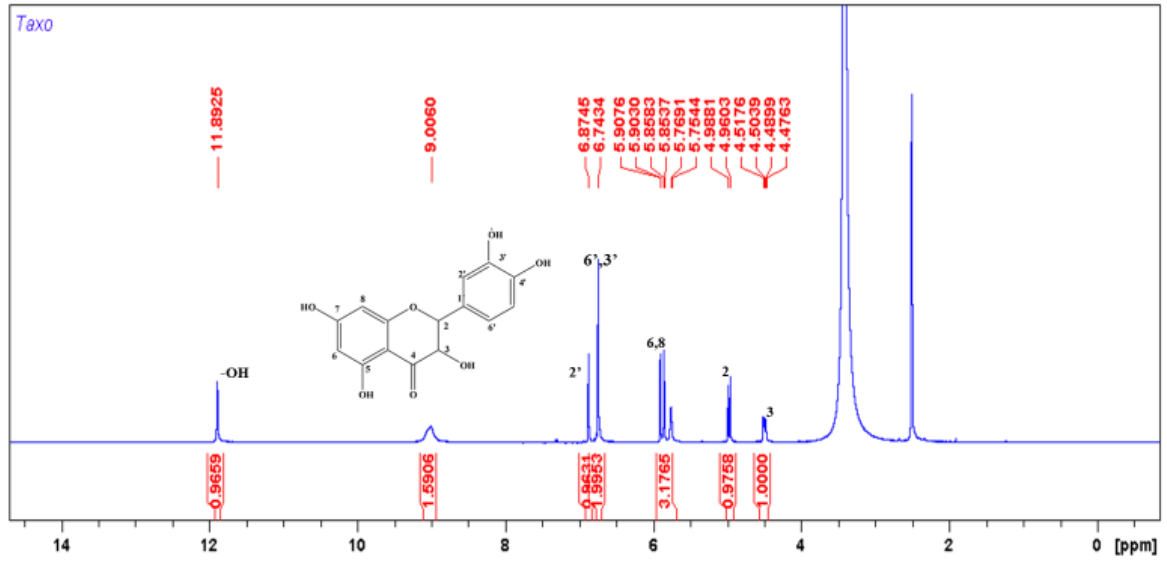
^{1}H NMR spectrum of Taxifolin

^{1}H NMR spectrum of Hesperidin

Expanded ^{1}H NMR spectrum of Hesperidin

^{1}H NMR spectrum of Hesperitin
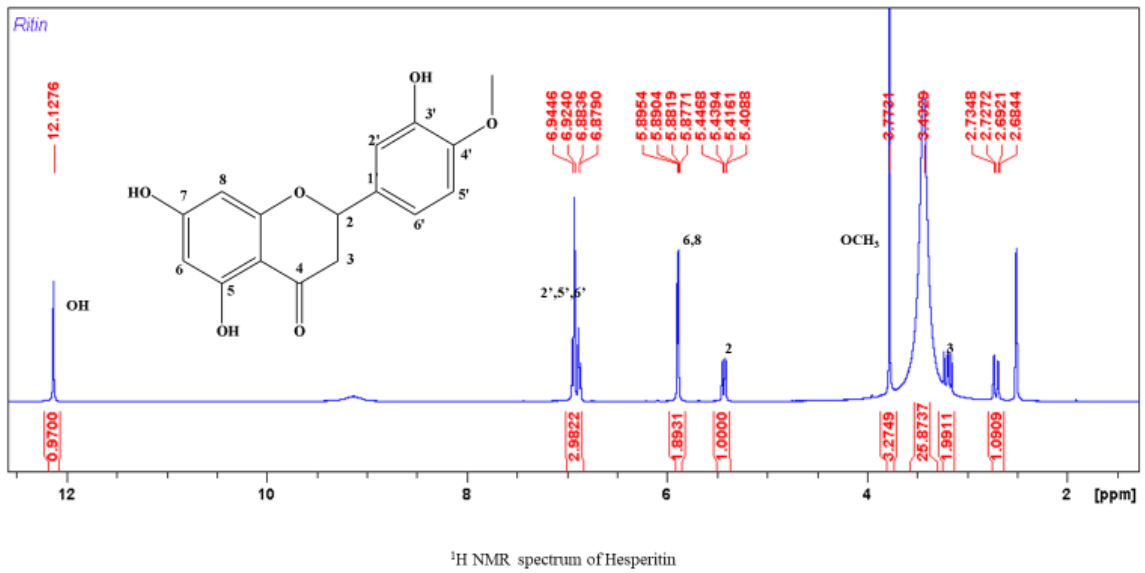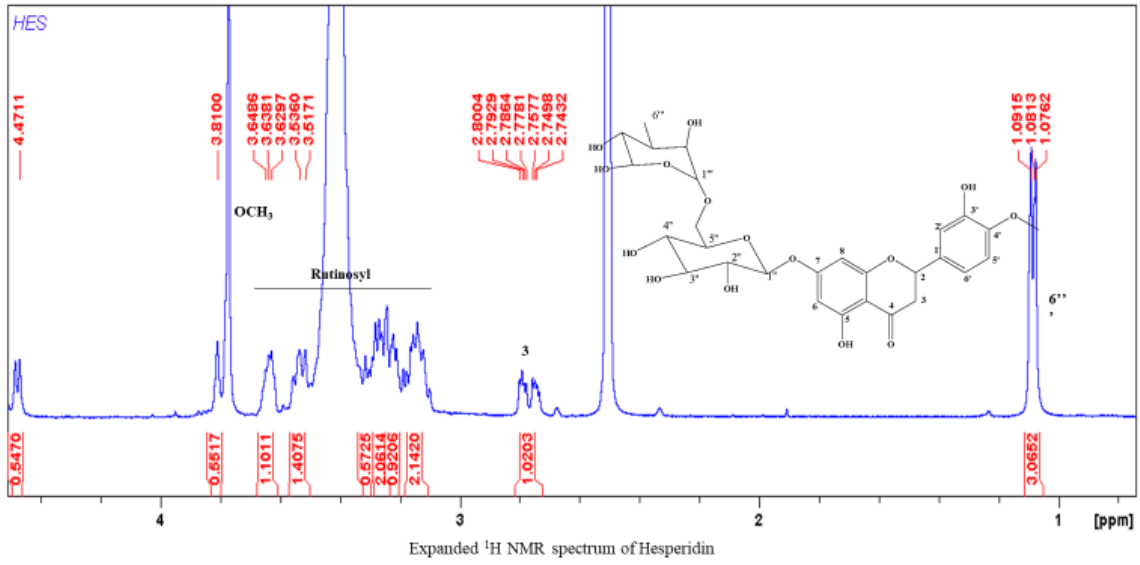
4.   CHAPTER FOUR: MANUSCRIPT THREE

4.1 Hesperidin-loaded nanoemulsions improve cytotoxicity, induces apoptosis and downregulates miR-21 and miR-155 expression in MCF-7

Submitted to: Journal of Drug Targeting

Chapter three demonstrated the therapeutic potential of the isolated flavonoids in breast cancer as evidenced by their effect on the apoptotic pathway, the expression of key apoptotic miRNAs and cell cycle progression in MCF-7, a luminal A breast cancer model. However, literature has shown flavonoids to generally have low bioavailability and poor solubility in aqueous media which often hampers their clinical application. During our preparations and experimental investigations, we also observed the acclaimed poor aqueous solubility; therefore, we designed nanosystems to circumvent these drawbacks. The biosafety evaluations of the hesperidin and luteolin nano-formulations proved the synthesised hesperidin-loaded nanoemulsions to be safe, in contrast to the luteolin nano-formulation. Therefore, chapter four details their synthesis and characterisation, and further explores the anticancer potential of the novel hesperidin-loaded nanoemulsions.

This chapter is formatted according to the journal specifications.

Hesperidin-loaded nanoemulsions improve cytotoxicity, induces apoptosis and downregulates miR-21 and miR-155 expression in MCF-7

Judie Magura[a], Daniel Hassan[b], Roshila Moodley[c*], Irene Mackraj[a].

[a] *School of Laboratory Medicine and Medical Sciences, University of KwaZulu–Natal, Durban, South Africa*

[b]*Discipline of Pharmaceutical Sciences, University of KwaZulu–Natal, Durban, South Africa*

[c]*School of Chemistry and Physics, University of KwaZulu–Natal, Durban, South Africa*

Abstract

Hesperidin, a ubiquitous plant-based flavanone, demonstrates excellent therapeutic properties, but due to poor solubility and bioavailability, its therapeutic effects are limited. Therefore, in this study, hesperidin was encapsulated into nanoemulsions (HP-NEM) to improve its solubility and achieve enhanced bioavailability and efficacy in breast cancer treatment using MCF-7 cell lines. Furthermore, this study assessed the cytotoxic and apoptotic effects of HP-NEM against MCF-7 and their effects on oncomiRs, microRNA-21 and microRNA-155 expression. A spontaneous emulsification method was used to formulate HP-NEM and its physicochemical properties were evaluated. The optimised HP-NEM displayed a spherical shape with 305 ± 40.8 nm, 0.308 ± 0.04, -11.6 ± 3.30 mV and $93 \pm 0.45\%$ for particle size, polydispersity index (PDI), zeta-potential (ζ) and encapsulation efficiency, respectively. The *in vitro* drug release profile demonstrated a sustained release of hesperidin from the nanoemulsions over a 48 h period. Cytotoxicity studies using MTT assay, showed selective toxicity of the HP-NEM against MCF-7, without affecting normal cells (HEK 293). Treatment with the HP-NEM induced cell death through apoptosis, cell cycle arrest in the G2/M phase

and downregulated miR-21 and miR-155 expression in MCF-7. This study supports the use of HP-NEM as a potential therapeutic agent in breast cancer treatment.

Introduction

Breast cancer is one of the most frequently diagnosed malignancies in women and is the second-highest cause of cancer death, worldwide [1,2]. Over the last ten years, there have been significant advancements in understanding the genetic and molecular basis of breast cancer [3], leading to a heightened interest in unravelling effective therapeutic approaches for the alleviation of the breast cancer pandemic.

Hesperidin, a naturally occurring 3',5,7-trihydroxy-4'-methoxy flavanone glycoside, commonly found in citrus fruits, was recently isolated from *Eriocephalus africanus* (wild rosemary) [4]**.** Hesperidin, and its aglycone hesperetin, have shown promising antioxidant and anticancer activity [5,6]. Furthermore, it has been implicated in several anticancer mechanisms, such as inhibition of angiogenesis, induction of apoptosis, cell cycle arrest, and modulation of regulatory proteins in cancer cells [7-9]. However, similar to most flavonoids, hesperidin has not yet been fully adopted, clinically, mainly due to its hydrophobic nature, resulting in poor bioavailability and low solubility in aqueous media [10,11]. Pharmacokinetic studies have shown that hesperidin is poorly absorbed and rapidly cleared, with less than 25% cumulative urinary recovery following oral administration, and non-detectable concentrations in circulating plasma after a single dose of 10 mg/kg *in vivo* [12,13]. Several lipid-based nanosystems, such as liposomes, solid lipid nanoparticles (SLN), microemulsions, micelles, and oil in water emulsions, have been reported as improving the solubility and bioavailability of flavonoids [14,15]. Additionally, hesperidin has previously been fabricated into a

chitosan/gelatin coated cargo known as hesperidin-loaded microparticles, hesperidin-PLGA/Poloxamer 407 nanoparticles and hesperidin-loaded solid lipid nanoparticles, to enhance its bioavailability, solubility, therapeutic effects and systemic circulation [16-18]. Furthermore, formulation of hesperidin into a nanosuspension demonstrated its enhancement due to the nanocrystalline formulation and not the micellar contribution of poloxamer 188 [19]. However, none of these studies, report on the nano emulsification of hesperidin or explore the use of polyethylene glycol (PEG) and Tween® 80 for the formulation of hesperidin nanoemulsions. Therefore, this study explores the use of Tween® 80, due to its self-emulsifying properties, safety and biocompatibility in cells, and PEG (a hydrophilic, non- toxic polymer) to formulate hesperidin-loaded nanoemulsions.

Nanoemulsions are colloidal oil-in-water/water-in-oil dispersions, ranging from 20 to 500 nm in size, that are appropriate for use in the formulation of drug vehicles for hydrophobic molecules [20]. Nanoemulsions could be advantageous in improving the efficacy of hesperidin in cancer treatment due to their ability to escape rapid renal clearance, minimal adverse effects to neighbouring healthy cells, enhanced drug solubility and bioavailability, and improved absorption [21]. Furthermore, nanoemulsions improve specificity in drug targeting by exploiting the differences between tumour cells and normal cells. For example, *in vivo,* rapidly growing cancer cells are often characterized by leaky vasculature and a poor lymphatic drainage system. Nanoemulsions due to their size can be exploited to passively accumulate in the tumour microenvironment through the enhanced permeability and retention effect (EPR), thereby improving targeting and enhancing efficacy [22]. The vascular pore size for most solid tumours varies between 380 nm and 780 nm depending on the tumour type and growth. Thus, nanoemulsions with a particle size less than 400 nm can easily permeate into the tumour microenvironment and be retained for long periods [22,23].

Cancer is a complex disease characterized by uncontrolled cell proliferation, influenced by dysregulated cellular and molecular pathways. Until recently, these dysregulations were mostly accredited to abnormalities in oncogenes and tumour suppressor genes. However, currently, there is a focus on the posttranscriptional regulatory role of miRNAs, which modulate crucial signalling pathways related to apoptosis, cell cycle progression, and proliferation [24]. Dysregulation of miRNAs has been implicated in the progression of carcinogenesis, and the aberrant expression of oncogenic miRNAs (oncomiRs), have been shown to influence tumour progression through suppressing apoptosis and allowing cell proliferation in various types of cancers [25]. Due to the ability of oncomiRs to act as oncogenes, they can be exploited as attractive therapeutic targets in cancer treatment. Overexpression of oncomiRs, miRNA-21 and miRNA-155 in breast and lung cancer has been implicated in cell differentiation, apoptosis, tumour progression and metastasis [26-29]. Previous *in vitro* studies have demonstrated that knockdown of miR-21 expression suppresses the growth and proliferation of cells in MCF-7 [30]. Furthermore, inhibition of miR-155 in an allograft mouse model suppressed the growth of the breast tumour in mice, and knockdown of miR-155 in breast cancer cell lines decreased cell proliferation [31,32]. These reports support the inhibition of miR-21 and miR-155 as therapeutic targets in breast cancer treatment.

Thus far, there are no known reports on the formulation of hesperidin into nanoemulsions, therapeutic potential of HP-NEM in breast cancer and epigenetic control. Therefore, this study evaluated the encapsulation of hesperidin into nanoemulsions, and compared the cytotoxicity of the optimised hesperidin-loaded nanoemulsions (HP-NEM) to hesperidin alone, in MCF-7. Thereafter, the effect of HP-NEM on apoptosis and cell cycle arrest in MCF-7, and the expression of oncomiRs (miR-21 and miR-155) was investigated.

Materials and Methods

Chemicals

Cell culture, dimethyl sulfoxide (DMSO), 3-(4,5-dimethyl-2-thiazolyl)-2,5-diphenyl-2H-tetrazolium bromide (MTT), polyethylene glycol 2000 (PEG-2000), Tween® 80 and hesperidin were purchased from Sigma-Aldrich, Germany. Foetal bovine serum (FBS), Dulbecco's phosphate-buffered saline (DPBS), Dulbecco's modified Eagle's medium (DMEM), and trypsin were obtained from Biowest, USA. Antibiotic-Antimycotic was obtained from Gibco by Life Technologies. Fresh sheep blood was purchased from Polychem Handelsges (South Africa). The kits used for the apoptosis and cell cycle analysis were obtained from BD Pharmingen™, California San Jose, USA. Purelink miRNA isolation kit (ThermoFischer Scientific, USA), SensiFast™ cDNA synthesis kit (Bioline, USA), SYBR green (Roche Diagnostics, IN, USA) and specific primers were synthesized from Inqaba Biotec™ laboratories, South Africa. All other reagents and solvents were of analytical grade.

Synthesis of hesperidin-loaded nanoemulsions

Hesperidin-loaded nanoemulsions (HP-NEM) were prepared based on a previously described spontaneous emulsification technique with some modifications [33]. Based on prior optimisation, 6.25 mg of hesperidin was dissolved in 1.25 mL of DSMO and sonicated for 30 min. Thereafter, 50 mg of Tween® 80 dissolved in 1.25 mL of DMSO was added to the hesperidin solution and homogenised for 30 min at room temperature. Thereafter, 50 mg of the stabilizer, PEG-2000 dissolved in 5 mL, was added. The nanoemulsions were obtained on stirring the hesperidin and Tween® 80 mixture in 20 mL of water for 24 h.

Physico-chemical properties (particle size, polydispersity index (PDI), zeta-potential (ζ)) and morphology characterisation

The particle size, polydispersity index (PDI), and zeta-potential (ζ) of the prepared HP-NEM diluted in deionised water in the ratio of 1:9 were obtained using a Zetasizer Nano ZS (Malvern Instruments Corp, UK) at room temperature. For the morphological characteristics, high resolution-transmission electron microscopy (HR-TEM) (Joel, JEM-1000, voltage of 100 kV) was used to capture the micrographs. The samples were prepared by the dropwise loading of the nanoemulsions onto a carbon-coated grid. These were allowed to dry then viewed using HR-TEM.

Encapsulation efficiency

The amount of hesperidin entrapped in the nanoemulsions was determined by a simple ultrafiltration method [34]. A 3 mL aliquot of nanoemulsions, with a calculated concentration of 250 µg/mL, was transferred into Amicon® Ultra-4 centrifugal filter tubes, pore size 10 kDa (Millipore Corp., USA), and centrifuged at 3000 rpm at room temperature for 30 minutes. Thereafter, the absorbance of the untrapped hesperidin, in the filtrate, was recorded at 280 nm using a Shimadzu UV-Vis 1601 (Japan) and calibration curve was employed to determine the amount of untrapped hesperidin. The encapsulation efficiency (EE) (percentage) was calculated from equation **1**:

$$EE\ \% = \left(\frac{\text{Weight of hesperidin in the nanoemulsion}}{\text{Weight of hesperidin initially added at preparation}} \right) \times 100 \ \dots\dots\dots Eq.\ 1$$

In vitro drug release

For the drug release study, 1 mL of the prepared nanoemulsions was filled into a sealed dialysis bag with a molecular-weight-cut-off of 14 kDa and 8 mm in diameter. The dialysis bag was immersed into a bottle of the release medium which was phosphate buffer saline (PBS) at pH

7.4 (40 mL) and incubated at 37 °C on an orbital shaker maintained at 100 rpm [35]. At time intervals of 0.5, 1, 2, 3, 4, 5, 6, 7, 8, 12, 24, and 48 h, samples of 3 mL were collected and replaced with the same amount of fresh release medium to maintain sink conditions. The concentration of the HP-NEM in the collected samples was quantified spectrophotometrically at 280 nm using a Shimadzu UV-Vis 1601 (Japan), with suitable blanks. The cumulative release percentage was computed using the standard calibration curve and equation **2**:

$$\% \text{ Cumulative release profile } = \left(\frac{At}{Ai}\right) \times 100\,\% \text{.................} Eq.\ 2$$

where A*t*, is the amount of hesperidin released from HP-NEM at time t and A*i* is the amount of hesperidin initially encapsulated into the nanoemulsions.

Haemolysis assay

The haemolysis assay was carried out to determine the blood compatibility of the prepared HP-NEM. Firstly, the nanoemulsions were diluted to concentrations of 50, 100, 150, 200, and 250 µg/mL in PBS (pH 7.4). Thereafter, 200 µL of fresh sheep blood was added to 800 µL of nanoemulsion at each concentration, followed by incubation at 37 °C for 1 h. PBS and pure water without the nanoemulsions served as the negative and positive controls, respectively. After incubation, the samples were centrifuged for 5 min at 10 000 rpm, and 200 µL of the supernatant was drawn and added to a 96-well plate. The absorbance was measured at 540 nm using a microplate reader (SPECTROstar Nano, BMG Germany). The percentage of haemolysis was calculated using equation **3**:

$$\text{Hemolysis \% } = \left(\frac{\text{Absorbance (sample)} - \text{Absorbance (−ve control)}}{\text{Absorbance (+ve control)} - \text{Absorbance (−ve control)}}\right) \times 10 \text{ ...... } Eq.\ 3$$

Cytotoxicity

Human breast cancer (MCF-7) cells and normal human (HEK 293) cells were obtained from the American Tissue Culture Collection (ATCC) (Virginia, USA). Cells were cultured in DMEM supplemented with 10% FBS and 1% antibiotic-antimycotic and incubated at 37 $^{\circ}$C, at a humidified atmosphere of 5% CO_2. When cells were in exponential growth, they were seeded into 96-wells plates (5 $\times$ 10^3/100 µL of medium). The MCF-7 cells were treated with the hesperidin alone for 24 and 48 h or HP-NEM for 24 h at 20, 60, 100, and 140 µg/mL. The untreated cells served as the control in this experiment. To evaluate for selective cytotoxicity of the nanoemulsions, normal HEK 293 cells treated at the same concentrations for 24 h were used. After treatment, cell viability was determined by the colorimetric MTT assay with absorbance recorded at 560 nm. Following the cytotoxicity assay, the EC_{50} value of the nanoemulsions was determined.

Apoptosis assay and cell cycle analysis

The apoptosis analysis was conducted using flow cytometry and the BD Pharmingen™ Annexin V Apoptosis Kit 1, according to the manufacturer's instructions. For cell cycle analysis, the BD Pharmingen™ FITC BrdU Flow Kit was employed. Briefly, treated cells were harvested, resuspended in 1 mL of medium, and labelled with 10 µL BrdU solution for 30 min at 37 $^{\circ}$C. Cells were fixed and permeabilized with BD cytofix buffer and cytoperm permeabilization buffer, respectively. Fixed and permeabilized cells were treated with DNase at 37 $^{\circ}$C for 1 h to expose the incorporated BrdU, then stained with anti-BrdU fluorescent antibodies. To stain for total DNA, 7-amino-actinomycin D (7-AAD) was subsequently added to the sample solution and incubated for 15 min at room temperature. Thereafter, the cell cycle analysis data was acquired using flow cytometry.

The quantitative real-time PCR analysis of miR-21 and miR-155

MiRNA from the MCF-7 cells treated with the EC_{50} concentration and 100 µg/mL of the nanoemulsions or medium (control) for 24 h was extracted using the PureLink miRNA isolation kit as per the manufacturer's instructions. The purity and concentration of the extracted miRNA were measured spectrophotometrically, with A260/280 ratio values greater than 1.8 considered as pure. The miRNA expression levels were detected using the synthesised cDNA template, SYBR green, and quantitative real-time PCR. The primer sequences used was as follows: miR-21; forward 5′-GGGGATTTCTTGGTTTGTGAA-3′ and reverse 5′-ATACAGCTAGAAAAGTCCCTGAAAA-3′ [36], and miR- 155; forward 5′-CGGTTTAATGCTAATCGTGA-3′ and reverse 5′-GAGCAGGGTCCGAGGT-3′ [37]. U6 was used as the reference gene for the miRNA and to normalise the results. The comparative method was used to calculate the fold-change (FT) of miR-21 and miR-155 expression [38]; $FT = 2^{-\Delta \Delta Cq}$ where C_q is the PCR cycle number in which the fluorescent signal from the amplification is detected.

Statistical analysis

All experiments were performed independently and in triplicate. Data was reported as the mean ± standard deviation from the three experiments and evaluated for statistical significance by one-way ANOVA and Tukey`s post hoc tests at $p < 0.05$. Flow cytometry data was analysed using the Kaluza analysis software, version 2.1.

Results

Synthesis of hesperidin-loaded nanoemulsions (HP-NEM)

Hesperidin-loaded nanoemulsions (HP-NEM) were successfully synthesised using the spontaneous emulsification method. Figure 1 illustrates the schematic formulation of the HP-NEM.
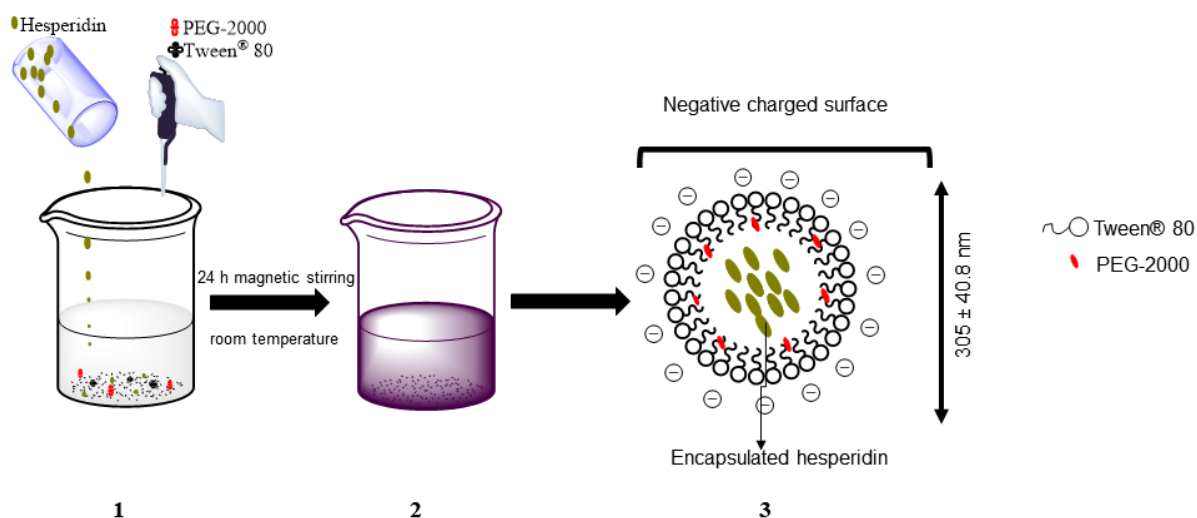
Figure 1. Formulation of hesperidin-loaded nanoemulsions (HP-NEM) (1) Drop-wise nano emulsification of hesperidin; (2) Formulation after 24 h stirring (3) As prepared hesperidin-loaded nanoemulsions (HP-NEM).

## *Particle size, polydispersity index, zeta potential, and morphology*

Particle size has a substantial impact on drug delivery to tumours due to its effects on cellular uptake and internalization. Various studies suggest that smaller molecules and particles have ease of entry and prolonged retention in tumours [39]. Particles with an average diameter less than 500 nm can be internalised into cells through an endocytotic mechanism called pinocytosis [40]. Table 1 shows the particle size of HP-NEM as 305 ± 40.8 nm. The polydispersity index (PDI) (0.0 to 1.0) describes the degree of uniformity of particle size populations in a sample, with 0.0 indicating perfect particle size distribution and 1.0 indicating multiple particle sizes [40]. The PDI for HP-NEM was recorded as 0.308 ± 0.04 (Table 1). The zeta potential of the HP-NEM was recorded as -11.6 ± 3.30 mV (Table 1).

Table 1: Particle size, zeta potential, PDI and EE of hesperidin-loaded nanoemulsions.

Hesperidin-loaded nanoemulsions physicochemical characteristics	
Size (nm)	305 ± 40.8
Zeta Potential (mV)	-11.6 ± 3.30
PDI	0.308 ± 0.04
EE %	93 ± 0.45

Values represented as mean $\pm$ SD.

The HR-TEM micrographs (Figure 2) show spherical nanoemulsions with moderate uniformity.
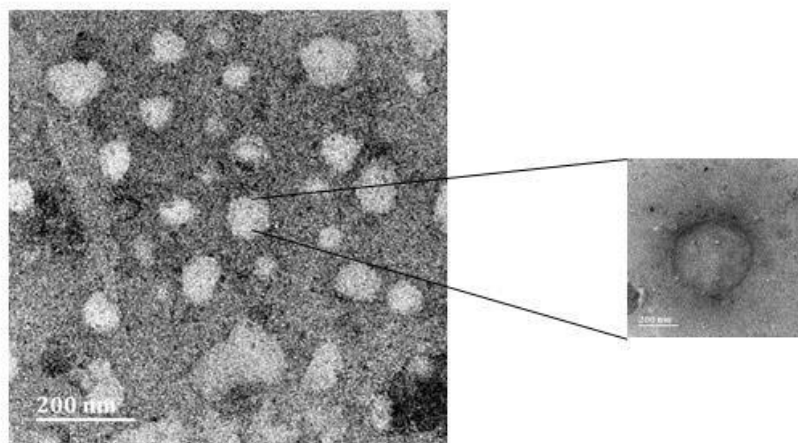
Figure 2. The HR-TEM micrographs showing the prepared spherical hesperidin-loaded nanoemulsions (HP-NEM).

Encapsulation efficiency

The encapsulation efficiency ($93 \pm 0.45\%$) of the HP-NEM is also shown in Table 1. Encapsulation efficiency is a vital parameter in drug formulations, which indicates the loading efficiency of the formulation. The prepared nanoemulsions show relatively high encapsulation efficiency, suggesting greater incorporation of hesperidin into the nanoemulsions.

In vitro drug release

The drug release profile of hesperidin (hesperidin alone) and HP-NEM is shown in Figure 3. Hesperidin showed a significantly low drug release, with 16.05 % being released in the first 2 h and slowing progressing to 26.66%, 36.29%, and 40.56 at 4 h, 8 h, and 24 h, respectively. In contrast, HP-NEM showed a higher release with, 24,85%, 45,93%, 86,90% and 97,34% of the hesperidin being release from the nanoemulsions at 2 h, 4 h, 8 h and 24 h respectively. Drug release from HP-NEM cumulated to 98.57 ± 0.39% (nearly complete drug release) over 48 h, compared to 46.35 ± 0.61% from hesperidin. The differences in the release rate could be due to insolubility of hesperidin in aqueous medium and the smaller particle size of the nanoemulsions, which could have improved their permeation across the membrane [41].
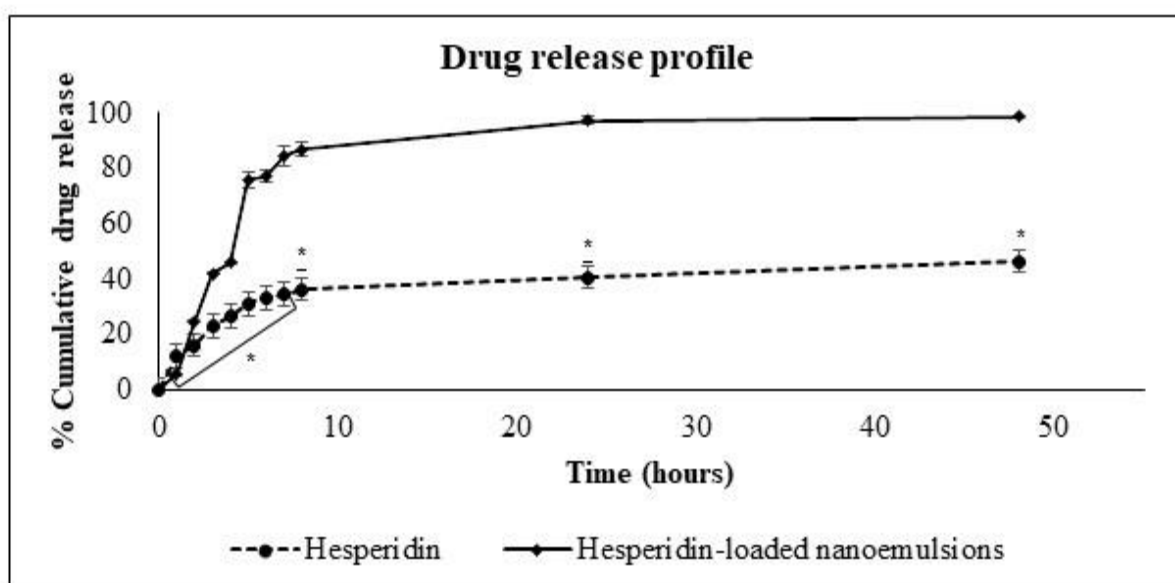
Figure 3. The drug release profile of hesperidin and hesperidin-loaded nanoemulsions (HP-NEM) over 48 h. Values represented as mean ± SD of three experimental replicates, * represents statistically significant difference of % cumulative drug release between hesperidin and hesperidin-loaded nanoemulsions at $p < 0.05$.

Haemolysis

Haemolysis induced by new formulations or molecules is a significant limitation in their applications. Therefore, to ascertain the safety of the prepared HP-NEM, their *in vitro* haemolytic activity was assessed. The results shown in Figure 4 indicated that the haemolytic activity of the nanoemulsions at various concentrations was comparable to the negative control PBS, suggesting HP-NEM to be hemocompatible.
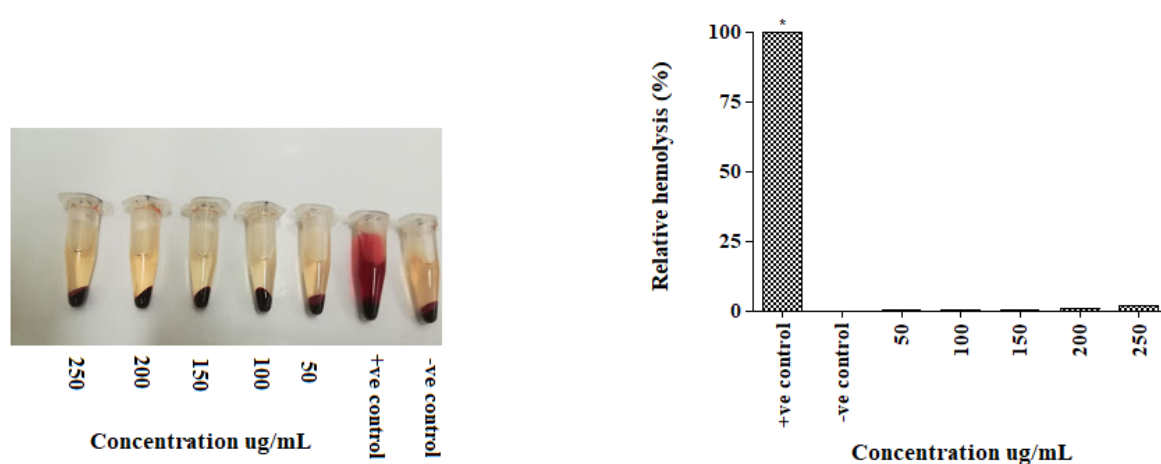

Figure 4. The haemolytic activity of hesperidin-loaded nanoemulsions (HP-NEM). Experiments were done in triplicates, and values are represented as mean ± SD, *significant difference at $p < 0.05$.

Cytotoxicity

The *in vitro* cytotoxicity of hesperidin and HP-NEM in MCF-7 cell lines is shown in Figure 5a. Treatment with HP-NEM for 24 h showed significantly lower cell viability at all tested concentrations from 20 -140 µg/mL relative to hesperidin at 24 h or 48 h. HP-NEM was most effective at concentrations of 60 to 140 µg/mL, decreasing cell viability to less than 10%. Based on these results, prolonged incubation for the nanoemulsions was not necessary, and all treatments, thereafter, were conducted at 24 h. The EC_{50} concentrations of hesperidin and HP-NEM in MCF-7 at 24 h were determined as 62.57 µg/mL and 29.36 µg/mL, respectively.

Hesperidin and HP-NEM showed low toxicity against normal HEK 293 cells (Figure 5b).
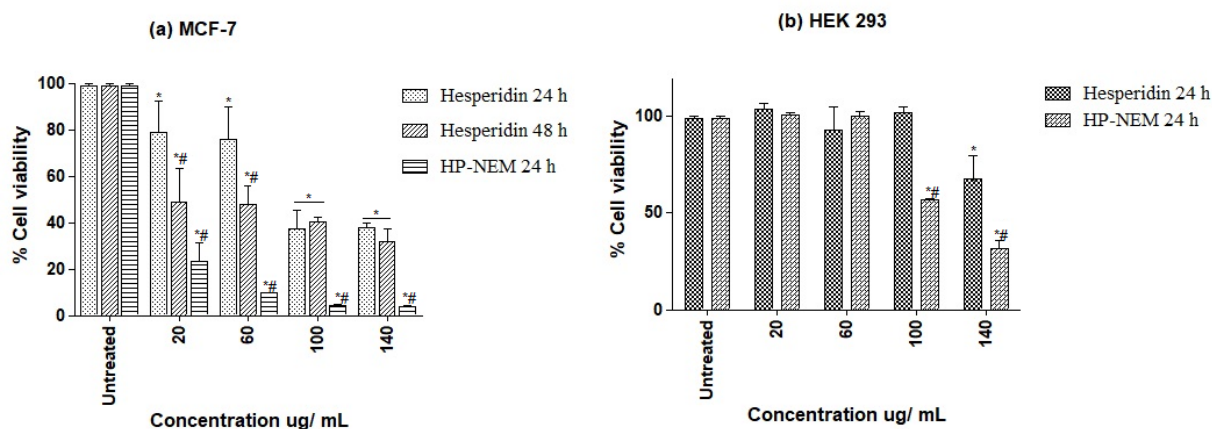
Figure 5. The comparative cytotoxic effect of hesperidin and hesperidin-loaded nanoemulsions (HP-NEM) against (a) MCF-7 and (b) HEK 293, untreated cells served as the control. Values represented as mean ± SD of three independent experimental replicates, * significant difference from the untreated group at p< 0.05 and # significant difference from the hesperidin 24 h treated group at p< 0.05.

Apoptosis

Following the cytotoxicity analysis, hesperidin and HP-NEM were further evaluated, to examine whether the induced cell death in MCF-7 was through apoptosis. Annexin and PI staining were used to evaluate the apoptotic activity. Treatment of MCF-7 cells with 100 ug/mL of hesperidin and HP-NEM for 24 h significantly increased the total percentage of apoptotic cells from 0.01% in the control (untreated cells) to 18.80% and 58.87%, respectively (Figure 6). This confirmed the induction of apoptosis in MCF-7 after treatment with hesperidin and HP-NEM, and potent efficacy of HP-NEM in comparison to hesperidin.
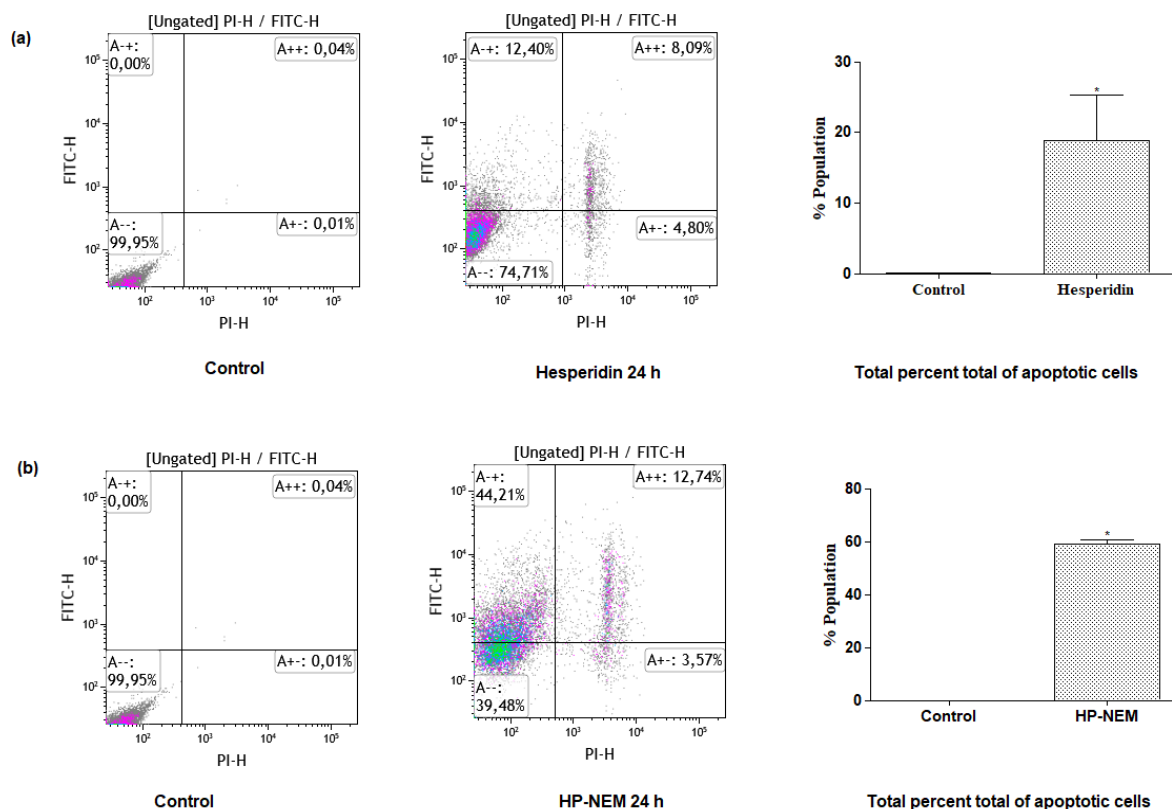
Figure 6. The apoptotic effect of (a) hesperidin and (b) hesperidin-loaded nanoemulsions (HP-NEM) on MCF-7 at 100 µg/mL for 24 h treatment. Quadrants represent A--, viable, A-+, early apoptotic, A++, late apoptotic, and A+-, necrotic cells. The bar chart represents the mean total percentage of the apoptotic cells' population. Values represented as mean ± SD of three independent experiments, *significant difference from the control at $p < 0.05$.

Cell cycle analysis

Figure 7 shows the cell cycle distribution of MCF-7 cells after treatment with 100 µg/mL of hesperidin and HP-NEM for 24 h. Compared to the control (untreated cells), hesperidin treated cells showed an increased percentage accumulation in the G0/G1 (38.72%), S (16.98%), and G2/M (25.12%) phases. However, HP-NEM treated cells showed an increased percentage accumulation in the G0/G1 (32.34%), S (6.4%), and G2/M (45.30%) phases. Higher accumulation in the G0/G1 phase (38.72%) and G2/M phase (45.30%) suggests cell cycle arrest in the G0/G1 and G2/M phase for hesperidin and HP-NEM, respectively.

113
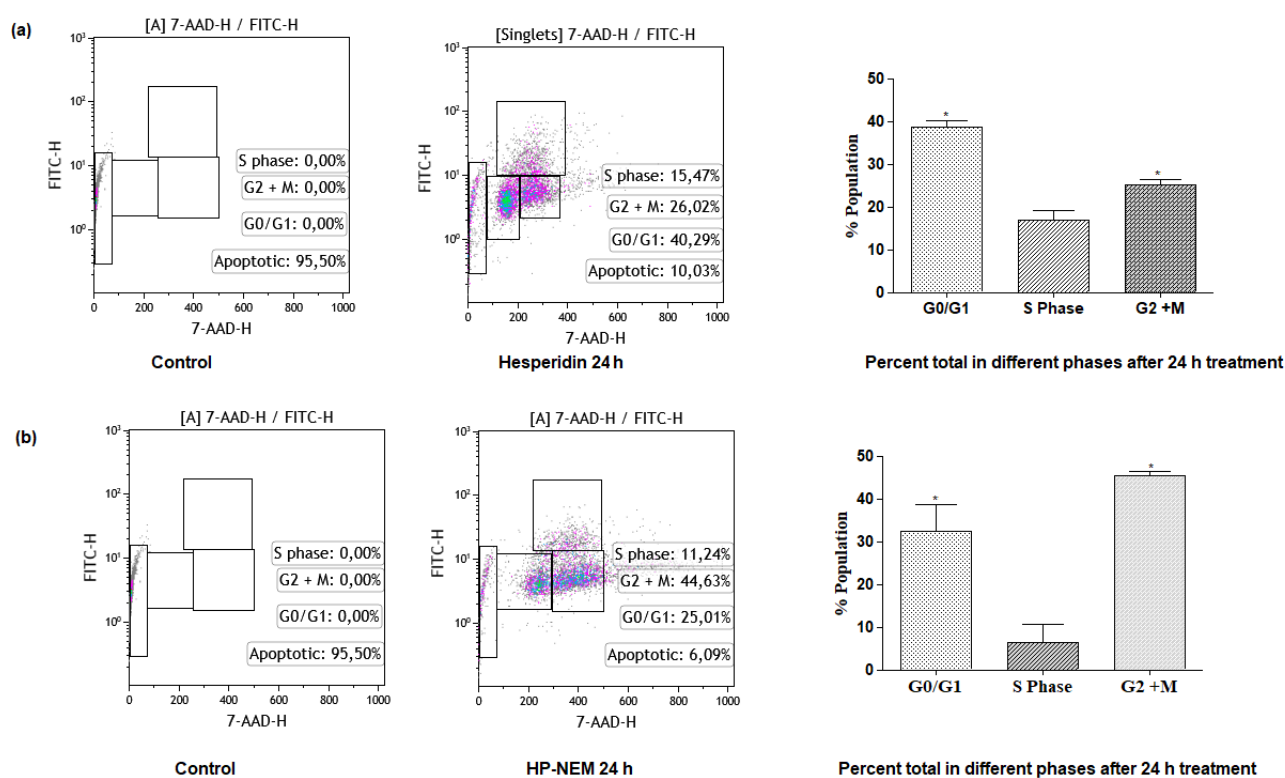
Figure 7. The effect of (a) hesperidin and (b) hesperidin-loaded nanoemulsions (HP-NEM) on cell cycle in MCF-7 after 24 h treatment at 100 µg/mL. The bar chart represents the mean percentage of cell populations in cell cycle phases G0/G1, S and G2/M. Values represented as mean ± SD of three experiments, * significant difference at p< 0.05.

miRNAs expression in HP-NEM treated MCF-7

To evaluate the potential of HP-NEM as a therapeutic agent in breast cancer, its effect on miR21 and miR-155, oncomiRs overexpressed in breast cancer [42], was investigated. The effect of HP-NEM on miR-21 and miR-155 expression in MCF-7 is illustrated in Figure 8. The results showed that the treatment of the MCF-7 cells with HP-NEM at concentrations of 29. 36 µg/mL (EC$_{50}$) and 100 µg/mL for 24 h, significantly decreased miR-21 and miR-155 expression relative to the control (untreated cells) at p < 0.05.
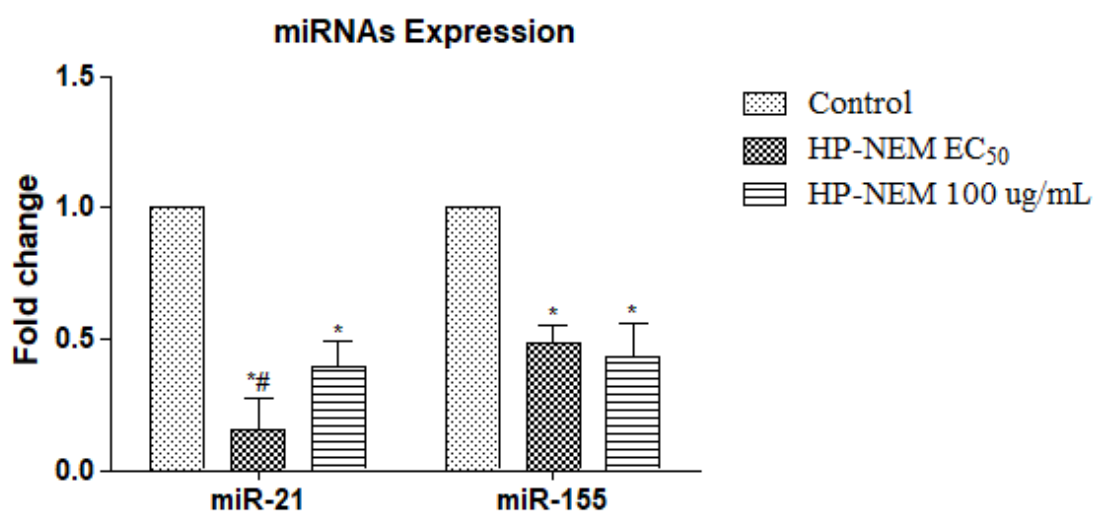
Figure 8. Hesperidin-loaded nanoemulsions (HP-NEM) downregulates miR-21 and miR-155 expression in MCF-7 after treatment at concentrations of 29.36 µg/mL (EC_{50}) and 100 µg/mL for 24 h. Values represented as mean $\pm$ SD of three experimental replicates, and *,# significant difference from the control group and HP-NEM 100 µg/mL at $p< 0.05$, respectively.

Discussion

The pharmacological use of hesperidin, a natural plant-based flavonoid, with potential neuroprotective, inflammatory, and anticancer activities (including promoting apoptosis as well as limiting tumour progression, metastasis and cell proliferation) [6,43], is hampered by low water solubility and poor bioavailability [11]. Nanoemulsions are widely accepted as an ideal delivery system for enhancing solubility and bioavailability of hydrophobic compounds [44]. Nanoemulsions have gained substantive recognition due to their stability, prolonged half-life, ability to protect drugs from enzymatic degradation, and non-toxicity [21]. However, the incorporation of hesperidin into nanoemulsions has not been studied.

In this study, we successfully synthesised hesperidin-loaded nanoemulsions (HP-NEM) with an average size of 305 nm and an encapsulation efficiency of 93% from an initial concentration of 250 µg/mL of the nanoemulsions. Characterisation of HP-NEM with HR-TEM confirmed

the spherical morphology (Figure 2), with moderate particle uniformity, indicated by a PDI value of 3.08 (Table 1). The net surface charge of nanoemulsions is reported to enhance drug stability, membrane permeation and efficacy [45] and in this regard, HP-NEM exhibited a negative surface charge of -11.6 mV (Table 1), contributing to the stability of HP-NEM, through electrostatic repulsion between particles. Furthermore, the negative surface charge has been reported to decrease binding to serum proteins and prolongs circulation [46]. The circulating half-life of nanoemulsions plays a critical role in their efficacy and studies have shown that coating nanoparticles with hydrophilic polymers such as polyethylene glycol (PEG), could prevent non-specific interactions and rapid renal clearance, as well as prolong the circulating half-life thereby improving efficacy [22]. In particular, long PEG chains such as PEG-2000 or PEG-5000, integrated into nanoemulsions, have been shown to improve their retention time and tumour circulation [47].

The ability of nano formulations to release its cargo at specifically targeted sites or over time for sustained medication, is also important for its efficacy as a delivery system [48]. The *in vitro* release profile (Figure 3) showed that both hesperidin and HP-NEM exhibited a sustained release pattern, with HP-NEM displaying a significantly higher cumulative release of 98.57 $\pm$ 0.39% in comparison to 46.4 $\pm$ 0.60% for hesperidin, over a 48 h period. The higher release of hesperidin from HP-NEM could be attributed to improved solubility resulting in increased diffusion through the membrane. These findings were similar to those previously reported on enhanced hydrophobic drug dissolution in eplerenone nanoemulsions, which resulted in a higher (90%) and sustained release from the nanoemulsions in contrast to the unformulated drug (39.6%) [49].

The efficacy of HP-NEM as an anticancer agent was determined through a comparative cytotoxicity study between hesperidin and HP-NEM in MCF-7. Hesperidin and HP-NEM showed dose and time-dependent cytotoxicity, with HP-NEM showing significantly higher

cytotoxic effects within a shorter incubation period, 24 h (Figure 5a). The potency of HP-NEM to induce cytotoxicity in MCF-7 was further confirmed by the EC_{50} values, where encapsulation of hesperidin reduced the EC_{50} value by half (62.57 µg/mL for hesperidin vs. 29.36 µg/mL for HP-NEM). Solubility and size could have possibly contributed to the more potent cytotoxicity of HP-NEM (particle size of 305 nm) in comparison to hesperidin (particle size of 1320 nm) [16]. Similarly, encapsulating kaempferol into nanoemulsions showed a significantly higher decreased cell viability in glioma cells (brain cancer) when compared to free kaempferol [50]. Furthermore, the safety of HP-NEM was supported by the lack of induction of haemolysis in red blood cells (Figure 4) and low toxic effects against normal HEK 293 cell lines (Figure 5b).

Induction of apoptosis is regarded as a vital strategy in cancer treatment [51], hence following the observed potent cytotoxicity of HP-NEM in MCF-7 cells, the form of cell death was further investigated. Several cell death mechanisms, including apoptosis, autophagy, and necrosis, have been implicated in drug cytotoxicity effects in cancer cells, with apoptosis being the target for most treatments [45]. Cells undergoing apoptosis have phosphatidylserine (PS), an apoptotic marker that binds to Annexin V externalised, and thus serves as a probe for flow cytometric analysis for apoptotic cells [52]. In addition, Annexin V is conjugated with propidium iodide (PI) to distinguish between apoptotic cells (PI-negative) and necrotic cells (PI-positive). In this study, the induction of apoptosis by hesperidin and HP-NEM in MCF-7 was confirmed through Annexin V/PI and flow cytometry, 24 h post-treatment. HP-NEM treated cells showed a higher increase in the total accumulation of apoptotic cell populations from the control, 58.87% versus 18.80% in hesperidin treated cells. This result further confirmed the potency of HP-NEM over hesperidin in MCF-7.

Cell cycle dysregulation associated with uncontrolled cell propagation and genomic instability, is one of the major characteristics of cancer. Regulation of cell cycle progression or cell cycle

arrest (stopping in-phase until DNA is repaired or cells undergo apoptosis) is regarded as an effective approach in tumour growth control [53]. In this study, HP-NEM demonstrated significant accumulation of apoptotic cell populations in the G2/M phase after 24 h treatment, which suggests that cell cycle arrest is one of the mechanisms HP-NEM employs to effect cytotoxicity in MCF-7. These results were consistent with other plant-based nanoemulsions, such as carvacrol (from thyme plants) which induced apoptosis and cell cycle arrest in doxorubicin-resistant A549 cell lines (lung cancer) [54].

Studies on post-transcriptional gene regulators, miRNAs, has revolutionised our understanding of cancer biology [55]. The regulatory role played by miRNAs in the progression of cancer has enhanced their potential as therapeutic targets in cancer treatment [56]. Examples of successful miRNA-targeting drugs in clinical trials include Miravirsen, which inhibits miR-122 responsible for viral replication in hepatitis C [57]; MRG 110, which inhibits miR-92 mostly overexpressed in non-small-cell-lung cancer; and RGLS5579 targeted miR-10b, which promotes metastasis in brain cancer [58]. Previous studies have reported the upregulation of miR-21 and miR-155 in breast cancer [28]. Therefore, targeting miR-21 and miR-155 could provide a possible new therapeutic approach in breast cancer. The effect of HP-NEM on oncomiRs has not previously been reported. In this study, we evaluated the expression of miR-21 and miR-155 in MCF-7 after treatment with HP-NEM for 24 h, using real-time PCR. HPNEM downregulated the expression of miR-21 and miR-155, supporting its therapeutic potential in breast cancer treatment.

Conclusion

Although hesperidin has experimentally shown potential therapeutic effects, its efficacy is hampered due to its hydrophobic nature and low bioavailability. This study shows encapsulation of hesperidin into nanoemulsions could improve its efficacy in breast cancer

treatment, as demonstrated by the significantly higher cytotoxicity of hesperidin-loaded nanoemulsions (HP-NEM) against MCF-7 compared to hesperidin. HP-NEM induced cytotoxicity in MCF-7 through apoptosis and cell cycle arrest in the G2/M phase and was found to be safe with no adverse side effects. Furthermore, this study shows the potential of HP-NEM as a therapeutic agent in breast cancer treatment by inhibiting the overexpressed miR-21 and miR-155 in MCF-7, which has never been reported before. Future studies on the mechanisms underlying the inhibition of oncomiRs by HP-NEM and the pharmacokinetics of HP-NEM are further required to assess its therapeutic potential in breast cancer.

Conflict of interest

The author(s) confirm no conflict of interest.

References

1. Cheng CW, Yu JC, Hsieh YH, et al. Increased cellular levels of MicroRNA-9 and MicroRNA-221 correlate with cancer stemness and predict poor outcome in human breast cancer. Cell Physiol Biochem. 2018;48(5):2205-2218.

2. Zuo J, Yu Y, Zhu M, et al. Inhibition of miR-155, a therapeutic target for breast cancer, prevented in cancer stem cell formation. Cancer Biomark. 2018;21(2):383-392.

3. Wang P, Du Y, Wang J. Indentification of breast cancer subtypes sensitive to HCQ-induced autophagy inhibition. Pathol Res Pract. 2019;215(10):152609.

4. Magura J. Moodley R, Maduray K, et al. Phytochemical constituents and in vitro anticancer screening of isolated compounds from Eriocephalus africanus. Nat Prod Res. DOI: 10.1080/14786419.2020.1744138

5. Ahmadi A, Shadboorestan A. Oxidative stress and cancer; the role of hesperidin, a citrus natural bioflavonoid, as a cancer chemoprotective agent. Nutr Cancer. 2016;68(1):29-39.

6. Stanisic D, Costa A, Fávaro W, et al. Anticancer activities of hesperidin and hesperetin in vivo and their potentiality against bladder cancer. J Nanomed Nanotechnol. 2018;9.

7. Hana R, Bawi B-. Hesperidin inhibits angiogenesis, induces apoptosis, and suppresses laryngeal cancer cell metastasis. Ibnosina J Med Biomed Sci Medknow. 2018;10(5):169.

8. Pandey P, Sayyed U, Tiwari RK, et al. Hesperidin induces ROS-Mediated apoptosis along with cell cycle arrest at G2/M phase in human gall bladder carcinoma. Nutr Cancer Routledge. 2019;71(4):676-687.

9. Cincin Z, Kiran B, Baran Y, et al. Hesperidin promotes programmed cell death by downregulation of nongenomic estrogen receptor signalling pathway in endometrial cancer cells. Biomed Pharmacother. 2018; 103:336-345.

10. Arbain NH, Salim N, Masoumi HRF, et al. In vitro evaluation of the inhalable quercetin loaded nanoemulsion for pulmonary delivery. Drug Deliv Transl Res Springer Verlag. 2019;9(2):497-507.

11. Hajialyani M, Hosein Farzaei M, Echeverría J, et al. Hesperidin as a neuroprotective agent: A review of animal and clinical evidence. Molecules. 2019;24(3):648.

12. Li Y-M, Li X-M, Li G-M, et al. In vivo pharmacokinetics of hesperidin are affected by treatment with glucosidase-like BglA protein isolated from yeasts. J Agric Food Chem. 2008;56(14):5550-5557.

13. Nectoux AM, Abe C, Huang S-W, et al. Absorption and metabolic behavior of hesperidin (Rutinosylated Hesperetin) after single oral administration to Sprague-dawley rats. J Agric Food Chem. 2019;67(35):9812-9819.

14. Zhang J, Wang D, Wu Y, et al. Lipid–polymer hybrid nanoparticles for oral delivery of tartary buckwheat flavonoids. J Agric Food Chem American Chemical Society. 2018;66(19):4923-4932.

15. Khan H, Ullah H, Martorell M, et al., editors. Flavonoids nanoparticles in cancer: Treatment, prevention and clinical prospects. Semin Cancer Biol; 2019: Elsevier.

16. Ali SH, Sulaiman GM, Al-Halbosiy MM, et al. Fabrication of hesperidin nanoparticles loaded by poly lactic co-Glycolic acid for improved therapeutic efficiency and cytotoxicity. Artif Cells, Nanomedicine, Biotechnol. 2019;47(1):378-394.

17. Ferrari PC, Correia MK, Somer A, et al. Hesperidin-loaded solid lipid nanoparticles: development and physicochemical properties evaluation. J Nanosci Nanotechnol American Scientific Publishers. 2019;19(8):4747-4757.

18. Tsirigotis-Maniecka M, Lamch Ł, Chojnacka I, et al. Microencapsulation of hesperidin in polyelectrolyte complex microbeads: Physico-chemical evaluation and release behavior. J Food Eng. 2017; 214:104-116.

19. Wei Q, Keck CM, Müller RH. Solidification of hesperidin nanosuspension by spray drying optimized by design of experiment (DoE). Drug Dev Ind Pharm. 2018;44(1):1-12.

20. Ostróżka Cieślik A, Sarecka Hujar B. The use of nanotechnology in modern pharmacotherapy. In: Multifunctional systems for combined delivery, biosensing and diagnostics. Elsevier: Elsevier; 2017. p. 139-158.

21. Sánchez López E, Guerra M, Dias Ferreira J, et al. Current applications of nanoemulsions in cancer therapeutics. Nanomaterials. 2019;9(6):821.

22. Ganta S, Talekar M, Singh A, et al. Nanoemulsions in translational research opportunities and challenges in targeted cancer therapy. AAPS Pharmscitech. 2014;15(3):694-708.

23. Alasvand N, Urbanska AM, Rahmati M, et al. Therapeutic nanoparticles for targeted delivery of anticancer drugs. In: Multifunctional systems for combined delivery, biosensing and diagnostics. Elsevier; 2017. p. 245-259.

24. Leichter AL, Sullivan MJ, Eccles MR, et al. MicroRNA expression patterns and signalling pathways in the development and progression of childhood solid tumours. Mol Cancer. 2017;16(1):15.

25. O'Bryan S, Dong S, Mathis JM, et al. The roles of oncogenic miRNAs and their therapeutic importance in breast cancer. European J Cancer. 2017; 72:1-11.

26. Tan W, Liu B, Qu S, et al. MicroRNAs and cancer: Key paradigms in molecular therapy. Oncology Letters. 2018;15(3):2735-2742.

27. Mattiske S, Suetani RJ, Neilsen PM, et al. The oncogenic role of miR-155 in breast cancer. Cancer Epidemiology Biomarkers and Prevention. 2012;21(8):1236-1243.

28. Chernyy V, Pustylnyak V, Kozlov V, et al. Increased expression of miR-155 and miR222 is associated with lymph node positive status. J Cancer Ivyspring Int Publisher. 2018;9(1):135.

29. Metawae E, Abd-Alhamid N, Abd-Allatif S, et al. Evaluation of microRNA-155 as a diagnostic serum-based biomarker in patients with breast cancer. Al-Azhar Assiut Med J Medknow. 2018;16(1):81.

30. Yan LX, Wu QN, Zhang Y, et al. Knockdown of miR-21 in human breast cancer cell lines inhibits proliferation, in vitro migration and in vivo tumor growth. Breast Cancer Res. 2011;13(1): R2.

31. Jiang S, Zhang H-W, Lu M-H, et al. MicroRNA-155 functions as an oncomiR in breast cancer by targeting the suppressor of cytokine signaling 1 gene. Cancer Res 2010;70(8):3119-3127.

32. Kim S, Song JH, Kim S, et al. Loss of oncogenic miR-155 in tumor cells promotes tumor growth by enhancing C/EBP-β-mediated MDSC infiltration. Oncotarget Impact Journals LLC. 2016;7(10):11094.

33. Sulaiman GM, Jabir MS, Hameed AH. Nanoscale modification of chrysin for improved of therapeutic efficiency and cytotoxicity. Artif Cells, Nanomedicine, Biotechnol. 2018;46(sup1):708-720.

34. Xu J, Chen Y, Jiang X, et al. Development of hydrophilic drug encapsulation and controlled release using a modified nanoprecipitation method. Processes. 2019;7(6):331.

35. Hassan D, Omolo CA, Gannimani R, et al. Delivery of novel vancomycin nanoplexes for combating methicillin resistant Staphylococcus aureus (MRSA) infections. Int J Pharm Elsevier BV. 2019; 558:143-156.

36. Hao B, Zhang J. miRNA-21 inhibition suppresses the human epithelial ovarian cancer by targeting PTEN signal pathway. Saudi J Biol Sci Elsevier. 2019;26(8):2026-2029.

37. Zhang Y, Li X, Zhang Y, et al. Pegylated interferon-α inhibits the proliferation of hepatocellular carcinoma cells by downregulating miR-155. Ann Hepatol Elsevier. 2019;18(3):494-500.

38. Schmittgen TD, Livak KJ. Analyzing real-time PCR data by the comparative CT method. Nat Protoc. 2008;3(6):1101.

39. Miyake M, Kakizawa Y, Tobori N, et al. Membrane permeation of giant unilamellar vesicles and corneal epithelial cells with lipophilic vitamin nanoemulsions. Colloids Surfaces B Biointerfaces Elsevier BV. 2018; 169:444-452.

40. Danaei M, Dehghankhold M, Ataei S, et al. Impact of particle size and polydispersity index on the clinical applications of lipidic nanocarrier systems. Pharmaceutics. 2018;10(2):57.

41. Lucca LG, de Matos SP, Weimer P, et al. Improved skin delivery and validation of novel stability indicating HPLC method for ketoprofen nanoemulsion. Arab J Chem Elsevier BV. 2020;13(2):4505-4511.

42. Wang W, Luo Y-p. MicroRNAs in breast cancer: oncogene and tumor suppressors with clinical potential. J Zhejiang Uni: Science B. 2015;16(1):18-31.

43. Hemanth Kumar B, Dinesh Kumar B, Diwan PV. Hesperidin, a citrus flavonoid, protects against l-methionine-induced hyper-homo-cysteinemia by abrogation of oxidative stress, endothelial dysfunction and neurotoxicity in Wistar rats. Pharm Biol. 2017;55(1):146-155.

44. Tubtimsri S, Limmatvapirat C, Limsirichaikul S, et al. Fabrication and characterization of spearmint oil loaded nanoemulsions as cytotoxic agents against oral cancer cell. Asian J Pharm Sci. 2018;13(5):425-437.

45. Khan I, Bahuguna A, Kumar P, et al. In vitro and in vivo antitumor potential of carvacrol nanoemulsion against human lung adenocarcinoma A549 cells via mitochondrial mediated apoptosis. Sci Rep Springer US. 2018;8(1):1-15.

46. Zhang Y, Li Y, Ma J, et al. Convenient preparation of charge-adaptive chitosan nanomedicines for extended blood circulation and accelerated endosomal escape. Nano Res Tsinghua University Press. 2018;11(8):4278-4292.

47. Muralidharan P, Mallory E, Malapit M, et al. Inhalable PEGylated phospholipid nanocarriers and PEGylated therapeutics for respiratory delivery as aerosolized colloidal dispersions and dry powder inhalers. Pharmaceutics. MDP AG. 2014;6(2):333-353.

48. Werzer O, Tumphart S, Keimel R, et al. Drug release from thin films encapsulated by a temperature-responsive hydrogel. Soft Matter Royal Society of Chemistry. 2019;15(8):1853-1859.

49. Khames A. Formulation and characterization of Eplerenone nanoemulsion liquisolids, an oral delivery system with higher release rate and improved bioavailability. Pharmaceutics. 2019;11(1):40.

50. Colombo M, Figueiró F, de Fraga Dias A, et al. Kaempferol-loaded mucoadhesive nanoemulsion for intranasal administration reduces glioma growth in vitro. Int J Pharm Elsevier BV. 2018;543(1-2):214-223.

51. Jaudan A, Sharma S, Malek SNA, et al. Induction of apoptosis by pinostrobin in human cervical cancer cells: Possible mechanism of action. PLoS One Public Library of Sci. 2018;13(2).

52. Lee S, Meng X, Flatten K, et al. Phosphatidylserine exposure during apoptosis reflects bidirectional trafficking between plasma membrane and cytoplasm. Cell Death Differ Nature Publishing Group. 2013;20(1):64-76.

53. Murad H, Hawat M, Ekhtiar A, et al. Induction of G1-phase cell cycle arrest and apoptosis pathway in MDA-MB-231 human breast cancer cells by sulfated polysaccharide extracted from Laurencia papillosa. Cancer Cell Int. 2016;16(1):39.

54. Khan I, Bahuguna A, Bhardwaj M, et al. Carvacrol nanoemulsion evokes cell cycle arrest, apoptosis induction and autophagy inhibition in doxorubicin resistant-A549 cell line. Artif Cells, Nanomedicine Biotechnol Taylor and Francis Ltd. 2018;46(sup1):664675.

55. Price C, Chen J. MicroRNAs in cancer biology and therapy: current status and perspectives. Genes Dis Elsevier Korea LLC. 2014;1(1):53-63.

56. Liu J, Huang W, Yang H, et al. Expression and function of miR-155 in breast cancer. Biotechnol Biotechnol Equip. 2015;29(5):840-843.

57. Yu L, Zhao J, Gao L. Predicting potential drugs for breast cancer based on miRNA and tissue specificity. Int J Biol Sci Ivyspring International Publisher. 2018;14(8):971.

58. Hanna J, Hossain GS, Kocerha J. The potential for microRNAs in clinical research. Frontiers in Genetics. 2019; 10:478.

5.   CHAPTER FIVE: SUMMARY

5.1 Synthesis

The plant kingdom continues to make significant contributions to modern medicine, offering structurally diverse compounds with a plethora of therapeutic effects and providing new entities for drug discovery and development. Currently, of the approximately half a million discovered world flora species, only 10% has been scientifically investigated. Historically, research into natural medicinal plants has given rise to potent anticancer drugs. Indeed plant-derived compounds as an alternative therapeutic approach has gained enormous momentum in cancer, targeting apoptotic pathways with a purported lower toxicity to cells. However, there remains an extensive gap between the scientific validation of promising plant-derived compounds and the biodiversity of the natural flora.

Optimised, selective therapeutic effects on cancerous cells with minimal toxicity on healthy cells is urgently required in current therapies. Nanotechnologically modified drugs and drug delivery systems have emerged as attractive entities in cancer treatment offering site-specific drug delivery, improved drug bioavailability and solubility. The incorporation of plant-derived compounds into novel nanotechnology systems could improve their pharmacokinetic limitations, target specificity and therapeutic effects. Therefore, this study aimed to isolate and characterise phytocompounds from *Eriocephalus africanus* L.*,* investigate their effect on apoptotic and epigenetic control in breast cancer using human breast adenocarcinoma cell lines (MCF-7), and develop nanosystems for their encapsulation and explore their safety and efficacy as anticancer agents.
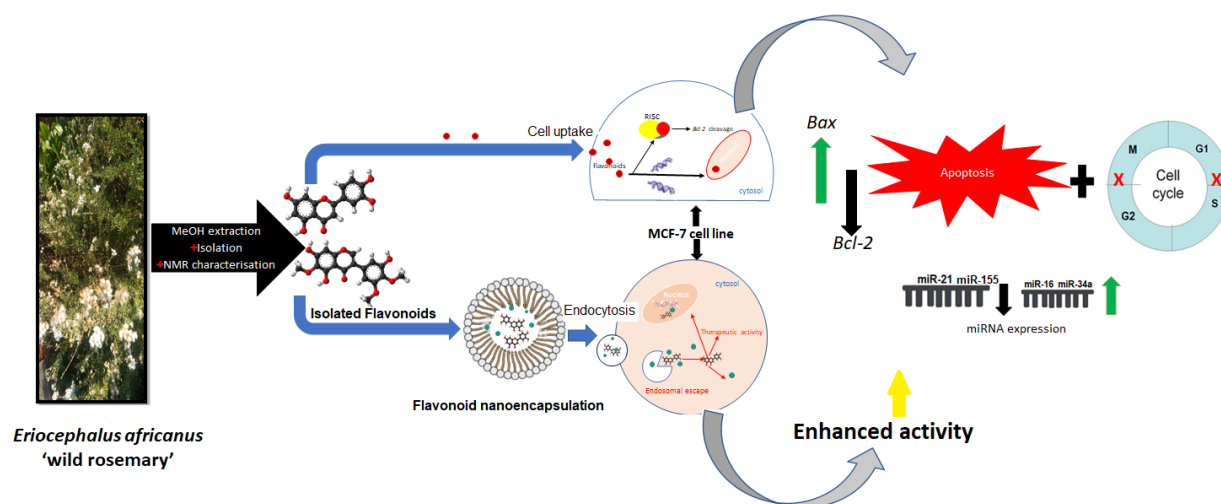
Figure 9. Schematic presentation of the study.

The phytochemical analysis of the methanolic extracts of *E. africanus* resulted in the isolation and identification of hesperidin, luteolin and apigenin. Preliminary screening of the methanolic extract and isolated compounds for anticancer activity in selected human carcinoma cell lines (MCF-7, HepG2 and A549), showed decreased cell viability in a dose dependent manner. Interestingly, the methanolic extract showed the highest effect against MCF-7 with EC_{50} of 45.47 µg/mL in contrast to the pure isolated compounds, which recorded EC_{50} values of 62.57 µg/mL for hesperidin, 70.34 µg/mL for luteolin and > 100 µg/mL for apigenin, demonstrating synergistic effects of the compounds. Hesperidin and luteolin, which demonstrated potential anticancer activity, were further investigated for their cytotoxicity in MCF-7, a model which represents luminal A breast cancer. The non-cancerous human embryonic kidney cells (HEK 293) are widely used in biomedical research as they are representative of healthy human cells and are easy to grow and maintain; therefore, they were used as a model in this study to evaluate the selective toxicity of the isolated compounds. The isolated compounds showed selective toxicity against HEK 293, with minimal decrease in cell viability in the order of hesperidin > luteolin > apigenin. This study revealed the methanolic extract of *E. africanus* to be a rich source of natural flavonoids, with major flavonoids being hesperidin, luteolin and apigenin.

Subsequent to profiling the cytotoxic effects demonstrated by hesperidin and luteolin in MCF7, we evaluated their effects on key molecular pathways implicated in the pathophysiology of breast cancer and cancer per se. Evasion of apoptosis is a hallmark of all cancers, including breast cancer, and is associated with uncontrolled tumour progression, metastasis and resistance to therapy. In this regard, recent drug developments have been focusing on anticancer agents

with the potential to induce or repair apoptotic function. Hesperidin and luteolin demonstrated MCF-7 cell death induced by apoptosis through the intrinsic and extrinsic pathways coupled with downregulation of antiapoptotic *Bcl-2* expression and upregulation of proapoptotic *Bax* expression. Dysregulated cell cycle machinery has also been indicated to promote tumour progression, hence therapeutic agents inhibiting the progression of cancerous cells through the cell cycle are of great importance in cancer treatment. In this regard, the effects of hesperidin and luteolin on cell cycle progression were evaluated and found to cause accumulation of cell populations in the G0/G1 and sub-G1 phases, respectively.

In light of the emerging evidence on the vital role of miRNA as post-transcriptional gene expression regulators through binding to target mRNA, we evaluated the expression of key apoptotic miRNA (*viz.* miR-16, -21 and -34a), upon treatment with hesperidin or luteolin. In addition, their relationship with the expression of target *Bcl-2* gene was evaluated. The findings from quantitative real-time PCR analysis revealed that treatment of MCF-7 with hesperidin or luteolin resulted in downregulation of miR-21 and upregulation of miR-16 and -34a. Furthermore, Pearson`s correlation analysis indicated positive correlation between the expression of *Bcl-2* and miR-21 and negative correlation between *Bcl-2*, miR-16 and -34a, indicating that treatment with flavonoids promote apoptosis through upregulation of proapoptotic miRNAs and downregulation of *Bcl-2*. Overall, findings from this study broadened the understanding of molecular mechanisms involved in flavonoid-induced cell death and provided new insights on their effects on expression of apoptotic miRNAs as well as their relations with target mRNA.

Nanotechnology was employed to improve the bioavailability and efficacy of hesperidin and luteolin. Hesperidin was successfully encapsulated into a nanoemulsion (HP-NEM), prepared using Tween® 80, PEG-2000 and water *via* a spontaneous emulsification technique. The prepared HP-NEM displayed a spherical shape with 305 nm, 0.308 and -11.6 mV and 93% for particle size, polydispersity index (PDI), zeta-potential (ζ) and encapsulation efficiency, respectively. Biosafety studies of HP-NEM performed through the MTT assay on HEK 293 together with a haemolytic assay, revealed the safety profile of HP-NEM. Exposure of MCF-7 cells to HP-NEM for 24 h, showed significantly lower cell viability at all tested concentrations from 20 -140 µg/mL relative to hesperidin at 24 h or 48 h, confirming enhanced cytotoxicity. This cytotoxicity was confirmed to be through induction of apoptosis using flow cytometric techniques. Furthermore, treatment of MCF-7 cells with HP-NEM resulted in accumulation of

cell populations in the G2/M of the cell cycle. Of note, treatment with hesperidin alone and HP-NEM resulted in cell accumulation at different phases G0/G1 and G2/M, respectively. This could suggest that the modification of hesperidin into HP-NEM influences activation of possibly different cell cycle signaling factors to that of hesperidin alone, resulting in halting of the cell cycle progression at different phases. Nevertheless, more details still need to be determined and investigated. miR-21 and miR-155 have been described as oncomirs overexpressed in breast cancer that influence tumour progression. In this study, treatment of MCF-7 with HP-NEM for 24 h downregulated the expression of miR-21 and miR155, showcasing the novelty of HP-NEM as a potential therapeutic agent in breast cancer treatment. An interesting finding was that treatment with the EC_{50} concentration (29.36 µg/mL) of HP-NEM resulted in further decreased expression of miR-21, in contrast to treatment at a concentration of 100 µg/mL. This may suggest that HP-NEM has a higher binding affinity to miR-21 at low concentrations, which resulted in the observed higher inhibition of miR-21 expression and could further contribute to its therapeutic potency in breast cancer treatment as an inhibitor of miR-21.

As part of our standardisation procedures we also investigated the synthesis, physicochemical properties and cytotoxic activity of luteolin-loaded solid-lipid nanoparticles (Appendix A). For the encapsulation of luteolin, solid-lipid nanoparticles generated from cleaved stearylamine were used. Solid-lipid nanoparticles are similar to nanoemulsions, but they employ a solid lipid instead of a liquid lipid as in the case of nanoemulsions. Luteolin-loaded solid-lipid nanoparticles (LUT-SA-SLN) were successfully formulated using an emulsion-solvent evaporation method and evaluated for their biosafety in HEK 293. Exposure of HEK 293 to LUT-SA-SLN, reduced cell viability drastically (< 10 %) at all tested treatments and several experimental replicates. These observations indicated that LUT-SA-SLN exhibited non-selective cytotoxicity and their use could cause adverse side effects therefore, no further experiments were conducted using LUT-SA-SLN, in this study.

5.2 Conclusion

Overall, findings presented in this study provide comprehensive insight into the anticancer potential of *E. africanus* from plant extract to nanodrug. The study identifies *E. africanus* as a source of natural flavonoids, possessing anticancer therapeutic effects mediated through the

apoptotic pathway and cell cycle regulation. This study provides new insight on the effects of flavonoids on the expression of apoptotic miRNAs, demonstrating their efficacy in targeting apoptosis in cancer treatment. The encapsulation of the flavonoids into newly designed nanosystems, highlights the potential of improved bioavailability and therapeutic efficacy of hesperidin-loaded nanoemulsions in breast cancer treatment mediated through apoptotic activity and downregulation of commonly overexpressed oncomirs. Importantly, this study makes a significant contribution in broadening the scientific basis for the potential use of plant-derived, nanotechnologically-modified flavonoids as alternative treatment options in breast cancer.

5.3 Recommendations for further work

In this study, apigenin proved to be less sensitive against MCF-7; however, it showed potent activity against HepG2 (EC_{50} = 11.93 µg/mL), therefore it could be explored for possible treatment of liver cancer.

The use of plant-derived flavonoids and flavonoid-loaded nanosystems in targeting the apoptotic pathway for breast cancer treatment promises to circumvent the challenges in current therapies. However, further research is needed to replicate the *in vitro* model represented in this study to further understand their use in cancer treatment. In this regard the following recommendations are proposed:

- Investigate the effects of flavonoids and flavonoid-loaded nanoemulsions in other *in vitro* and *in vivo* cancer models and comprehensively investigate the pathways implicated in the pathogenesis and treatment of cancer
- Perform *in vivo* studies and evaluate the pharmacokinetics, toxicity and degree of accumulation at the diseased site of the synthesised flavonoid-loaded nanosytems
- Functionalise and optimise the synthesised flavonoid-loaded nanosystems for possible clinical application in breast cancer treatment.
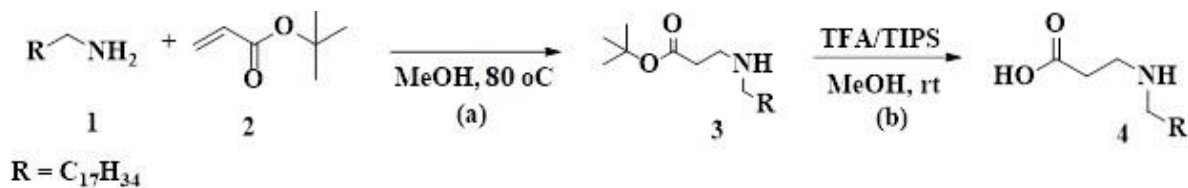
Appendix A

Luteolin-loaded solid lipid nanoparticles

Synthesis of the novel lipid used for the encapsulation of luteolin

The bicephalic surfactant (novel lipid) was synthesised as illustrated in Scheme A1.

Scheme A1. a). Methanol (MeOH), reflux with constant stirring at 80 ℃, 24 h, and b). MeOH + trifluoroacetic acid (TFA)/triisopropylsilane (TIPS) at room temperature for 8 h.

*Synthesis of Compound 3 (di-tert-butyl 3,3'-(octadecylazanediyl) dipropionate)*

Compound **3** was synthesised following a previously reported procedure (Hassan et al. 2020). Briefly, *tert*-butyl acrylate **2** (1.75 g; 13.65 mmol) was dissolved in methanol (15 mL) and the solution was added to stearylamine **1** in methanol (1.7 g; 6.3 mmol) (10 mL). The mixture was stirred and refluxed at 80 ℃ for 24 h and the progress of the reaction was monitored *via* thin layer chromatography. The crude product was washed with chloroform several times to remove excess *tert*-butyl acrylate (BA), then the solvent (chloroform) and excess BA were removed using a rotary evaporator. The crude product was purified *via* column chromatography (silica, mesh size 60 - 100) (hexane: ethyl acetate, 7: 3) to obtain a white solid compound **3** (1.85 g; yield 49.52 %).

Synthesis of Compound 4 (3, 3'-(octadecyl-azanediyl) dipropionic acid)

To a solution of compound **3** (1.03 g; 0.46 mmol) in methanol (20 mL), TFA/TIPS (1.81g; 23 mmol) was added at room temperature, as reported in the literature (Makhathini et al. 2019). The resulting mixture was stirred vigorously at room temperature for 6 h and evaporated to dryness using a rotary evaporator. The subsequent residue was washed several times with hexane to obtain a white semi-white compound **4** (SA) (0.28 g; yield 56.45 %).

Synthesis of luteolin-loaded solid lipid nanoparticles (LUT-SA- SLN)

The luteolin-loaded solid lipid nanoparticles (LUT-SA-SLN) were prepared using the emulsion-solvent evaporation method (Umerska et al. 2018). Briefly, luteolin and the novel lipid (SA) were both dissolved in tetrahydrofuran (THF) separately and added dropwise to deionized water under ultrasound sonication. Thereafter, the solution was gently stirred using a magnetic stirrer at room temperature for 24 h, to allow for solvent evaporation and formation of the nanoparticles (Figure A1).
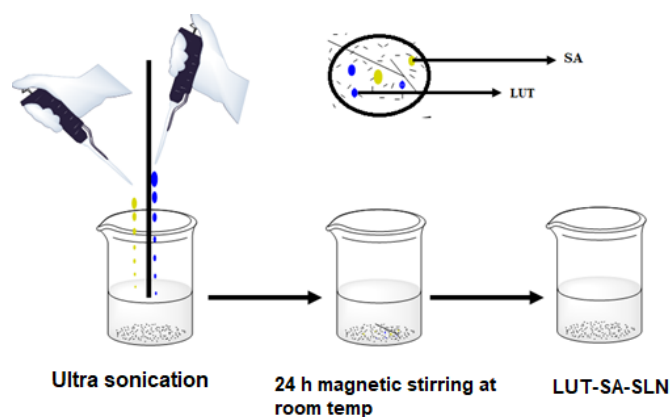
Figure A1. Synthesis of luteolin-loaded solid lipid nanoparticles (LUT-SA-SLN) using the emulsion-solvent evaporation method.

Physicochemical properties of the synthesised LUT-SA-SLN

The particle size, polydispersity index, zeta potential, and the encapsulation efficiency of LUT-SA-SLN is shown in Table A1

Table A1. Particle size, zeta potential, PDI and EE of luteolin-loaded solid lipid nanoparticles.

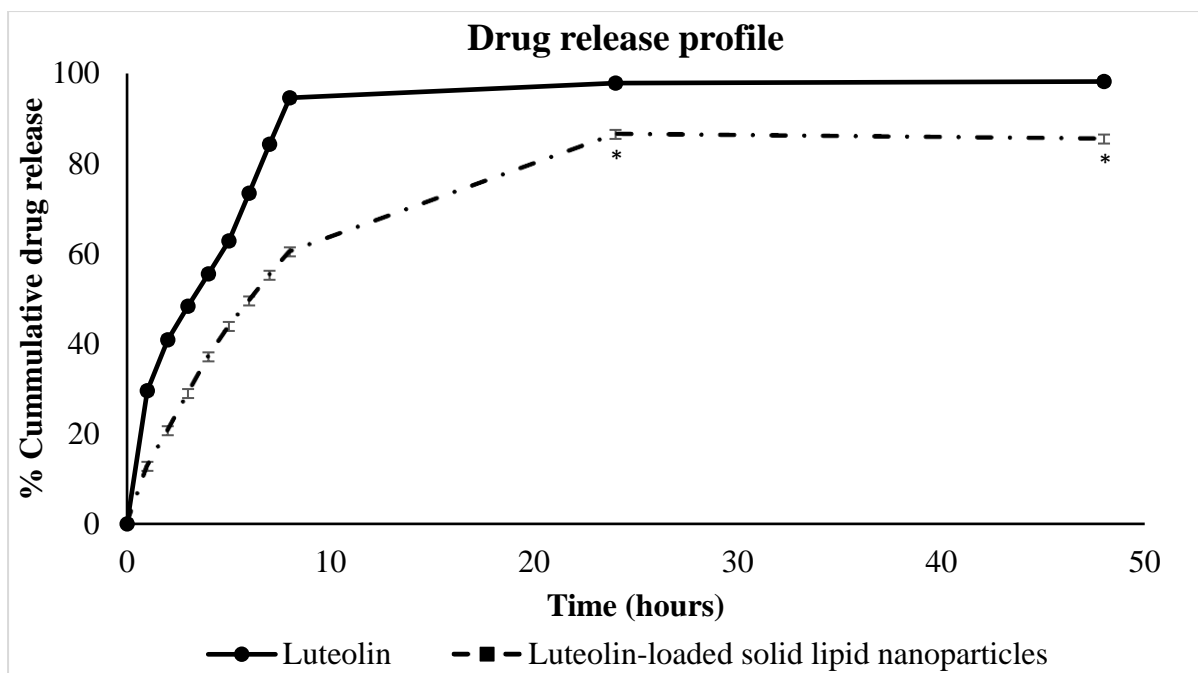| Luteolin-loaded solid lipid nanoparticle physicochemical characteristics	
Size (nm)	227.1 ± 53.98
Zeta Potential (mV)	-30.4 ± 5.51
PDI	0.371 ± 0.08
EE %	95 ± 0.01

Values represented as mean $\pm$ SD.

Morphology

The morphology of the synthesised luteolin-loaded solid lipid nanoparticles recorded using the HR-TEM, was shown to be spherical in shape (Figure A2)
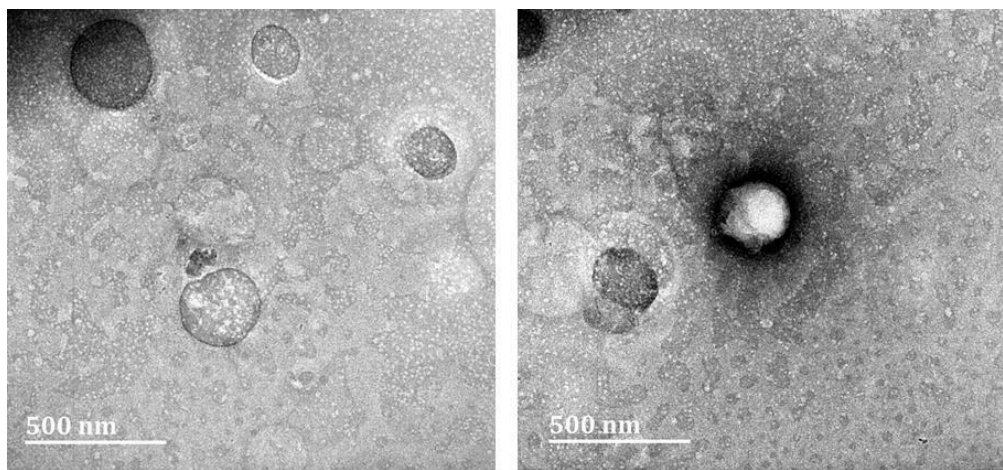
Figure A2. HR-TEM micrographs of synthesised luteolin-loaded solid lipid nanoparticles

In vitro drug release

The drug release study was carried out as described in **Chapter four, manuscript three**. The drug release profile for luteolin and LUT-SA-SLN (Figure A3), showed a rapid drug release from luteolin with up 94% released in the first 8 h. In contrast, LUT-SA-SLN showed a slower drug release with 60% released in the first 8 h then progressing to plateau at 86% from 24 h to 48 h. Previous studies have attributed the slower release to internal interactions between the encapsulated drug and the polymer of the nanoparticles (Cristina Puhl et al. 2011). Furthermore, similar luteolin release was observed for stearylamine-chitosan nanoparticles (Dang et al. 2014).

Figure A3. The drug release profile of luteolin and luteolin-loaded solid lipid nanoparticles (LUT-SA-SLN) over 48 h. Values represented as mean ± SD from experimental triplicates, * represents statistically significant difference of % cumulative drug release between luteolin and luteolin-loaded solid lipid nanoparticles at $p < 0.05$.

Cytotoxicity of LUT-SA-SLN

Based on the calculated concentration (5 µg/mL) of luteolin in the synthesised nanoparticles, cells (MCF-7 and HEK 293) were treated with LUT-SA-SLN in dilutions of 20, 40, 60, and 100 µL in supplemented DMEM (100 µL, total volume per well), 5- fluorouracil (5-FU) served as the positive control in this experiment. The cell viability was determined by the colorimetric MTT assay with absorbance recorded at 560 nm. As illustrated in Figure A4, treatment with LUT-SA-SLN, resulted in decreased cell viability of < 10% in both cell lines, indicating the non-selective toxicity of the prepared LUT-SA-SLN.
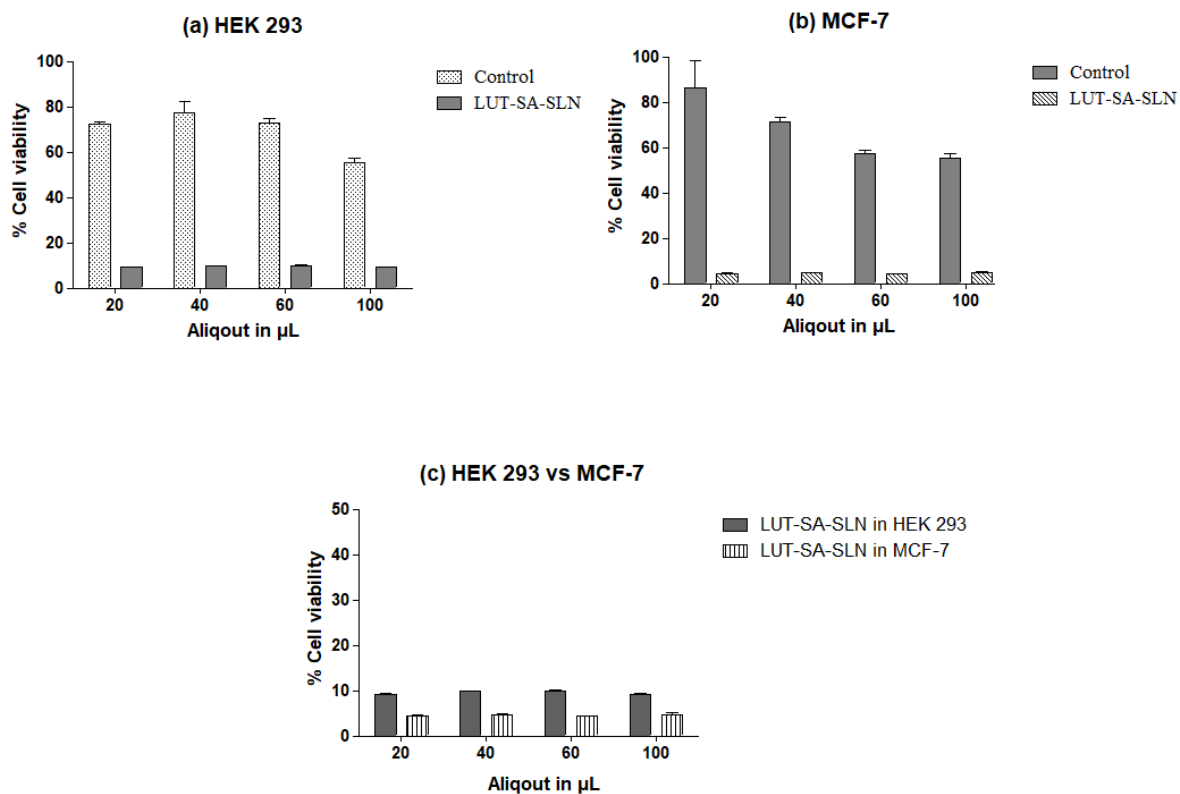
Figure A4. Cytotoxicity of luteolin-loaded solid lipid nanoparticles (LUT-SA-SLN) against (a) HEK 293, (b) MCF-7 and (c) comparison of LUT-SA-SLN cytotoxicity in HEK 293 and MCF-7. Values are represented as mean ± SD of six experimental replicates.

UNIVERSITY OF
KWAZULU-NATAL

INYUVESI
YAKWAZULU-NATALI

RESEARCH OFFICE
BIOMEDICAL RESEARCH ETHICS ADMINISTRATION
Westville Campus
Govan Mbeki Building
Private Bag X 54001
Durban
4000
KwaZulu-Natal, SOUTH AFRICA
Tel: 27 31 2604769 - Fax: 27 31 260-4609
Email: BREC@ukzn.ac.za
Website: http://research.ukzn.ac.za/Research-Ethics/Biomedical-Research-Ethics.aspx

04 March 2020

MRS J Magura (214585401)
School of Laboratory Medicine and Medical Sciences
College of Health Sciences
214585401@stu.ukzn.ac.za

Dear Mrs Magura

Protocol: Investigating the effects of nano-encapsulated phytocompounds from Eriocephalus africanus on cancer
Degree: PhD
BREC REF: EXM095/19
NewTitle: The effect of isolated and nanoencapsulated flavonoids from Eriocephalus africanus on apoptotic and epigenetic effects in cancer

We wish to advise you that your application for amendments received on 18 February 2020 to change the title to the above has been noted and approved by a subcommittee of the Biomedical Research Ethics Committee.

The committee will be advised of the above at its next meeting to be held on 14 April 2020.

Yours sincerely

Prof V Rambiritch
Chair: Biomedical Research Ethics Committee

cc: (supervisor) mackraji@ukzn.ac.za

Assignments
Students
Grade Book
Libraries
Calendar
Discussion
Preferences
About this page

This is your assignment inbox. To view a paper, select the paper's title. To view a Similarity Report, select the paper's Similarity Report icon in the similarity column. A ghosted icon indicates that the Similarity Report has not yet been generated.

Thesis

Inbox | Now Viewing: new papers ▼

Submit File Online Grading Report | Edit assignment settings | Email non-submitters

Delete | Download | move to...

	Author	Title	Similarity	web	publication	student papers	Grade	response	File	Paper ID	Date
☐	Judie Magura	Thesis	12% / 12%	9%	9%	8%	✏️	●	download paper	1350597533	28-Jun-2020